university of groningen

The functional relationship between peroxisomes, bile salts and lipid rafts in the liver

Paranimfen:
Jan Freark de Boer
Mark Hoekstra

ISBN: 978-90-367-6045-4
ISBN (e-book): 978-90-367-6048-5

Cover and page layout: K.P.Rembacz
Photograph: CLSM image of rat hepatocytes stained for the Peroxisomal membrane protein of 70 kDa (Pmp70)
Printed by: cyfrowa**drukarnia.pl**

Rijksuniversiteit Groningen

The functional relationship between peroxisomes, bile salts and lipid rafts in the liver

Proefschrift

ter verkrijging van het doctoraat in de
Medische Wetenschappen
aan de Rijksuniversiteit Groningen
op gezag van de
Rector Magnificus, dr. E. Sterken,
in het openbaar te verdedigen op
maandag 11 februari 2013
om 11:00 uur

door

Krzysztof Przemysław Rembacz

geboren op 13 april 1977

te Wrocław, Polen

Promotores:	**Prof. Dr. K. N. Faber**
	Prof. Dr. H. Moshage
Beoordelingscommissie:	**Prof. Dr. I. van der Klei**
	Prof. Dr. D.-J. Reijngoud
	Prof. Dr. Bruno Stieger

Table of contents

Chapter 1 7
Introduction.

Chapter 2 29
Unconjugated bile salts shuttle through hepatocyte peroxisomes for taurine conjugation.

Chapter 3 47
Involvement of Pmp70 in the intrahepatocyte bile salt shuttle.

Chapter 4 67
Lipid rafts are essential for peroxisome biogenesis in HepG2 cells.

Chapter 5 87
Caveolin-1 is enriched in the peroxisomal membrane of rat hepatocytes.

Chapter 6 107
General discussion and future perspectives.

Chapter 7 119
Summaries.

CHAPTER 1

General Introduction & Aim of this thesis

1. General features of the liver
2. Bile salt physiology
3. Bile salt modifications, de-conjugation and re-conjugation.
4. Bile salt metabolism in peroxisome disorders.
5. Peroxisomes and peroxisomal membrane proteins (PMPs)
6. Peroxisome proliferator-activated receptors (PPARs) affect peroxisome biogenesis and bile salt synthesis
7. Lipid rafts in cellular and peroxisomal membranes.
8. Aim and outline of this thesis

1. General features of the liver

The liver is a central organ in whole body metabolism, thermoregulation, and physiological homeostasis. The predominant cells in the liver are the hepatocytes. These cells comprise up to 70-80% of the total cell population. Other cell types include bile duct epithelial cells (cholangiocytes), endothelial cells, Kupffer cells (liver-specific macrophages), hepatic stellate cells, portal myofibroblasts and hepatic progenitor (or oval) cells (Figure 1).
Hepatocytes are polarized parenchymal cells. Their basolateral membrane is in contact with the blood circulation, while the apical (or canalicular) membrane lines the bile canaliculi.

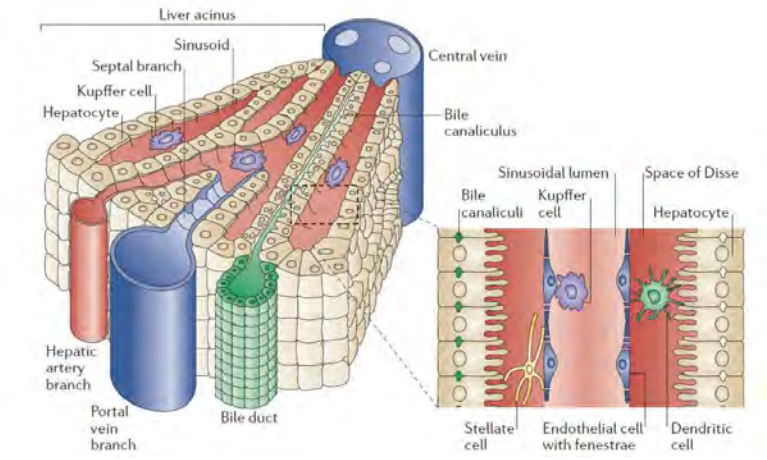

Figure 1. Three-dimensional structure of a liver lobule
The portal vein and hepatic artery supply the liver with nutrients and oxygenated blood, respectively. Hepatic blood flows through sinusoids towards the central vein. Hepatocytes are organized in plates and secrete bile into bile canaliculi, which merge in bile ducts. Hepatocytes are separated from sinusoidal endothelial cells by the space of Disse, which contains Kupffer cells as well as hepatic stellate cells. Reprinted by permission from Macmillan Publishers Ltd: Nature Reviews Immunology (Adams *et al* Aberrant homing of mucosal T cells and extra-intestinal manifestations of inflammatory bowel disease), copyright (2006)

The bile canaliculi merge into bile-collecting bile ductules. The bile is stored in the gall bladder and released into the intestine (duodenum) triggered by food intake.
Blood enters the liver via the portal vein and the hepatic artery. Most of the blood flowing through the liver comes from the intestines (approximately 75%) and is rich in nutrients and low in oxygen. The hepatic artery supplies the liver with oxygen-rich blood.

2. Bile salt physiology

Bile salt synthesis

A major function of the liver is the production of bile, which aids in the digestion of fat-soluble nutrients and the excretion of (fat-soluble) waste products and toxins. The functional compounds in bile are bile salts and phospholipids. After secretion into the bile, bile salts and phospholipids form mixed-micelles, which are the carriers of fat-soluble compounds that facilitate their absorption (for nutrients) in the gut or their secretion (of waste products/toxins) via the feces. Bile salts are synthesized in the liver, specifically in the hepatocytes, in a multistep enzymatic pathway using cholesterol as starting substrate (1). Conversion of cholesterol to bile salts involves at least 13 different enzymes and is of key importance to control cholesterol homeostasis. Approximately 500 mg of cholesterol is converted on a daily base into the primary bile acids cholic acid (CA) and chenodeoxycholic acid (CDCA).

Three different types of modifications are required for the complete conversion of cholesterol into a bile salt: 1) hydroxylation of the steroid nucleus, 2) shortening of the side chain, and 3) conjugation (amidation) of the side chain to either taurine or glycine. The main bile salts formed in human are glycine conjugates, while in rodents the taurine conjugates predominate (2).

Bile salt are synthesized largely via two main routes, the classic (or neutral) and the alternative (or acidic) pathway. These two metabolic processes only differ in the order of reactions that transform cholesterol to CA or CDCA and intracellular sites where the first reaction takes place (3, 4). Each pathway contains only one unique enzyme that is responsible for the hydroxylation of the C-7 position. All other enzymes are active in both pathways.

The classic (neutral) route starts with the hydroxylation at the C-7 position in the steroid nucleus by 7α-hydroxylase (CYP7A1), an enzyme residing in the endoplasmic reticulum (ER). CYP7A is considered to be the rate-limiting step in the whole process of bile salt biosynthesis (3, 4). The alternative (acidic) pathway is initiated by the hydroxylation of the cholesterol side chain, at carbon C-27, by the enzyme sterol 27-hydroxylase (CYP27A1) residing in mitochondria. The resulting product, cholesten-3β-27-diol, is subsequently hydroxylated at the C-7 position by CYP7B1.

From this point, the acidic and neutral pathways overlap. The different enzymes introducing various changes to the bile salt intermediates are shown in Figure 2.

The ring modifications are catalyzed by 3β-hydroxy C27-steroid dehydrogenase-isomerase (3βHSD/HSD3β7) and CYP8B1 in the ER.

Sterol 12-α-hydroxylase (CYP8B1) (1) leads to the formation of tri-hydroxycholestanoic acids (THCA) (5) leading to the production of CA. Cyp8B1 is therefore a central factor in controlling the ratio of CA over CDCA synthesis and thereby regulates the hydrophobicity index of the bile salt pool.

The following steps occur in the cytoplasm by Δ4-3-ketosteroid-5-β-reductase (AKR1D1) and 3α-hydroxysteroid dehydrogenase AKR1C4. The last steps in bile salt biosynthesis take place in the peroxisomal matrix, where bile salt intermediates are subjected to a single cycle of β-oxidation. This yields C24 bile acid CoA-esters, which are subsequently conjugated to glycine or taurine by the peroxisomal enzyme bile acid coenzyme A:amino acid N-transferase (BAAT) (5). After conjugation, bile salts are exported out of the peroxisome to the hepatocyte cytoplasm by a yet unidentified transporter. Cytosolic bile salts are exported to the bile by the canalicular bile salt export pump (BSEP) and enter the enterohepatic circulation.

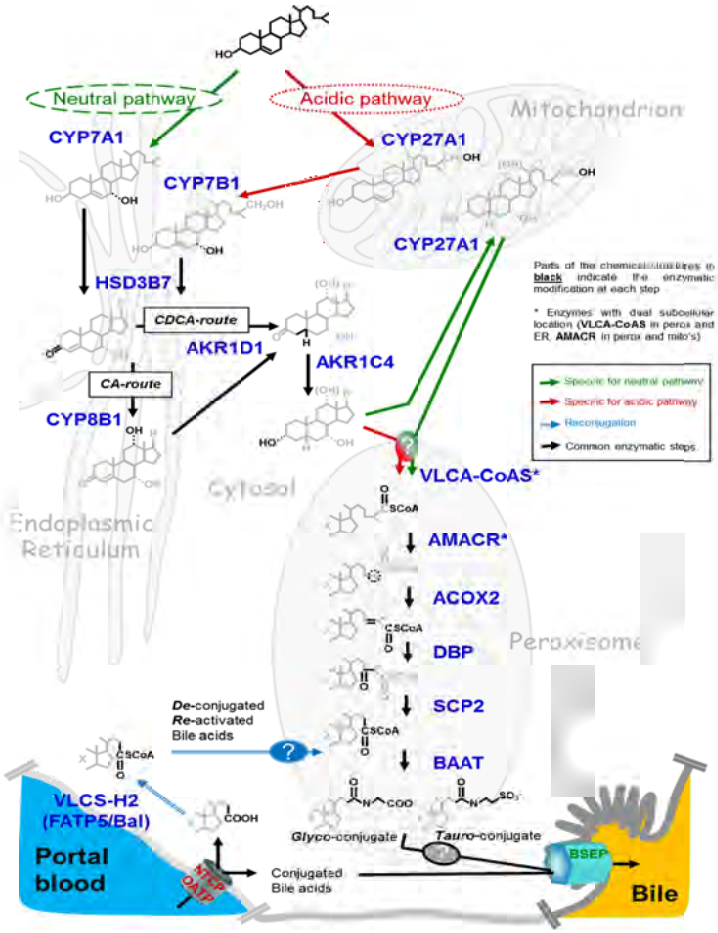

Figure2.: Enzymes and organelles involved in bile salt biosynthesis.
Bile salts are synthesized *de novo* in hepatocytes. Different enzymes involved (depicted in blue) are localized to different intracellular compartments. Changes to the cholesterol backbone along the synthesis route are given in bold. Cyp7A1 is considered the rate-limiting enzyme of the neutral pathway and is located to the endoplasmic reticulum. The first step of the acidic route is catalyzed by mitochondrial CYP27A1. Subsequent enzymatic reactions occur in the cytosol, endoplasmic reticulum and peroxisomes. The final step (bile salt conjugation) takes place in peroxisomes. This step is also essential in the reconjugation pathway of bile salts returning from enterohepatic circulation (blue arrows), where bile salts first need to be re-activated with CoA by FATP5/Bal. After transport to the cytosol, bile salts are exported by BSEP to the bile. Adapted from (4).

Enterohepatic circulation of bile salts

Food intake triggers the contraction of the gallbladder and releases bile into the intestinal lumen. The bile salt/phospholipid mixed-micelles take up fat-soluble compounds and carry them through the intestinal tract so they can be absorbed in the gut or efficiently secreted in the feces (6). At the terminal ileum, the majority (~95%) of bile salts is reabsorbed and return to the liver. Arriving at the liver through the portal vein, bile salts are taken up by the hepatocytes and re-secreted to the bile, thus completing the enterohepatic cycle (6, 7).

Dedicated bile salt transporters maintain the unidirectional cycling of bile salts between the liver and intestine (see Figure 3).

Bile salts are exported to the bile by the Bile Salt Export Pump (BSEP/*ABCD11*). Bile salt concentrations are 100-1000 fold higher in bile as compared to the hepatocyte cytoplasm. Thus, BSEP transports these compounds against a steep concentration gradient and is able to do so at the expense of ATP hydrolysis. The substrate specificity of BSEP is narrow and restricted to conjugated bile salts (4, 8).

Bile salt secretion is followed by a passive inflow of water and must be closely coordinated with canalicular phospholipid secretion to prevent bile salt-induced damage to bile ductular cells (9, 10). Phospholipids are secreted by the phospholipid flippase (MDR3/*ABCB4*) in humans and Mdr2 in rats (10)). The major phospholipid in the bile is phosphatidylcholine. Free cholesterol is secreted to bile via the ABCG5/G8 heterodimer. Conversion of cholesterol to bile salts and cholesterol secretion by ABCG5/G8 are the two major routes of hepatic cholesterol elimination (11).

In the terminal ileum, bile salts are reabsorbed to blood. The first step is uptake from the intestinal lumen by the apical sodium-dependent bile acid transporter (ASBT/*SLC10A2*) present in the apical membrane of ileal enterocytes (4, 12, 13). Inside enterocytes, bile acids bind to the intestinal bile acid binding protein (I-BABP) and are transferred to the basolateral membrane for secretion by the heterodimeric sodium-independent organic solute transporter Ostα-Ostβ (Ostα/β) (4, 14).

From the ileum, bile salts are transported back to the liver via the portal circulation. Import of conjugated bile salts into the hepatocyte is mediated mainly by the sodium-dependent taurocholate-co-transporting polypeptide (NTCP/SLC10A1). Like ASBT, NTCP is a member of the SLC10 family of sodium bile salt co-transporters (4, 15, 16, 17). NTCP is exclusively expressed in the liver (4, 15) and is localized to the sinusoidal/basolateral membrane of hepatocytes (4, 16, 18). A significant fraction of the bile salt pool is deconjugated by intestinal bacteria (see below). NTCP has a very low affinity for unconjugated bile acids. Recently, Oatp1b2 has been shown to be the primary transporter in mice to absorb unconjugated from the portal blood into the hepatocytes (19).

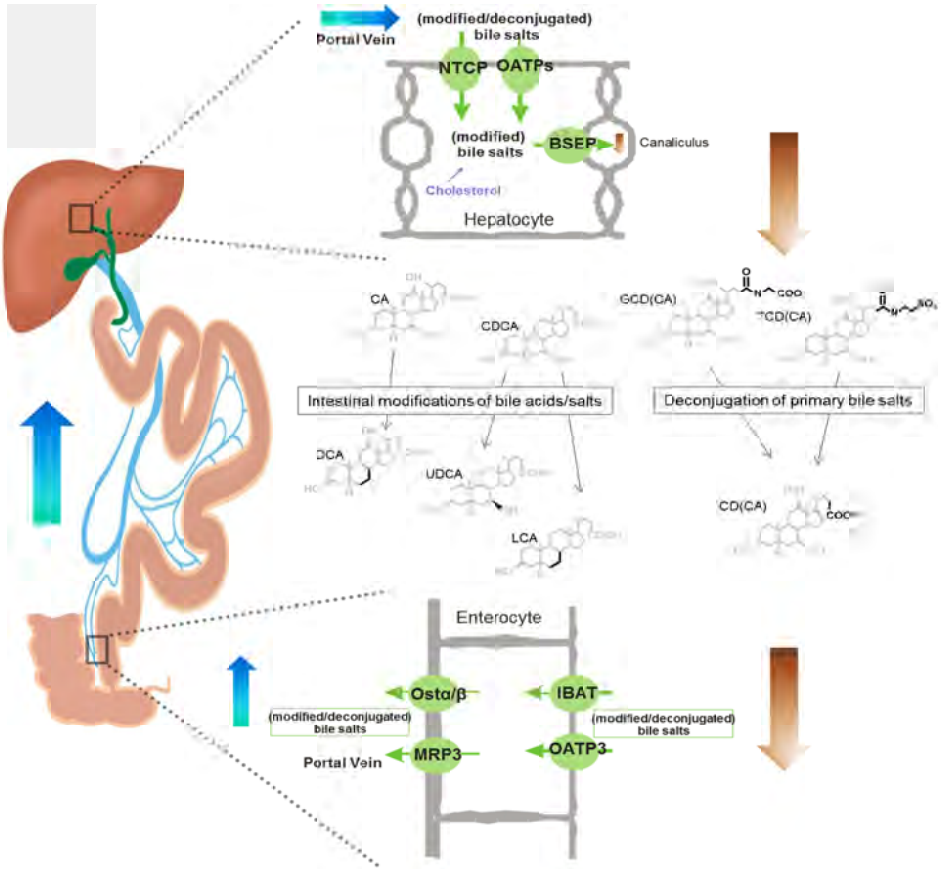

Figure 3. Bile salts are maintained in the enterohepatic circulation
Bile salts are synthesized in hepatocytes and are exported by the canalicular bile salt export pump (BSEP). A portion of bile salts is subjected to structural changes (depicted in black in the chemical structures) by the intestinal bacterial flora. After passing through the small intestine (brown arrows), bile salts are reabsorbed in the terminal ileum by the apical sodium-dependent bile acid transporter (ASBT) in the apical membrane of ileal enterocytes. Bile salts are secreted into the blood circulation (blue arrow) by the heterodimeric organic solute transporter OSTα/β and transported back to the liver. In the liver, bile salts are imported into hepatocytes from the blood by the sodium-dependent taurocholate cotransporting polypeptide (NTCP) and organic anion transporting polypeptides (OATPs) in the basolateral membrane of hepatocytes.

3. Bile salt modifications, de-conjugation and re-conjugation.

Intestinal modifications

Bile salts may undergo structural changes when exposed to the intestinal flora. A significant portion of bile salts is deconjugated (Figure 3), removing the glycine or taurine moiety from the side chain (20). In addition, the C7 hydroxyl group may be removed from the steroid nucleus converting the primary bile salts CA and CDCA to the secondary bile acids deoxycholic acid (DCA) and lithocholic acid (LCA), respectively (Figure 3).
Secondary bile acids may accumulate to high levels in the bile acid pool, aggravate cholestasis, and contribute to gallstone formation and colon cancer, because of their increased hydrophobicity compared to the primary bile salts. Human biliary bile is a mixture of CA (35%), CDCA (35%), DCA (25%), LCA (1%), UDCA (2%) and a residual fraction containing six different oxo- and 3β-hydroxy- derivatives (2%). In contrast, fecal bile consists of DCA (34%), LCA (29%), UDCA (2%), CDCA (2%), CA (2%) and the secondary bile acid-derived oxo- and hydroxy- forms (isocholic-; 7-oxodeoxycholic-; 7-epicholic-; 12-oxochenodeoxycholic- and 12-epicholic acid) which amount over 30% of the excreted bile salt pool (20).
In healthy humans, approximately one-third of the bile salt pool may become de-conjugated on a daily basis, but biliary bile almost exclusively contains conjugated bile salts (4, 21). Thus, the liver very effectively reconjugates bile acids that have lost their glycine/taurine side chain in the intestine. In contrast, modifications of the hydroxyl groups largely persist during enterohepatic cycling of (secondary) bile salts.

Bile salt reactivation with coenzyme A

Unconjugated (C_{24}-)bile salts entering the hepatocyte first need to be activated with coenzyme A (CoA) by the fatty acid transport protein 5 (FATP5/ SLC27A5/ ACSVL6 / ACSB / BACS / VLCS-H2 in human, VLACSR in mice or BAL in rat) (22, 23). FATP5 is specific for reconjugation of C_{24} bile acids that are present in the enterohepatic cycle. CoA activation (thioesterification) is also a crucial step in the *de novo* bile salt synthesis, where the C_{27}-precursors of cholic acid and chenodeoxycholic acid THCA and DHCA are CoA-activated before peroxisomal side chain shortening and conjugation (amidation) to taurine or glycine. However, this activation step is performed by a different enzyme, Very Long-chain acyl-CoA Synthetase (VLCS), which is present both in peroxisomes and in the ER (Figure 2) (22, 23). FATP5 is present at the basal membrane of hepatocytes (24), a location that fits well with the site of entrance of its substrates into hepatocytes (see Figure 2 and 4). The majority of gall bladder bile acids are unconjugated in Fatp5 (or Bacs)-/- mice, stressing the important contribution of reconjugating bile acids that are cycling between intestine and liver.

Peroxisomes are involved in the final step of biosynthesis and reconjugation of bile salts

In contrast to the 2 separate enzymes for CoA-activation of bile acid intermediates in *de novo* synthesis and in the enterohepatic cycle, there is only one enzyme, bile acid coenzyme A:amino acid N-transferase (BAAT), that conjugates glycine or taurine to these precursors. The supply of substrates for BAAT from 2 different sources that appear either in the peroxisome (in bile salt synthesis) or in the cytosol (in the enterohepatic cycle) make the subcellular location of this enzyme highly relevant for the putative existence of intracellular bile salt transporters. The existence of a peroxisomal pool of BAAT has never been disputed. However, clear controversy exists whether or not a significant amount of BAAT also resides in the cytosol that could be responsible for reconjugation of cycling C_{24} bile salts. The existence of a cytosolic pool of BAAT was concluded from the fact that in subcellular fractionation experiments BAAT was always detected in both peroxisomal and cytosolic fractions (25-29). However, peroxisomes are fragile organelles and are easily ruptured during cell fractionation experiments. As a consequence, over 80% of peroxisomal matrix proteins may leak out during this procedure and incorrectly designated as "cytosolic" (4, 30, 31). In addition, artificially expressed BAAT tagged with the green fluorescent protein (GFP) was found predominantly in the cytosol of fibroblasts and HeLa cells (32, 33). In contrast, GFP-BAAT was efficiently sorted to peroxisomes of primary rat hepatocytes and endogenous rat and human BAAT were detected predominantly, if not solely, in peroxisomes of hepatocytes by immunofluorescence microscopy and differential membrane permeabilisation by digitonin (34). This implies that CoA-activated C_{24} bile acids need to be transported into hepatocyte peroxisomes for their reconjugation (Figure 4) (34). Biochemical evidence for the shuttle of C_{24} bile acids into peroxisomes has recently been obtained (see chapter 2; Rembacz *et al.*, 2010 (35).

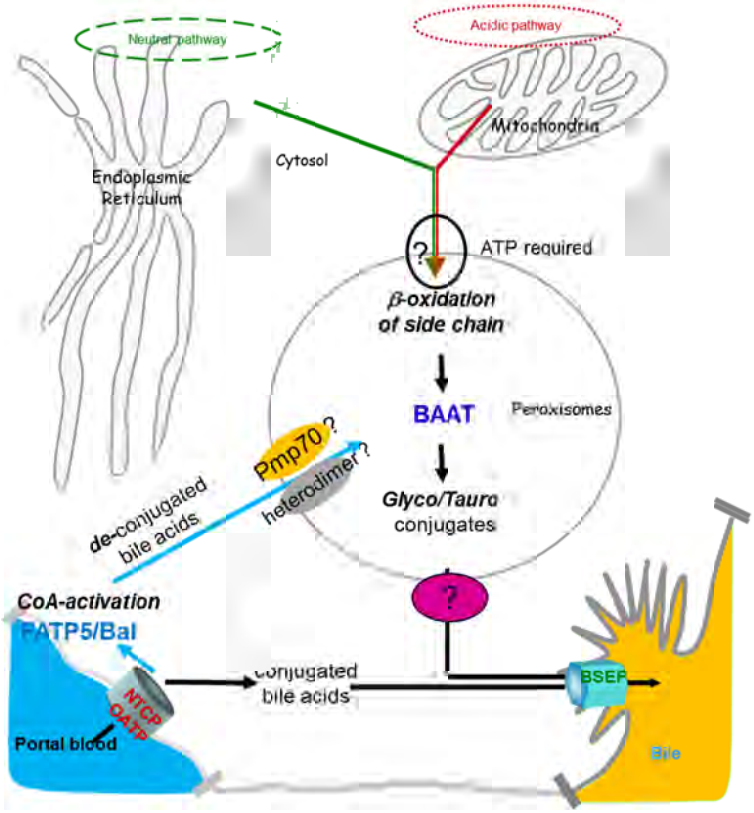

Figure 4. Bile acids are conjugated inside hepatocyte peroxisomes
Bile acids are synthesized from cholesterol in a cascade of enzymatic reactions that take place in different subcellular compartments. The bile acid biosynthesis intermediates di- and trihydroxycholestanoic acid (D- and THCA) are transported into peroxisomes by a yet unidentified transporter protein. It is known however, that ATP is required for the translocation of bile salt intermediates for their peroxisomal β–oxidation. Multiple side chain oxidation reactions lead to the production of (chenodeoxy) cholic acid, which is conjugated to glycine or taurine by BAAT. After transport to the cytosol via an unknown transporter, bile salts are exported by BSEP to bile.
Re-conjugation pathway: Unconjugated bile acids returning from the enterohepatic circulation are imported by OATP(s) or NTCP into hepatocytes. Subsequently, a FATP5/Bal-mediated reactivation with CoA takes place. CoA-re-activated bile acids are imported into peroxisomes via an unknown transporter and conjugated to glycine or taurine by BAAT. It is not known whether PMP70 plays a role in this process and if so, whether it acts as a homodimer or a heterodimer with one of its presumed partners (ALDP, ALDPR, P70R). Like in the bile salt biosynthesis pathway, bile salts are transported to the cytosol and exported by BSEP.

Established activities for bile salt (-intermediates) peroxisomal transport

The identity of proteins that facilitate the transport of bile salt(intermediates) in or out the peroxisomes is unknown to date. However, some biochemical characteristics of these transport processes have been established and linked to candidate proteins.
Two studies have biochemically assessed the transport of bile salt (-intermediates) across peroxisomal membranes (36, 37). In an indirect assay, Une *et al*. (37) studied the conversion of the cholic acid-precursors 3alpha,7alpha,12alpha-trihydroxy-5beta-cholestanoic acid (THCA) and THCA-CoA to cholic acid when incubated with purified rat liver peroxisomes. Cholic acid production was largely dependent on ATP and was more efficient starting from THCA-CoA compared to THCA. Moreover, CA production form THCA-CoA was inhibited when intact peroxisomes were pretreated with proteinase K or by N-ethylmaleimide, sodium azide and verapamil, known inhibitors of ATP-binding cassette (ABC)-transporters (37). This suggests that the CoA-activated form of THCA is the preferred substrate for import into peroxisomes, which largely depends on a protein with ABC-transporter-type characteristics (see Figure 4).
After conjugation to taurine or glycine, bile salts are exported from peroxisomes to the cytosol. This activity was studied by Visser *et al*. (36), who reconstituted peroxisomal membrane proteins in liposomes and measured uptake of radiolabeled GCA and TCA. The transport activity was insensitive to sodium, potassium, glycine, ATP or NEM, indicating that this transporter facilitates passive unidirectional transport driven by the substrate concentration gradient. A putative limitation of the later study is that peroxisomal membrane proteins were isolated form *Bos taurus* kidneys, which are not involved in bile salt synthesis and/or enterohepatic cycling (36). A putative liver-specific peroxisomal bile salt transporter may therefore be missed in this analysis.

4. Bile salt metabolism in peroxisome disorders.

Peroxisomal biogenesis disorders impair the bile salt biosynthesis
There are genetic disorders that directly affect the formation or function of peroxisomes. Collectively, these disorders are known as peroxisomal disorders, which can be subdivided in peroxisome biogenesis disorders (PBD) and single enzyme defects. The PBD include Zellweger syndrome (ZS), neonatal adrenoleukodystrophy (NALD) and infantile Refsum disease (IRD) and are characterized by the absence or malformation of peroxisomes. Besides involvement in bile salt biosynthesis in the liver, peroxisomes harbor a great variety of metabolic activities all over the body, including catabolism of very long chain fatty acids, D-amino acids, polyamines, and biosynthesis of plasmalogens. Therefore, malfunction of these organelles results in a variety of symptoms that often present in early childhood and include skeletal and craniofacial dysmorphism, liver dysfunction, progressive sensorineural hearing loss, and retinopathy (38-40). PBD

result from mutations in *PEX* genes that code for proteins (peroxins) that are required for the proper formation of the organelle, e.g. formation of the organellar membrane, targeting of enzymes to peroxisomes, proliferation and inheritance of peroxisomes during cell division.
The absence of normal peroxisomes also severely affects bile salt biosynthesis. In fact, the accumulation of bile salt synthesis intermediates DHCA and THCA in plasma are diagnostic markers for PBD (41-43). Normal plasma levels of DHCA and THCA in healthy subjects are low and are on average 0,77% and 0,12% of total pool of bile acids, respectively, while the biosynthetic end products CDCA (53%) and CA (14%) predominate the bile salt pool detected in plasma. The ratios of THCA/CA and DHCA/CDCA in serum are used as diagnostic measures where ratio's >0.04 and >0.01, respectively, are indicative for Zellweger syndrome (44, 45).
In ZS patients, serum CDCA and CA concentration are strongly reduced , but show a normal conjugation profile. Remarkably, also part of THCA and DHCA are conjugated to taurine (46). As BAAT is likely to reside in the cytosol of hepatocytes of Zellweger syndrome patients, this indicates that the enzyme is at least partly active in this abnormal cellular location. It is unknown whether BAAT is also responsible for the taurine conjugation of bile salt intermediates in ZS subjects. Similarly, C27- bile acid biosynthetic intermediates accumulate in bile, liver and serum in *pex2*-/- mice, a rodent model for Zellweger Syndrome (47), and remain largely unconjugated, while the small pool of C24-bile acids are mainly conjugated. However, when these mice are fed a CA-containing diet, the bile acid pool remains largely unconjugated, whereas control animals effectively conjugate dietary CA. These data show that peroxisome deficiency leads to a generalized defect in bile acid conjugation (47).
One of the single peroxisomal enzyme defects is BAAT deficiency that has been described in two Amish children. These patients presented with pruritus, fat malabsorption and vitamin K coagulopathy and high levels of unconjugated bile acids in serum and increased urinary excretion of mainly unconjugated and glucuronidated/sulfated bile acids (48, 49). The complete absence of conjugated bile acids in the serum of these patients reconfirms that BAAT is the sole enzyme able to conjugate bile acids to glycine or taurine.

5. Peroxisomes and peroxisomal membrane proteins (PMPs)

Peroxisomes are organelles surrounded by a single membrane that are particularly abundant in the mammalian liver. The focus in this thesis is on their role in synthesis and enterohepatic cycling of bile salts, but in fact, they may harbor a great variety of metabolic and catabolic activities, dependent on the organism, tissue, cell type, and environmental conditions. Peroxisomes are conserved throughout the eukaryotic kingdom and perform vital functions in organisms ranging from yeast, plants, insects, mammals and human. Their involvement in metabolism varies from methanol utilization in yeast, photorespiration in plants

and a multitude of different reactions in mammals. Besides their role in bile salts synthesis, hepatic peroxisomes are also necessary for β-oxidation of very long chain fatty acids (50).
During the last two decades, much research in this field has been focused on identifying and characterizing proteins that are involved in formation of peroxisomes, the so-called peroxins. These proteins are involved in peroxisomal matrix protein import, membrane biogenesis, peroxisome proliferation, and inheritance. The nomenclature established for these proteins states the acronym *PEX*# for the genes and Pex#p for the proteins, where # indicates a number that reflects the order of discovery (51). Many of the peroxins are embedded in –or associated with- the peroxisomal membrane. In addition, the peroxisomal membrane contains proteins that transport solutes that are substrates or products from peroxisomal metabolism. Best studied are the peroxisomal ABC transporters.

Peroxisomal ABC transporters and other peroxisomal substrate transporters

Most eukaryotic ABC transporters are a single protein composed of two homologous halves each of them consisting of a hydrophobic transmembrane domain and a nucleotide-binding fold (NBD). Alternatively, a functional ABC transporter can be build from two separate polypeptides, each containing 1 transmembrane domain and 1 NBD. All peroxisomal ABC transporters are such half-transporters belonging to the subclass D of the ABC protein family (ABCD) (52, 53).
To date 4 peroxisomal ABC half transporters have been identified, in order of discovery: the peroxisomal membrane protein of 70 kDa PMP70 (54) (encoded by the *ABCD3* gene (55)), the adrenoleukodystrophy protein ALDP encoded by *ABCD1* (56), the ALDP-related protein ALDPR (*ABCD2*) (57) and the PMP70-related protein PMP70R/PMP69/P70R (*ABCD4*) (52, 53, 58, 59).

The best-studied protein of this subfamily is ALDP. Mutations in the *ABCD1* gene are the cause of X-linked Adrenoleukodystrophy (X-ALD), an inherited disease that particularly affects the nervous system and adrenal glands. Biochemically, these patients are characterized by the accumulation of very-long chain fatty acids (VLCFAs) in blood and other body fluids. It appears that ALDP is required to transport these VLCFAs in to peroxisomes to become metabolized to LCFAs, which in turn are transported to mitochondria for further chain shortening.
ALDPR (*ABCD2*) exhibits overlapping functions to ALDP, as demonstrated by normalization of VLCFA levels and increased oxidation of C24:0 and C26:0 in *ABCD1-/-* human and *Abcd1-/-* mouse cells overexpressing ALDPR (52, 60, 61, 62, 63). However, *Abcd2-/-* mice do not show significant abnormalities in VLCFA metabolism and, so far, no mutations in human *ABCD2* have been found to be associated with adrenoleukodystrophy. Thus, the specific physiological relevance of this transporter remains unclear.

The 70-kDa peroxisomal membrane protein (PMP70) is a major protein component of peroxisomal membrane in the liver. The *ABCD3* gene has been characterized already over 20 years ago, still a clear physiological function for PMP70 has not been
established yet. Its ATP binding site faces the cytosol (54), which suggests that it transports substrates from the cytosol into the peroxisomal matrix. PMP70 has been shown to transport CoA esters of LCFAs across the peroxisomal membrane in *in vitro* assays, but a physiological role has not been established in mice or human (64). Some unpublished reports have suggested a role for PMP70 in transport of bile salt intermediates, but these data await publication in peer-reviewed journals. When overexpressed in *ABCD1-/-* cells, PMP70 is able to correct the defect in C24:0 oxidation. Thus, PMP70 and ALDP have partly overlapping substrate specificities (52, 60).

It has been suggested that peroxisomal ABC half transporters may functionally organize both in homodimers and in heterodimers. Formation of heterodimers could potentially broaden the range of substrates that are transported by the peroxisomal ABC transporters. Hypothetically, 10 different combinations could be formed of the 4 peroxisomal ABC transporters enabling 10 different substrates (or families of substrates) to cross the peroxisomal membrane. However, potential heterodimerization of these proteins has been solely observed in experiments where the proteins were artificially expressed. Endogenous PMP70 and ALDP in mouse liver were found to exist predominantly as homodimers (53). In addition, the 4 peroxisomal ABC transporters all show a unique tissue distribution and little is known about their cell type specific expression in these tissues. So the presence and physiological relevance of peroxisomal ABC transporter-heterodimers remains unclear.

Besides the four ABC transporters, also a few other peroxisomal substrate transporters have been identified. PMP34 (SLC25A17) was shown to transport ATP into the peroxisomal matrix, which is used for the activation of fatty acids (65). Little is known about the putative transporters PMP22 (PXMP2) (66), MPV17 (possibly involved in the reactive oxygen species metabolism (67)) and PXMP4.

6. Peroxisome proliferator-activated receptors (PPARs) affect peroxisome biogenesis and bile salt synthesis.

Peroxisome proliferator-activated receptors (PPARs) are three, genetically and functionally distinct, ligand-activated transcription factors influencing the mammalian development, physiology and homeostasis (68). PPARα ligands fall into a large group of "peroxisome proliferators" (clofibrate, bezafibrate, ciprofibrate and Wy-14,643) and in rodents, but not in humans, they dramatically increase the size and number of hepatic and renal peroxisomes as well as their metabolic activities (68, 69, 70). Ligand-activated PPARα strongly induces the

expression of *PEX11*. Pex11p exists in two isoforms Pex11pα and Pex11pβ and promotes peroxisome proliferation (71, 72, 73). Consequently, the number of peroxisomes is strongly decreased in *Pex11α-/-* mice that are unresponsive to PPARα ligands (11, 72).
PPARα is also involved in regulation of *de novo* synthesis of bile salts and transport. The first enzyme in the classical route of bile acid biosynthesis from cholesterol, CYP7A1 is repressed by fibrates (11). Further analyses revealed, that PPARα down-regulates CYP7A1 by decreasing the levels of Hepatocyte Nuclear Factor 4α (11). In contrast, PPARα increases CYP8B1 expression and was shown to directly bind to the promoter element of this gene (11, 74).
It is known that peroxisome proliferators induce ABCD3/PMP70.
Fibrates have a differential effect on the expression of peroxisomal ABC transporters. PPARα does not influence the *Abcd1*/Aldp and *Abcd4*/Pmp70r expression levels (75). It does, however, strongly induce *Abcd2*/Aldpr (76) and *Abcd3*/Pmp70 (52) expression. In line with a direct role of Pparα in regulation of *Abcd3*, fenofibrate failed to induce its expression in *Pparα-/-* mice (77). It was also shown, that PPARα agonists downregulate Bsep, Ntcp and Oatp1 (11, 78), however, this effect is most likely a result of reduced expression of Hnf4α, which is a key transcriptional regulator of these genes (22, 79). In a similar indirect way, also Baat expression is reduced by PPARα (28). Since no apparent PPRE could be identified in the *BAAT/Baat* promoter region, it seems most likely that Hnf4α is the central factor as Baat expression is strongly decreased in *Hnf4α-/-* mice (22).

7. Lipid rafts in cellular and peroxisomal membranes.

Lipid rafts in cell membranes

The plasma membrane is a lipid bilayer with embedded (trans-) membrane proteins. The main lipid components of cellular membranes are glycerolipids, glycerophospholipids, ceramides, glycosphingolipids, sphingomyelins and cholesterol (80).
Biological membranes exist in a fluid or liquid-crystalline phase (so-called l_c phase). In addition, most cellular and organellar membranes contain certain membrane domains, which are especially enriched in sphingolipids and sterols (cholesterol) that locally change the membrane physical characteristics. Such domains exist in a liquid-ordered (l_o) phase (81). Biochemically, they are characterized by their resistance to solubilization by detergents (e.g. Triton X-100 and Lubrol WX) at low temperatures (0-4^{o}C) and are therefore called Detergent Resistant Membranes (DRMs) or lipid rafts. After extraction by detergents, lipid rafts can be isolated by flotation gradient centrifugation. The majority of DRMs in mammalian cells originate from the plasma membrane. However, they are also present in intracellular membranes.
Besides certain lipids, lipid rafts are enriched in specific proteins. Such proteins may preferentially associate with lipid rafts because they contain lipid moieties,

like myristate, palmitate or a glycosylphospatidylinositol (GPI) anchor, or a specific hydrophobic architecture. In the pioneering work of Simons and Ikonen (Nature 1997), lipid microdomains were proposed to serve as platforms for transport of selected membrane proteins or as relay stations in intracellular signaling (82). At present, lipid rafts are defined as dynamic, nanoscale sterol-sphingolipid – enriched assemblies of proteins and lipids. They can further organize into larger raft domains by specific lipid-lipid, protein-lipid or protein-protein interactions.
The general concept nowadays implements three levels of lipid raft organization in cellular membranes (83). Lipid rafts of the first level are *nanoscale assemblies* (>50 nm) of cholesterol, sphingolipids and proteins with variable composition. They contain GPI-anchored proteins, transmembrane raft proteins and acylated cytosolic proteins, which can be modulated by actin filaments. A higher level of organization is achieved when nanoscale assemblies cluster into *raft platforms* that are formed in response to membrane trafficking event or external signals that give rise to lipid–lipid, lipid–protein and protein–protein oligomerizing interactions. These are the structures mainly referred to in the literature involved in membrane trafficking and signaling. The highest and the largest (micrometer scale) raft structure is a *raft phase*, observed *in vitro* in Giant Unilamellar Vesicles (GUVs).
A subclass of lipid rafts are caveolae and are involved in cell signaling and lipid transport (84). They are 50 to 100 nm in size and cholesterol and sphingolipids are the predominant lipid components. Caveolae are flask-shaped invaginations of the plasma membrane and contain coat proteins (Caveolin-1, -2 and -3) that bind directly to cholesterol and support proteins (cavins) (80, 83, 84). Caveolin-1 fulfils important functions in the liver as caveolin-1 knock-out mice show impaired lipidogenesis and liver regeneration after partial hepatectomy (85).

ABC transporter activity depends on the membrane lipid composition

ABC transporters are localized to lipid rafts, which directly regulate their activity. The human P-glycoprotein (Pgp/MDR1/*ABCB1*) is an example of an ABC transporter, which transport activity depends on the lipid environment in the plasma membrane. Cellular membranes can be depleted from cholesterol using methyl-β-cyclodextrin treatment and/or cholesterol synthesis inhibitors. This disrupts the association of Pgp to lipid rafts an strongly inhibited the transport of BODIPY-verapamil, a typical substrate of Pgp. Cholesterol repletion re-established the transport of BODIPY-verapamil in a dose-dependent manner. This demonstrates that Pgp function strongly depends on the cholesterol content of the plasma membrane (86). Similar observations were made for breast cancer resistance protein (BCRP/*ABCG2*). Cholesterol depletion decreased, while cholesterol repletion increased BCRP activity in MDCKII cells with recombinant expression of human BCRP. Moreover, co-immunoprecipitation experiments suggested an interaction between BCRP and caveolin-1 in these cells (87).

Bile salt transporter activity is modulated by cholesterol

The hepatocyte plasma membranes also contain lipid microdomains and they are involved in controlling bile secretion (88). Lipid rafts reside in both the basolateral and apical plasma membranes of hepatocytes and contain cholesterol and caveolin. There are, however, differences in the specific lipid content. The lipid rafts in the apical membrane contain higher amounts of gangliosides, whereas the basolateral lipid rafts are more enriched in sphingolipids. The cholesterol content is similar, but the apical rafts have a higher cholesterol/phospholipid ratio versus the non-raft portion of the apical membrane, while the basolateral rafts do not show such enrichment. This results in a higher density of basolateral rafts with a lower cholesterol:sphingolipid ratio and thus a reduced buoyancy in the flotation gradients than rafts isolated from the apical membrane (89).

The typical hepatic bile acid transporters Ntcp and Bsep, as well as several members of the Oatp superfamily were found in a proteome analysis of the lipid raft-enriched fraction from rat liver (90). More recently, Ntcp was indeed shown to be associated to (non-caveolar) lipid rafts in rat liver and its transport activity appears to be dependent on the membranous cholesterol content (91). Remarkably, the activity of Ntcp increased when cholesterol was depleted in an *in vitro* experiment using HEK293 cells with recombinant expression of Ntcp. Subsequent cholesterol repletion reduced the Ntcp transport activity back to control levels (91).
In addition, BSEP activity has recently been analyzed for its dependence on membranous cholesterol content, with opposite results compared to Ntcp. Human, rat and mouse BSEP/Bsep were expressed using the baculo virus system and the bile salt export activity increased upon cholesterol loading of the insect cell membrane vesicles. Cholesterol loading had the most potent effect on rat Bsep, where transport activities for TCA, GCA and TCDCA increased 3- to 5-fold. Interestingly, cholesterol loading had no significant effect on GCDCA transport (92).
The intestinal bile acid transporter ASBT has also been found to reside in lipid rafts in the apical membrane of enterocytes. Methyl-β-cyclodextrin-mediated cholesterol depletion abolished the ASBT lipid raft localization and reduced the sodium dependent taurocholate transport (93). As described above, cholesterol depletion increased the activity of NTCP, the closest homolog of ASBT. The effect of cholesterol on the activity of bile acid transporters may in fact be primarily dependent on the specific cellular membrane they reside in, as BSEP and ASBT both are located in the apical membrane and NTCP in the basolateral membrane.

Thus, all bile acid transporters for which a possible association to lipid rafts has been studied so far have been found to reside in such lipid rafts. Moreover, their transport activity is modulated by the membranous cholesterol content. The peroxisomal membrane also contains -yet to be identified- transporters for bile acid (intermediates). It seems likely that also peroxisomal bile acid transporters are

associated to some kind of lipid raft. However, prior to the studies in this thesis, peroxisomal lipid rafts had not been described yet. Two observations point toward the putative existence of peroxisomal lipid rafts: 1. the identification of lipid raft-like domains in the membrane of peroxisomes of the yeast *Yarrowia lipolytica* (94) and the presence of PMP70 (ABCD3) in the proteome analysis of the lipid raft-enriched fractions of rat liver (90).

This thesis therefore focused on two interrelated research questions:

1) do hepatocyte peroxisomes play a role in re-conjugation of C_{24} bile acids and thereby are an integral part of the enterohepatic cycle of bile acids?
2) do hepatocyte peroxisomes contain lipid rafts and what is their function?

In both research questions, we were particularly interested in PMP70 as this peroxisomal ABC transporter is a likely candidate to be a transporter for bile acid (intermediates).

Aim and outline of this thesis.

The aim of this thesis is to determine the role of hepatocyte peroxisomes in the enterohepatic cycling of bile acids and to identify and characterize the putative peroxisomal bile acid transporters involved.

In chapter 1, we provide the necessary background of the essential functions of the liver and in particular bile salt synthesis and transport. We introduce peroxisomes and their established function in bile acid synthesis. Moreover, we provide details of known peroxisomal substrate transporters and the relevance of specific lipid microdomains in the activity of bile acid transporters.

In chapter 2, we aim to develop a novel experimental procedure to study intracellular sorting and glycine/taurine conjugation of cholic acid in rat hepatocytes in order to establish a putative role of peroxisomes in this process. We make use of stable isotope-labeled CA (D_4CA) to be able to differentiate between endogenously produced CA and externally added CA by mass spectrometry, the latter representing the bile acids that return from the intestine to the liver.

In Chapter 3, we use the novel "CA-conjugation and intracellular transport assay" to study the putative role of PMP70 (ABCD3) in transporting bile acids into peroxisomes for glycine/taurine conjugation. Expression of PMP70 in primary hepatocytes is induced by the PPARα agonist fenofibric acid or inhibited by RNA interference and the effect on glycine/taurine conjugation and transcellular transport of CA is analyzed.

In chapter 4, we analyze the putative presence of lipid rafts in the peroxisomal membrane of HepG2 cells and rat hepatocytes, with particular focus on PMP70. Lipid rafts are isolated from HepG2 cells and rat hepatocytes after solubilization with Triton X-100 or Lubrol WX. In addition, they are analyzed for the presence of various peroxins and peroxisomal ABC transporters. Cholesterol depletion and repletion experiments are performed with HepG2 cells and the effect on subcellular location of peroxisomal membrane proteins and peroxisome biogenesis is analyzed.

In chapter 5, we further characterize peroxisomal lipid rafts and particularly focus on the putative presence of caveolin-1 therein. Livers from caveolin-1 knockout mice are analyzed for possible defects in peroxisome biogenesis.

In chapter 6, we provide an integrated discussion of the role of peroxisomes and peroxisomal lipid rafts in bile salt synthesis in the liver.

References

1. Russell DW. The Enzymes, Regulation, and Genetics of Bile Acid Synthesis. Annu Rev Biochem 2003; 72:137-74.
2. Hayashi H, Takada T, Suzuki H, Onuki R, Hofmann AF, Sugiyama Y. Transport by vesicles of glycine- and taurine-conjugated bile salts and taurolithocholate 3-sulfate: a comparison of human BSEP with rat Bsep. Biochim Biophys Acta. 2005 Dec 30;1738(1-3):54-62. Epub 2005 Nov 15.
3. Myant NB, Mitropoulos KA. Cholesterol 7Alpha-Hydroxylase. J. Lipid Res. 1977;18(2):135-153.
4. Pellicoro A, Faber KN. The function and regulation of proteins involved in bile salt biosynthesis and transport. Aliment Pharmacol Ther. (2007)
5. Falany CN, Johnson MR, Barnes S, Diasio RB. Glycine and taurine conjugation of bile acids by a single enzyme. Molecular cloning and expression of human liver bile acid CoA:amino acid N-acyltransferase. J Biol Chem 1994; 269:19375-9.
6. Hofmann AF. Bile Acids: The Good, the Bad, and the Ugly. News Physiol Sci 1999; 14:24-9.
7. Meier PJ, Stieger B. Bile salt transporters. Annu Rev Physiol 2002; 64:635-61.
8. Mikkaichi T, Suzuki T, Tanemoto M, Ito S, Abe T. The organic anion transporter (OATP) family. Drug Metab Pharmacokinet 2004; 19: 171–9.
9. Oude Elferink RP, Groen AK. Mechanisms of biliary lipid secretion and their role in lipid homeostasis. Semin Liver Dis. 2000;20(3):293-305.
10. Meier PJ, Stieger B. Molecular Mechanisms in Bile Formation. News Physiol Sci. 2000 Apr;15:89-93.
11. Li T, Chiang JY. Regulation of Bile Acid and Cholesterol Metabolism by PPARs. PPAR Res. 2009;2009:501739
12. Gerloff T, Stieger B, Hagenbuch B, et al. The sister of P-glycoprotein represents the canalicular bile salt export pump of mammalian liver. J Biol Chem 1998; 273: 10046–50.
13. Borst P, Elferink RO. Mammalian ABC transporters in health and disease. Annu Rev Biochem 2002; 71: 537–92.
14. Stieger B, Meier Y, Meier PJ. The bile salt export pump. Pflugers Arch-Eur J Physiol 2007; 453: 611–20.
15. Zelcer N, Saeki T, Bot I, Kuil A, Borst P. Transport of bile acids in multidrugresistance-protein 3-overexpressing cells co-transfected with the ileal Na+-dependent bile-acid transporter. Biochem J 2003; 369: 23–30.
16. Zelcer N, Reid G, Wielinga P, et al. Steroid and bile acid conjugates are substrates of human multidrug-resistance protein (MRP) 4 (ATP-binding cassette C4). Biochem J 2003; 371: 361–7.
17. Dawson PA, Hubbert M, Haywood J, et al. The heteromeric organic solute transporter alpha-beta, ost alpha-ost beta, is an ileal basolateral bile acid transporter. J Biol Chem 2005; 280:6960–8.
18. Keitel V, Burdelski M, Warskulat U, et al. Expression and localization of hepatobiliary transport proteins in progressive familial intrahepatic cholestasis. Hepatology 2005; 41: 1160–72.
19. Csanaky IL, Lu H, Zhang Y, Ogura K, Choudhuri S, Klaassen CD. Organic anion-transporting polypeptide 1b2 (Oatp1b2) is important for the hepatic uptake of unconjugated bile acids: Studies in Oatp1b2-null mice. Hepatology. 2011 Jan;53(1):272-81
20. Jason M. Ridlon, Dae-Joong Kang, and Phillip B. Hylemon Bile salt biotransformations by human intestinal bacteria J. Lipid Res. 2006. 47: 241–259.
21. Shneider BL, Dawson PA, Christie DM, Hardikar W, Wong MH, Suchy FJ. Cloning and molecular characterization of the ontogeny of a rat ileal sodium dependent bile-acid transporter. J Clin Invest 1995; 95: 745–54.
22. Inoue Y, Yu AM, Inoue J, Gonzalez FJ. Hepatocyte nuclear factor 4alpha is a central regulator of bile acid conjugation. J Biol Chem. 2004 Jan 23;279(4):2480-9.
23. Watkins PA. Very-long-chain acyl-CoA synthetases. J Biol Chem. 2008 Jan 25;283(4):1773-7.
24. Doege H, Baillie RA, Ortegon AM, Tsang B, Wu Q, Punreddy S, Hirsch D, Watson N, Gimeno RE, Stahl A. Targeted deletion of FATP5 reveals multiple functions in liver metabolism: alterations in hepatic lipid homeostasis. Gastroenterology. 2006 Apr;130(4):1245-58.
25. Van Mil SWC, Van Der Woerd WL, Van Der Brugge G, et al. Benign recurrent intrahepatic cholestasis type 2 is caused by mutations in ABCB11. Gastroenterology 2004; 127: 379–84.
26. Crawford AR, Smith AJ, Hatch VC, Oude Elferink RP, Borst P, Crawford JM. Hepatic secretion of phospholipid vesicles in the mouse critically depends on mdr2 or MDR3 P-glycoprotein expression. Visualization by electron microscopy. J Clin Invest 1997; 100:2562–7.
27. Smit JJ, Schinkel AH, Oude Elferink RP, et al. Homozygous disruption of the murine mdr2 P-glycoprotein gene leads to a complete absence of phospholipidfrom bile and to liver disease. Cell 1993; 75: 451–62.
28. Solaas K, Kase BF, Pham V, Bamberg K, Hunt MC, Alexson SE. Differential regulation of cytosolic and peroxisomal bile acid amidation by PPAR alpha activation favors the formation of unconjugated bile acids. J Lipid Res. 2004 Jun;45(6):1051-60.
29. Solaas K, Ulvestad A, Söreide O, Kase BF. Subcellular organization of bile acid amidation in human liver: a key issue in regulating the biosynthesis of bile salts. J Lipid Res. 2000 Jul;41(7):1154-62.
30. Deleuze JF, Jacquemin E, Dubuisson C, et al. Defect of multidrug-resistance 3 gene expression in a subtype of progressive familial intrahepatic cholestasis. Hepatology 1996; 23: 904–8.
31. Styles NA, Falany JL, Barnes S, Falany CN. Quantification and regulation of the subcellular distribution of bile acid coenzyme A:amino acid N-acyltransferase activity in rat liver. J Lipid Res. 2007 Jun;48(6):1305-15.
32. Buch C, Hunt MC, Alexson SE, Hallberg E. Localization of peroxisomal matrix proteins by photobleaching. Biochem Biophys Res Commun. 2009 Oct 16;388(2):355-9.
33. O'Byrne J, Hunt MC, Rai DK, Saeki M, Alexson SE. The human bile acid-CoA:amino acid N-acyltransferase functions in the conjugation of fatty acids to glycine. J Biol Chem. 2003 Sep 5;278(36):34237-44
34. Pellicoro A, van den Heuvel FA, Geuken M *et al.* Human and rat bile acid-CoA:amino acid N-acyltransferase are liver-specific peroxisomal enzymes: implications for intracellular bile salt transport. Hepatology. 2007 Feb;45(2):340-8.
35. Rembacz KP, Woudenberg J, Hoekstra M, Jonkers EZ, van den Heuvel FA, Buist-Homan M,

Woudenberg-Vrenken TE, Rohacova J, Marin ML, Miranda MA, Moshage H, Stellaard F, Faber KN. Unconjugated bile salts shuttle through hepatocyte peroxisomes for taurine conjugation. Hepatology. 2010 Dec;52(6):2167-76.
36. Visser W.F., van Roermund C.W., Ijlst L., Waterham H.R., Wanders R.J.: Demonstration of bile acid transport across the mammalian peroxisomal membrane. Biochem. Biophys. Res. Commun., 2007; 357: 335–340
37. Une M, Iguchi Y, Sakamoto T, Tomita T, Suzuki Y, Morita M, Imanaka T. ATP-dependent transport of bile acid intermediates across rat liver peroxisomal membranes. J Biochem. 2003 Aug;134(2):225-30
38. Steinberg SJ, Dodt G, Raymond GV, Braverman NE, Moser AB, Moser HW. Peroxisome biogenesis disorders. Biochimica et Biophysica Acta-Molecular Cell Research 2006; 1763(12):1733-1748.
39. Wanders RJA, Waterham HR. Peroxisomal disorders I: biochemistry and genetics of peroxisome biogenesis disorders. Clinical Genetics 2005; 67(2):107-133.
40. Wanders RJA, Waterham HR. Peroxisomal disorders: The single peroxisomal enzyme deficiencies. Biochimica et Biophysica Acta-Molecular Cell Research 2006; 1763(12):1707-1720.
41. Eyssen H, Parmentier G, Compernolle F, Boon J, Eggermont E Trihydroxycoprostanic acid in the duodenal fluid of two children with intrahepatic bile duct anomalies. Biochim Biophys Acta. 1972 Jun 26;273(1):212-21
42. Monnens L. [A patient with anemia, hemorrhagic diathesis and anuria] (Article in Dutch) Ned Tijdschr Geneeskd. 1980 Aug 9;124(32):1356-7
43. Hanson RF, Szczepanik-VanLeeuwen P, Williams GC, Grabowski G, Sharp HL. Defects of bile acid synthesis in Zellweger's syndrome. Science. 1979 Mar 16;203(4385):1107-8.
44. Wanders RJ, Casteels M, Mannaerts GP, van Roermund CW, Schutgens RB, Kozich V, Zeman J, Hyanek J. Accumulation and impaired in vivo metabolism of di- and trihydroxycholestanoic acid in two patients. Clin Chim Acta. 1991 Oct 31;202(3):123-32.
45. Bootsma AH, Overmars H, van Rooij A, van Lint AE, Wanders RJ, van Gennip AH, Vreken P. Rapid analysis of conjugated bile acids in plasma using electrospray tandem mass spectrometry: application for selective screening of peroxisomal disorders. J Inherit Metab Dis. 1999 May;22(3):307-10.
46. Ferdinandusse S, Overmars H, Denis S, Waterham HR, Wanders RJ, Vreken P. Plasma analysis of di- and trihydroxycholestanoic acid diastereoisomers in peroxisomal alpha-methylacyl-CoA racemase deficiency. J Lipid Res. 2001 Jan;42(1):137-41.
47. Keane MH, Overmars H, Wikander TM, Ferdinandusse S, Duran M, Wanders RJ, Faust PL. Bile acid treatment alters hepatic disease and bile acid transport in peroxisome-deficient PEX2 Zellweger mice. Hepatology. 2007 Apr;45(4):982-97.
48. Carlton VE, Harris BZ, Puffenberger EG, Batta AK, Knisely AS, Robinson DL, Strauss KA, Shneider BL, Lim WA, Salen G, Morton DH, Bull LN. Complex inheritance of familial hypercholanemia with associated mutations in TJP2 and BAAT. Nat Genet. 2003 May;34(1):91-6.
49. Barbarito E, Batta AK, Salen G, Morton HD., Carlton V, Bull LN, Shneider BL. High serum and urinary unconjugated bile acid concentrations are associated with homozygous mutation in bile acid coenzyme A: Amino acid N-acyltransferase (BAAT). Gastroenterology 2003;124(4); supplement 1:A60
50. Rippin SJ, Hagenbuch B, Meier PJ, Stieger B. Cholestatic expression pattern of sinusoidal and canalicular organic anion transport systems in primary cultured rat hepatocytes. Hepatology 2001; 33(4):776-782.
51. Distel,B., Erdmann,R., Gould,S.J., Blobel,G., Crane,D.I., Cregg,J.M., Dodt,G., Fujiki,Y., Goodman,J.M., Just,W.W., Kiel,J.A., Kunau,W.H., Lazarow,P.B., Mannaerts,G.P., Moser,H.W., Osumi,T., Rachubinski,R.A., Roscher,A., Subramani,S., Tabak,H.F., Tsukamoto,T., Valle,D., van der Klei,I., Van Veldhoven,P.P., Veenhuis,M. Unified nomenclature for peroxisome biogenesis factors. Journal of Cell Biology 1996; 135(1):1-3.
52. Wanders RJA, Visser WF, van Roermund CW, Kemp S, Waterham HR. The peroxisomal ABC transporter family. Pflugers Arch. 2007 Feb;453(5):719-34.
53. Guimarães CP, Domingues P, Aubourg P, Fouquet F, Pujol A, Jimenez-Sanchez G, Sá-Miranda C, Azevedo JE. Mouse liver PMP70 and ALDP: homomeric interactions prevail in vivo. Biochim Biophys Acta. 2004 Aug 4;1689(3):235-43.
54. Kamijo K, Taketani S, Yokota S, Osumi T, Hashimoto T The 70-kDa peroxisomal membrane protein is a member of the Mdr (P-glycoprotein)-related ATP-binding protein superfamily. J Biol Chem. 1990; 265:4534–4540.
55. Kamijo K, Kamijo T, Ueno I, Osumi T, Hashimoto T. Nucleotide sequence of the human 70 kDa peroxisomal membrane protein: a member of ATP-binding cassette transporters. Biochim Biophys Acta 1992; 1129:323–327.
56. J. Mosser, A.M. Douar, C.O. Sarde, P. Kioschis, R. Feil, H. Moser, A.M. Poustka, J.L. Mandel, P. Aubourg, Putative X-linked adrenoleukodystrophy gene shares unexpected homology with ABC transporters, Nature 1993; 361:726– 730.
57. G. Lombard-Platet, S. Savary, C.O. Sarde, J.L. Mandel, G. Chimini, A close relative of the adrenoleukodystrophy (ALD) gene codes for a peroxisomal protein with a specific expression pattern, Proc. Natl. Acad. Sci. U. S. A. 1996; 93:1265–1269.
58. A. Holzinger, S. Kammerer, A.A. Roscher, Primary structure of human PMP69, a putative peroxisomal ABC-transporter, Biochem. Biophys. Res. Commun. 237 (1997) 152–157.
59. N. Shani, G. Jimenez-Sanchez, G. Steel, M. Dean, D. Valle, Identification of a fourth half ABC transporter in the human peroxisomal membrane, Hum. Mol. Genet. 6 (1997) 1925–1931.
60. Braiterman LT, Zheng S, Watkins PA, Geraghty MT, Johnson G, McGuinness MC, Moser AB, Smith KD. Suppression of peroxisomal membrane protein defects by peroxisomal ATP binding cassette (ABC) proteins. Hum Mol Genet. 1998 Feb;7(2):239-47.
61. Kemp S, Wei HM, Lu JF, Braiterman LT, McGuinness MC, Moser AB, Watkins PA, Smith KD. Gene redundancy and pharmacological gene therapy: implications for X-linked adrenoleukodystrophy. Nat Med. 1998; 4:1261–1268
62. Flavigny E, Sanhaj A, Aubourg P, Cartier N. Retroviral mediated adrenoleukodystrophy-related gene transfer corrects very long chain fatty acid metabolism in adrenoleukodystrophy fibroblasts:

implications for therapy. FEBS Lett 1999; 448:261–264
63. Netik A, Forss-Petter S, Holzinger A, Molzer B, Unterrainer G, Berger J. Adrenoleukodystrophy-related protein can compensate functionally for adrenoleukodystrophy protein deficiency (X-ALD): implications for therapy. Hum Mol Genet 1999; 8:907–913.
64. Imanaka T, Aihara K, Takano T, Yamashita A, Sato R, Suzuki Y, Yokota S, Osumi T. Characterization of the 70-kDa peroxisomal membrane protein, an ATP binding cassette transporter. J Biol Chem. 1999 Apr 23;274(17):11968-76.
65. Visser, W. F., van Roermund, C. W., Waterham, H. R. & Wanders, R. J. Identification of human PMP34 as a peroxisomal ATP transporter. *Biochem. Biophys. Res. Commun.* 2002; 299, 494-497.
66. Hartl, F. U. & Just, W. W. Integral membrane polypeptides of rat liver peroxisomes: topology and response to different metabolic states. *Arch. Biochem. Biophys.* 1987; 255, 109-119.
67. Iida, R. *et al.* Human Mpv17-like protein is localized in peroxisomes and regulates expression of antioxidant enzymes. *Biochem. Biophys. Res. Commun.* 2006; 344, 948-954.
68. Sinal CJ, Yoon M, Gonzalez FJ. Antagonism of the actions of peroxisome proliferator-activated receptor-alpha by bile acids. J Biol Chem. 2001 Dec 14;276(50):47154-62
69. Issemann, I. & Green, S. Activation of a member of the steroid hormone receptor superfamily by peroxisome proliferators. Nature 347, 645-650 (1990).
70. Forman BM, Chen J, Evans RM. The peroxisome proliferator-activated receptors: ligands and activators. Ann N Y Acad Sci. 1996 Dec 27;804:266-75.
71. Li,X., Baumgart,E., Dong,G.X., Morrell,J.C., Jimenez-Sanchez,G., Valle,D., Smith,K.D., & Gould,S.J. PEX11alpha is required for peroxisome proliferation in response to 4-phenylbutyrate but is dispensable for peroxisome proliferator-activated receptor alpha-mediated peroxisome proliferation. Mol Cell Biol. 22, 8226-8240 (2002).
72. Abe I, Okumoto K, Tamura S, Fujiki Y. Clofibrate-inducible, 28-kDa peroxisomal integral membrane protein is encoded by PEX11. FEBS Lett. 1998 Jul 24;431(3):468-72.
73. Erdmann, R., Blobel, G. Giant peroxisomes in oleic acid-induced Saccharomyces cerevisiae lacking the peroxisomal membrane protein Pmp27p. J. Cell Biol. 128, 509-523 (1995).
74. Hunt MC, Yang YZ, Eggertsen G, Carneheim CM, Gåfvels M, Einarsson C, Alexson SE. The peroxisome proliferator-activated receptor alpha (PPARalpha) regulates bile acid biosynthesis. J Biol Chem. 2000 Sep 15;275(37):28947-53.
75. Berger J, Albet S, Bentejac M, Netik A, Holzinger A, Roscher AA, Bugaut M, Forss-Petter S. The four murine peroxisomal ABC-transporter genes differ in constitutive, inducible and developmental expression. Eur J Biochem. 1999 Oct;265(2):719-27.
76. Albet S, Causeret C, Bentejac M, Mandel JL, Aubourg P, Maurice B. Fenofibrate differently alters expression of genes encoding ATP-binding transporter proteins of the peroxisomal membrane. FEBS Lett. 1997 Apr 1;405(3):394-7.
77. Fourcade S, Savary S, Albet S, Gauthé D, Gondcaille C, Pineau T, Bellenger J, Bentejac M, Holzinger A, Berger J, Bugaut M. Fibrate induction of the adrenoleukodystrophy-related gene (ABCD2): promoter analysis and role of the peroxisome proliferator-activated receptor PPARalpha. Eur J Biochem. 2001 Jun;268(12):3490-500.
78. Kok T, Bloks VW, Wolters H, Havinga R, Jansen PL, Staels B, Kuipers F. Peroxisome proliferator-activated receptor alpha (PPARalpha)-mediated regulation of multidrug resistance 2 (Mdr2) expression and function in mice. Biochem J. 2003 Feb 1;369(Pt 3):539-47.
79, Hayhurst GP, Lee YH, Lambert G, Ward JM, Gonzalez FJ. Hepatocyte nuclear factor 4alpha (nuclear receptor 2A1) is essential for maintenance of hepatic gene expression and lipid homeostasis. Mol Cell Biol. 2001 Feb;21(4):1393-403.
80. Mayor S, Rao M. Rafts: scale-dependent, active lipid organization at the cell surface. Traffic. 2004 Apr;5(4):231-40.
81. Brown DA, London E. Functions of lipid rafts in biological membranes. Annu Rev Cell Dev Biol. 1998;14:111-36.
82. Simons K, Ikonen E. Functional rafts in cell membranes. Nature. 1997 Jun 5;387(6633):569-72.
83. Simons K, Gerl MJ. Revitalizing membrane rafts: new tools and insights. Nat Rev Mol Cell Biol. 2010 Oct;11(10):688-99.
84. Chidlow JH Jr, Sessa WC. Caveolae, caveolins, and cavins: complex control of cellular signalling and inflammation. Cardiovasc Res 2010;86:219–25.
85. Fernández MA, Albor C, Ingelmo-Torres M, Nixon SJ, Ferguson C, Kurzchalia T, Tebar F, Enrich C, Parton RG, Pol A. Caveolin-1 is essential for liver regeneration. Science. 2006 Sep 15;313(5793):1628-32.
86. Troost J, Lindenmaier H, Haefeli WE, Weiss J. Modulation of cellular cholesterol alters P-glycoprotein activity in multidrug-resistant cells. Mol Pharmacol. 2004 Nov;66(5):1332-9.
87. Storch CH, Ehehalt R, Haefeli WE, Weiss J. Localization of the human breast cancer resistance protein (BCRP/ABCG2) in lipid rafts/caveolae and modulation of its activity by cholesterol in vitro. J Pharmacol Exp Ther. 2007 Oct;323(1):257-64.
88. Tietz P, Jefferson J, Pagano R, Larusso NF. Membrane microdomains in hepatocytes: potential target areas for proteins involved in canalicular bile secretion. J Lipid Res. 2005 Jul;46(7):1426-32.
89. Mazzone A, Tietz P, Jefferson J, Pagano R, LaRusso NF. Isolation and characterization of lipid microdomains from apical and basolateral plasma membranes of rat hepatocytes. Hepatology. 2006 Feb;43(2):287-96.
90. Bae TJ, Kim MS, Kim JW, Kim BW, Choo HJ, Lee JW, Kim KB, Lee CS, Kim JH, Chang SY, Kang CY, Lee SW, Ko YG. Lipid raft proteome reveals ATP synthase complex in the cell surface. Proteomics. 2004 Nov;4(11):3536-48.
91. Molina H, Azocar L, Ananthanarayanan M, Arrese M, Miquel JF. Localization of the Sodium-Taurocholate cotransporting polypeptide in membrane rafts and modulation of its activity by cholesterol in vitro. Biochim Biophys Acta. 2008 May;1778(5):1283-91.
92. Kis E, Ioja E, Nagy T, Szente L, Herédi-Szabó K, Krajcsi P. Effect of membrane cholesterol on BSEP/Bsep activity: species specificity studies for substrates and inhibitors. Drug Metab Dispos. 2009 Sep;37(9):1878-86.
93. Annaba F, Sarwar Z, Kumar P, Saksena S, Turner JR, Dudeja PK, Gill RK, Alrefai WA. Modulation of

ileal bile acid transporter (ASBT) activity by depletion of plasma membrane cholesterol: association with lipid rafts. Am J Physiol Gastrointest Liver Physiol. 2008 Feb;294(2):G489-97.
94. Boukh-Viner T, Guo T, Alexandrian A, Cerracchio A, Gregg C, Haile S, Kyskan R, Milijevic S, Oren D, Solomon J, Wong V, Nicaud JM, Rachubinski RA, English AM, Titorenko VI. Dynamic ergosterol- and ceramide-rich domains in the peroxisomal membrane serve as an organizing platform for peroxisome fusion. J Cell Biol. 2005 Feb 28;168(5):761-73.

CHAPTER 2

Unconjugated bile salts shuttle through hepatocyte peroxisomes for taurine conjugation.

Krzysztof P. Rembacz[1], Jannes Woudenberg[1,], Mark Hoekstra[1], Elles Z. Jonkers[2], Fiona A.J. van den Heuvel[1], Manon Buist-Homan[1], Titia E. Woudenberg-Vrenken[1], Jana Rohacova[3], M. Luisa Marin[3], Miguel A. Miranda[3], Han Moshage[1], Frans Stellaard[2], Klaas Nico Faber[1]

[1]Department of Gastroenterology and Hepatology, University Medical Center Groningen, University of Groningen, Groningen, The Netherlands
[2]Department of Laboratory Medicine, University Medical Center Groningen, University of Groningen, Groningen, The Netherlands
[3]Instituto de Tecnología Química, Departamento de Química (UPV-CSIC), Valencia, Spain

Hepatology. 2010 Dec;52(6):2167-76

Unconjugated bile salts shuttle through hepatocyte peroxisomes for taurine conjugation

ABSTRACT

Introduction: Bile acid-CoA:amino acid N-acyltransferase (Baat) conjugates bile salts to glycine or taurine, which is the final step in bile salt biosynthesis. In addition, Baat is required for reconjugation of bile salts in the enterohepatic circulation. Recently, we showed that Baat is a peroxisomal protein, implying shuttling of bile salts through peroxisomes for reconjugation. However, the subcellular location of Baat remains a topic of debate. The aim of this study was to obtain direct proof for reconjugation of bile salts in peroxisomes.

Methods: Primary rat hepatocytes were incubated with deuterium-labeled cholic acid (D_4CA). Over time, media and cells were collected and the levels of D_4CA, D_4-tauro-CA (D_4TCA) and D_4-glyco-CA (D_4GCA) were quantified by liquid chromatography-tandem mass spectrometry (LC/MS/MS). Subcellular accumulation of D_4-labeled bile salts was analyzed by digitonin permeabilization assays and subcellular fractionation experiments.

Results: Within 24 hours, cultured rat hepatocytes efficiently (> 90%) converted and secreted 100 µM D_4CA to D_4TCA and D_4GCA. The relative amounts of D_4TCA and D_4GCA produced were dependent on the presence of glycine or taurine in the medium. Treatment of D_4CA-exposed hepatocytes with 30-150 µg/ml digitonin led to the complete release of D_4CA, D_4GCA and Gapdh (cytosolic marker). Full release of D_4TCA, catalase and Baat was only observed at 500 µg/ml digitonin, indicating the presence of D_4TCA in membrane-enclosed organelles. D_4TCA was detected in fractions of purified peroxisomes, which did not contain D_4CA and D_4GCA.

Conclusion: We established a novel assay to study conjugation and intra- and trans-cellular transport of bile salts. Using this assay, we show that cholic acid shuttles through peroxisomes for taurine-conjugation.

INTRODUCTION

Bile salts are synthesized in the liver and are the driving force of bile flow. Bile is crucial for intestinal absorption of fats and fat-soluble vitamins, as well as the elimination of excess cholesterol and waste products from the body. In the terminal ileum, 90-95% of the bile salts are reabsorbed and transported back to the liver. Import and export of bile salts in hepatocytes and enterocytes is mediated by well-characterized transmembrane substrate transporters (1).

Fecal loss of bile salts is compensated by de novo bile salt synthesis in the liver. Hepatic bile salt synthesis involves at least 13 different enzymes that are located in different subcellular compartments, including the endoplasmic reticulum (ER), mitochondria, peroxisomes and the cytosol. Bile salts are made from cholesterol and this requires three key modifications of the cholesterol backbone: (1) hydroxylation of the steroid nucleus, (2) shortening of the side chain and (3) conjugation/amidation of glycine or taurine to the side chain. The last two modifications take place in peroxisomes (2). Bile acid-coenzyme A:amino acid N-acyltransferase (BAAT) catalyzes the third and final modification of bile salts before they enter the enterohepatic cycle (3).

The activity of BAAT remains crucial also during enterohepatic cycling of bile salts. A significant portion of bile salts is deconjugated by intestinal bacteria. Approximately one-third of the bile salt pool may undergo deconjugation on a daily basis in healthy humans (4). Still, unconjugated bile salts are also reabsorbed in the enterohepatic circulation and transported back to the liver. However, the fraction of unconjugated bile salts in the total bile salt pool is very low, indicating an efficient reconjugation process. The efficiency of bile salt reconjugation is further stressed by the fact that over 97% of the therapeutic bile salt ursodeoxycholate (UDCA) is conjugated to taurine or glycine after a single pass through isolated perfused rat livers (5).

Unconjugated bile salts are first activated with coenzyme A (CoA) by the fatty acid transport protein 5 (FATP5; *SLC27A5*), which is located at the basolateral membrane of hepatocytes (6, 7). Next, the CoA-activated C_{24}-bile salts are the substrate for BAAT. It has been postulated that a cytosolic pool of BAAT is responsible for reconjugating the recycling pool of unconjugated bile salts (8-10). However, we recently applied digitonin permeabilization assays and immunofluorescence microscopy on endogenous and GFP-tagged human BAAT/rat Baat and found that it is predominantly, if not solely, present in peroxisomes of hepatocytes (11). An exclusive peroxisomal location of BAAT implies that CoA-activated unconjugated bile acids need to be transported into peroxisomes, followed by glycine/taurine conjugation and export out of these organelles, a yet unexplored bile salt transport process.

In this study, we sought further proof for the transit of unconjugated bile salts through peroxisomes. For that purpose, we established a novel assay that allows the detection of (un)conjugated bile salts in peroxisomes. Rat hepatocytes were exposed to deuterated cholic acid (D_4CA). Over time, the concentrations of taurine-

and glycine-conjugated D_4CA in cells and medium were determined. At peak intracellular accumulation of D_4TCA and D_4GCA, digitonin permeabilization assays and cell fractionation experiments were performed. Our data show for the first time that unconjugated bile salts shuttle through peroxisomes to become conjugated to taurine.

EXPERIMENTAL PROCEDURES

Animals
Specified pathogen-free male Wistar rats (220–250 g; Charles River Laboratories Inc., Wilmington, MA, USA) were housed under standard laboratory conditions with free access to standard laboratory chow and water. Experiments were performed following the guidelines of the local Committee for Care and Use of laboratory animals.

Primary cells and culture conditions
Rat hepatocytes were isolated and cultured in William's medium E in a humidified incubator at 37 °C and 5% CO2, as described previously (12). In selected experiments (see below), hepatocytes were cultured in minimal essential medium (MEM, Invitrogen, Breda, The Netherlands). Hepatocyte viability and purity were over 90%.

Uptake and conversion of deuterated cholic acid by primary rat hepatocytes
Primary rat hepatocytes were plated at a density of 1.0 x 105 cells/cm2. After a 24 hour attachment period, cells were incubated with 25, 100 or 300 µM [2,2,4,4-D]Cholic acid (D_4CA; isotopic purity 98%, ISOTEC, Miamisburg, OH, USA) for 0 to 24 h. For taurine or glycine conjugation preference assays, hepatocytes were cultured in MEM, supplemented with 666 µM glycine (Sigma-Aldrich, St. Louis, MO, USA) and/or 666 µM taurine (Sigma-Aldrich) in the presence of 100 µM D4CA. At indicated time points, media and cells were collected followed by subcellular fractionation or immediate storage at -20^{o} C.

Subcellular fractionation and isolation of peroxisomes
The subcellular fractionation and isolation of peroxisomes from rat liver was performed essentially as described previously (13) using PEG1500-containing homogenization buffer (isolation medium-3). Peroxisomes were purified from the 500 x g supernatant (post-nuclear supernatant-PNS) using Nycodenz density gradient centrifugation according to the method described by Verheyden et al. (14). 12 mL PNS was loaded on top of a discontinuous Nycodenz gradient (2mL 56%, 3 mL 45% , 15 mL 30% and 5 mL 18%) and spun in a vertical rotor (Sorvall, SV288, Thermo Fisher Scientific, Waltham, MA, USA) at 20,000 rpm for 2 hours at 4 °C in a slow acceleration/deceleration mode. Equal volumes of all supernatants, pellets

and gradient fractions were analyzed by western blotting or were further purified for mass spectrometry.

Digitonin Assay
Digitonin assays were performed essentially as described before (11), with the basic difference that digitonin treatments were performed on rat hepatocytes attached to collagen-coated culture discs in stead of treated in suspension. Equal volumes of supernatant and pellet fractions were analyzed by western blotting or further processed for mass spectrometry.

Quantification of cell death.
Apoptotic cell death was visualized by acridine orange nuclear staining (15) and quantified by determining caspase-3 activity (16). The arbitrary fluorescence unit (AFU) was corrected for the amount of total protein in the cell lysate. Necrotic cell death was quantified by determining lactate dehydrogenase (LDH) leakage (17) and Sytox green® (Invitrogen) according to the suppliers' protocol.

SDS-PAGE and western blotting.
Protein samples were separated by SDS-PAGE and analyzed by western blotting according to established procedures (11). Protein concentrations were determined using the Bio-Rad Protein Assay system (Bio-Rad, Hercules, CA, USA) using bovine serum albumin as standard. Primary antibody dilutions used in this study are shown in Supplementary Table S1. Proteins signals were detected and quantified in a ChemiDoc XRS system (Bio-Rad). Protein band intensities were quantified using Quantity One software (Bio-Rad).

Purification of bile salts for mass spectrometry
Media samples (0.1-1.5 mL) from D_4CA-exposed hepatocytes were collected at indicated time points and diluted 1,000-fold in an internal standard (IS) solution (containing 100 ng/mL each of CA, TCA and GCA in H2O). Hepatocytes were washed twice in 1x ice-cold Hank's buffered salt solution (HBSS; Invitrogen), scraped in 250 µL 75% (v/v) methanol and 1,000-fold diluted in IS solution. Digitonin assay samples (1 mL, both representing supernatant and pellet fraction) were diluted 200-fold in IS solution. Nycodenz gradient fractions were 1,000-fold diluted in IS solution. Total bile salts were purified using reversed phase C18 columns (Sep-Pak C18 cartridge; Waters, Milford, MA, USA) as described before (18).

LC/MS/MS analysis of bile salts
A detailed description of the LC/MS/MS analysis of bile salts is given in the supplementary Material and Methods. In short, LC/MS/MS analysis was performed using a triple quadrupole mass spectrometer API 3000 (Applied Biosystems, Foster City, CA, USA) using ESI ionization in the negative mode. CA and D_4CA were detected using single ion monitoring at m/z 407 and m/z 411,

respectively. Detection of GCA, D_4GCA, TCA and D_4TCA was performed using the selected reaction-monitoring mode. Two LC-200 HPLC pumps (Perkin-Elmer, Waltham, MA, USA) coupled to a series 200 autosampler (Perkin-Elmer) were used. Chromatography was performed with a Luna C18(2) (Phenomenex, Torrance, CA, USA) analytical column (50x2.0 mm; particle size 3 µm).

Calculation and interpretation of LC/MS/MS data
The peak area for the D_4-labelled bile salt was determined and related to the corresponding unlabeled bile salt added as IS. This ratio was corrected for the natural isotope abundance of the IS. For the calculation of intracellular bile salt concentrations, the cellular volume of one million hepatocytes was set at 20 µL, being the higher limit of estimations reported by others (19-24).

Statistical analysis
All numerical results are reported as the mean of at least 3 independent experiments ± standard error of the mean.

RESULTS

In vitro cultured rat hepatocytes efficiently convert exogenously added cholate to taurocholate and glycocholate

We first determined the rate and specificity by which primary rat hepatocytes convert exogenously added cholic acid (CA) to taurocholic acid (TCA) and/or glycocholic acid (GCA). 24 h-attached hepatocytes were exposed to various concentrations deuterated CA (25, 100 and 300 µM D_4CA; Fig. 1. left, middle and right panels, respectively). Media (Fig. 1A) and cells (Fig. 1B) were collected after 3 and 24 h of incubation. D_4TCA and D_4GCA and the input-bile salt (D_4CA) were readily detectable in the medium after 3 h of incubation (Fig. 1A). D_4CA concentrations were below input levels (7, 60 and 225 µM for the input of 25, 100 and 300 µM, respectively). The presence of D_4TCA (6, 10 and 10 µM, respectively) and D_4GCA (6, 15 and 15 µM, respectively) in the medium after 3 h exposure time indicates that D_4CA is taken up, CoA-activated, taurine/glycine conjugated by and exported from the hepatocytes. After 24 h, D_4CA was absent in medium of cells exposed to 25 µM (Fig 1A,B. left panels). Instead, D_4TCA (12 µM) and D_4GCA (10 µM) were detected in these samples. Only small amounts (5 µM) of D_4CA were detected in the medium of hepatocytes exposed to 100 uM D_4CA for 24 h, which was effectively converted to D_4TCA (23 µM) and D_4GCA (68 µM) (Fig. 1A. middle panel). After 24 h-exposure of hepatocytes to 300 µM D_4CA, 70 µM D_4CA, 40 µM D_4TCA and 160 µM D_4GCA were detected in the medium (Fig. 1A. right panel).

Intracellular accumulation of taurocholate and glycocholate in cholate-exposed rat hepatocytes

Simultaneously with the media samples, hepatocytes were harvested in order to determine intracellular bile salt accumulation (Fig. 1B). After 3 hours exposure to

D_4CA, a large intracellular accumulation of conjugated D_4-labelled bile salts was detected. D_4TCA concentrations were approximately 200 µM for all 3 conditions, while D_4GCA levels (120, 400 and 600 µM, respectively) were dependent on the D_4CA input concentration (25, 100, 300 µM, respectively. Fig 1B. left, middle and right panel, respectively. D_4CA was undetectable in cells exposed to 25 µM D_4CA, while the cellular concentrations of this bile salt (80 and 310 µM, respectively) were close to the input levels of the other conditions (100 and 300 µM, respectively). After 24 h, the cellular concentrations of all these bile salts were strongly reduced again (Fig. 1B).

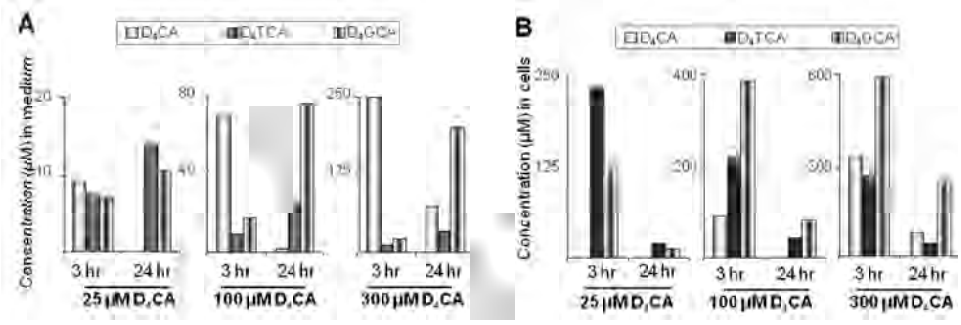

Figure 1. Unconjugated bile acids are efficiently converted by rat hepatocytes to their taurine and glycine conjugates *in vitro*. Primary rat hepatocytes were incubated with either 25, 100 or 300 µM D_4CA for 3 or 24 h. At indicated time points, media (A) and cells (B) were collected and the concentrations of D_4CA, D_4TCA and D_4GCA determined by mass spectrometry. Representative data from 3 independent experiments are shown.

To study the dynamic changes in intracellular and extracellular D_4-bile salts, hepatocytes were exposed to 100 µM D4CA and medium and hepatocytes were harvested at additional time points from 5 minutes to 24 h (Fig. 2). Medium concentrations of conjugated D_4-bile salts steadily increased in the first 4 h (10 µM D_4TCA and 21 µM D_4GCA) (Fig. 2A).

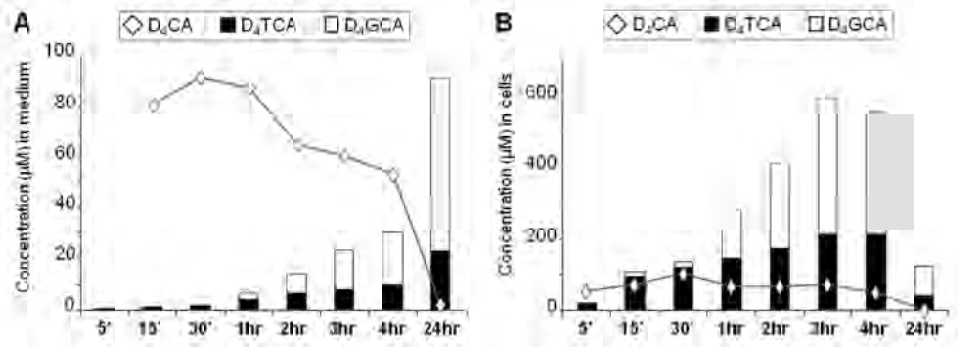

Figure 2. Transient accumulation of conjugated bile salts after exposure to D_4CA. Primary rat hepatocytes were exposed to 100 µM D_4CA and medium (A) and cells (B) were harvested at time points from 5 minutes to 24 h, followed by bile salt purification and analysis as in Fig. 1.

Almost complete conversion of D_4CA to D_4TCA and D_4GCA was detected after 24 h. Maximum intracellular accumulation of D_4TCA (200 µM) and D_4GCA (400 µM) was detected after 3 h exposure to D_4CA. Notably, in the first hour, only D_4TCA was detected in the medium and hepatocytes, while D_4GCA started to appear after 1 h and increased to higher levels compared to D_4TCA (Fig. 2).

D_4CA does not induce cell death in cultured rat hepatocytes

Specific bile salts may be toxic for hepatocytes inducing either apoptotic or necrotic cell death (25)). We analyzed the caspase-3 activity in cultured rat hepatocytes exposed to 100 µM D_4CA (Fig. 3A). After 3 hours of incubation with 100 µM D_4CA, we observed no significant increase in caspase-3 activity, while 50 µM glycochenodeoxycholic acid (GCDCA) induced a very strong apoptotic response (13-fold induction). In line with these findings, many apoptotic cells were detected after 24 h GCDCA exposure by acridine orange staining, which were absent in de D_4CA-exposed hepatocyte cultures (Fig. 3C). In addition, no cellular leakage of LDH was observed in hepatocytes treated for 4 h with 100 µM D_4CA indicating that no significant induction of necrotic cell death had occurred (Fig. 3B). These findings were confirmed by Sytox green® staining (see Supplementary Fig. S1).

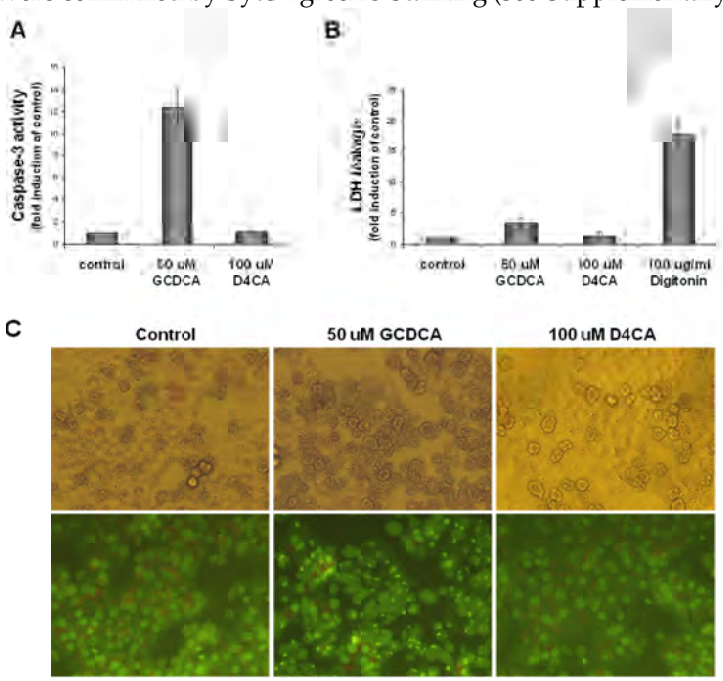

Figure 3. Incubation of rat hepatocytes with 100 µM D_4CA does not induce apoptosis or necrosis. Primary rat hepatocytes were incubated with either 100 µM D_4CA or 50 µM GCDCA for 3 h followed by caspase-3 activity measurements in total cell lysates (A) or LDH activity measurements in the medium (B). Treatment with 100 µg/ml digitonin was used as positive control for LDH leakage. Results are presented as fold induction compared to untreated control hepatocytes, which are set to 1. In addition, hepatocytes exposed for 24 h to 50 uM GCDCA or 100 uM D_4CA were stained using acridine orange to detect condensed nuclei, characteristic of apoptotic cells (C, top panels: bright field image, bottom panels: fluorescence image).

Taurine is the preferred substrate for conjugation to cholate in rat hepatocytes

Taurine-conjugated bile salts predominate in the bile salt pool of rats. The standard culture medium for rat hepatocytes (Williams' E medium) contains high concentrations of glycine (666 µM) with no additional taurine present, which may result in the high D_4GCA formation, especially at later time points. To determine whether the presence of glycine and taurine in the medium affects D_4TCA and/or D_4TCA production, we exposed rat hepatocytes for 24 h to 100 µM D_4CA in minimal medium with or without 666 µM glycine and/or 666 µM taurine (Fig. 4). Excess of either glycine or taurine in the culture medium leads to a concomitant D_4GCA and D_4TCA production, respectively, both extracellularly (Fig. 4A) and intracellularly (Fig. 4B). When both glycine and taurine are present in excess in the medium, D_4CA was predominantly converted to D_4TCA (70 µM, compared to only 2 µM D_4GCA).

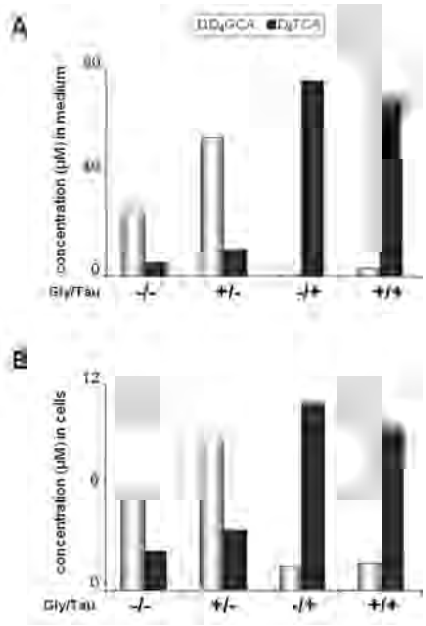

Figure 4. Rat hepatocytes prefer taurine over glycine as a substrate for bile salt conjugation. Primary rat hepatocytes were incubated for 24 h with D_4CA in Minimal Essential Medium in the absence or presence of 666 µM taurine and/or glycine. Media (A) and cells (B) were collected, followed by bile salt purification and analysis as in Fig. 1.

Selective membrane permeabilization of rat hepatocytes reveals peroxisomes as bile salt accumulation sites

Peak accumulation of D_4TCA (200 µM) and D_4GCA (400 µM) in hepatocytes was observed after a 3 h exposure to D_4CA (Fig 2). Hepatocytes exposed to these conditions were analyzed by digitonin permeabilization assays to determine whether D_4-labelled bile salts accumulate in membrane-enclosed intracellular compartments. Low concentrations of digitonin (30 µg/mL) disrupt the plasma membrane and cytosolic components are effectively released from the cellular fraction (Fig. 5A; Gapdh is shown as a cytosolic marker protein, quantification in 5B). D_4CA and D_4GCA are fully released from hepatocytes at this concentration (Fig. 5B, shown only for D_4CA). The peroxisomal membrane is more resistant to digitonin permeabilization and is only fully permeabilized at 500 µg/mL. Partial release of the peroxisomal marker proteins catalase and Baat is observed at digitonin concentrations of 30 and 150 µg/mL (Fig. 5A, quantification in 5B). The digitonin-extractability of D_4TCA lies in between the profile for Gapdh/D_4CA and catalase (Fig. 5B), suggesting that D_4TCA accumulates, at least partly, in membrane-enclosed organelles with peroxisomal characteristics.

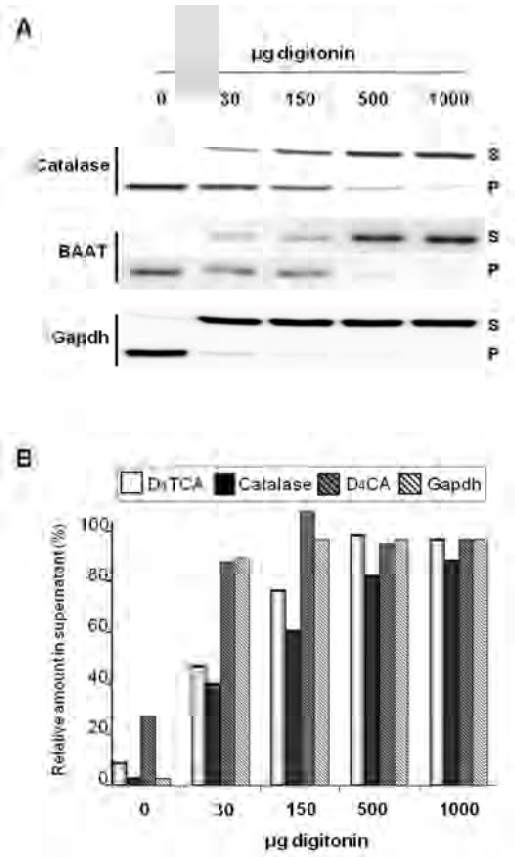

Figure 5. Digitonin-mediated membrane permeabilization of rat hepatocytes reveals peroxisomes as bile salt accumulation sites. Primary rat hepatocytes were incubated with 100 µM D_4CA for 3 h. Subsequently, hepatocytes were exposed to increasing concentrations of digitonin. Equal volumes of supernatant (S) and pellet fractions (P) were analyzed by western blotting using specific antibodies against the cytosolic marker Gapdh and the peroxisomal markers catalase and Baat (A; quantification of the Gapdh and Baat signal intensities is included in Fig. 5B) or collected for bile salt purification and analysis by mass spectrometry (B). For quantification, the cumulative (arbitrary) units for western blot signals or MS peak intensities detected in the supernatant and the pellet fraction was set to 100 for every digitionin-extraction condition. The relative amount detected in the supernatant fractions is given. Representative data from 3 independent experiments are shown.

D_4TCA is detected in peroxisomes of D_4CA-exposed hepatocytes

To obtain further evidence for the accumulation of D_4TCA in peroxisomes, we purified these organelles from a post-nuclear supernatant (PNS) fraction of D_4CA-exposed rat hepatocytes (Fig. 6). After Nycodenz density gradient centrifugation of the PNS, all 20 gradient fractions were analyzed for the presence of D_4TCA, D_4CA and markers for various cellular compartments. A PMP70/Baat-enriched peak was detected at high density fractions 3-5, separated from mitochondria (Cyt C; fractions 10-11) and cytosol (Gapdh; fractions 15-20) (Fig. 6A). Highest concentrations of D_4TCA were detected at the top of the gradient (Fig. 6B). In addition, minor but significant amounts of D_4TCA were detected in fractions 3-5, revealing a similar concentration profile as the peroxisomal marker proteins (Fig. 6C). In contrast, D_4CA and D_4GCA were not detected in the peroxisome-enriched fractions.

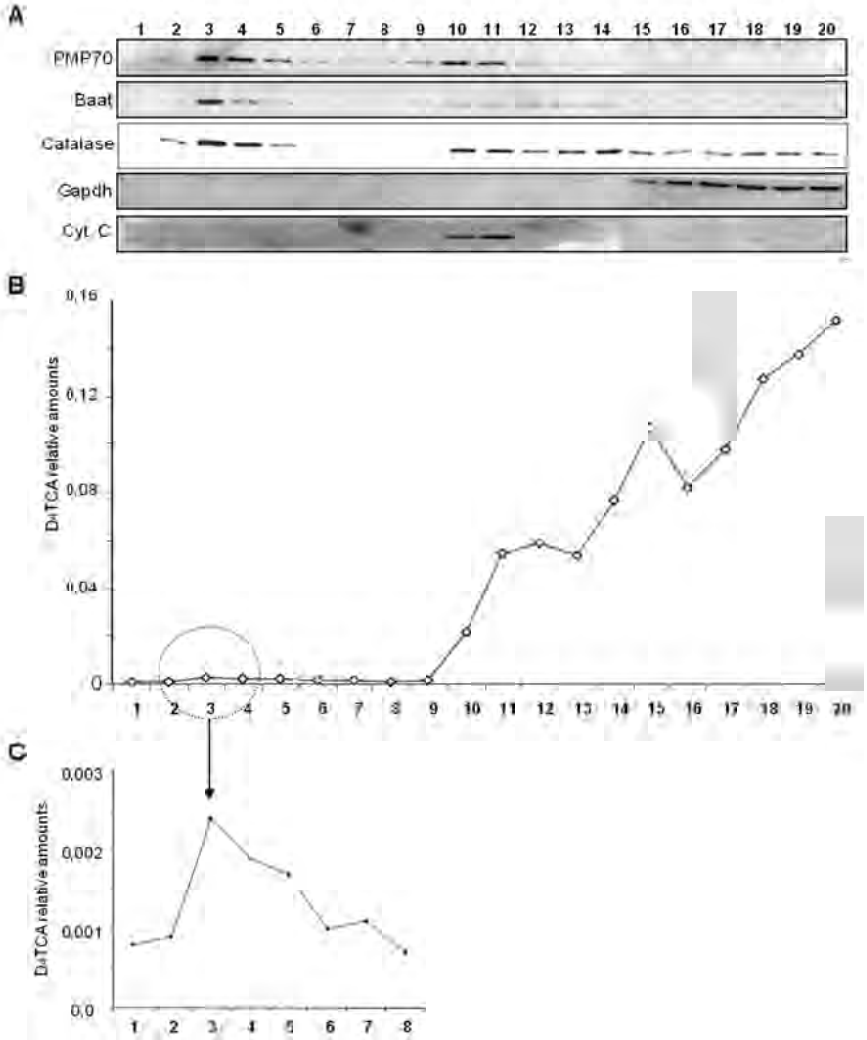

Figure 6. D_4TCA is detected in peroxisomes of D_4CA-exposed hepatocytes. Primary rat hepatocytes were incubated with 100 µM D_4CA for 3 h. Cells were homogenized and the post-nuclear supernatant was separated using Nycodenz density gradient centrifugation. Equal volumes of all gradient fractions were analyzed by western blotting, using specific antibodies against PMP70, Baat, Catalase, Gapdh and cytochrome C (A) or collected for bile salt purification and analysis (B). C shows an enlargement of the bottom 8 fractions of the gradient.

DISCUSSION

In this study, we established a novel assay that allows the study of transcellular and intracellular transport and conjugation of bile salts by rat hepatocytes in vitro. Primary rat hepatocytes effectively convert exogenously added deuterated cholic acid (D_4CA) to its taurine and/or glycine conjugates (D_4TCA and D_4GCA, respectively). Using digitonin permeabilization assays and peroxisome isolations, we demonstrate that D_4TCA transiently resides in peroxisomes. This provides direct evidence that unconjugated bile salts shuttle through peroxisomes to become (re-)conjugated.

Reconjugation of deconjugated bile salts is an important process. Over 30% of the total bile salt pool may become deconjugated by intestinal bacteria on a daily basis (4). Our previous study showed that the enzyme catalyzing bile salt conjugation, BAAT, is localized predominantly, if not solely, in peroxisomes (11). This suggests that bile salts need to shuttle through peroxisomes for reconjugation. However, the possible existence of a cytosolic pool of BAAT remains a matter of debate (8-11). Therefore, we developed this novel assay to study trans- and intracellular transport and conjugation of D_4CA. The use of D_4CA allowed us to specifically follow its (re-)conjugation route, independent from endogenous-produced CA.

In the intact liver, bile salt reconjugation is highly efficient as 97% of infused UDCA is conjugated to taurine or glycine after one single pass through rat livers (5). The in vitro cultured hepatocytes also perform this function with significant efficiency with less than 10% of the D_4CA unaccounted for after 24 h. This part of deuterium-labeled bile salts may still reside in the hepatocytes, be present as (CoA-)intermediate or is metabolized to other products. The ratio between the amounts of GCA and TCA formed can be strongly manipulated by the levels of glycine and taurine in the growth medium. A high preference for TCA formation is observed when both amino acids are present in excess. This is in line with the predominant presence of taurine-conjugated bile salts in rats (26). However, in the presence of only glycine, GCA is efficiently formed. These data show that the availability of glycine and/or taurine strongly determines the final conjugation profile. Glycine-conjugated bile salts are generally more cytotoxic compared to their taurine-equivalents (25). Taurine supplementation in cholestatic diseases may therefore limit liver damage. This is especially relevant in humans that have a predominance of glycine-conjugated bile salts.

Cultured rat hepatocytes accumulated high concentrations of D_4TCA and D_4GCA after exposure to 100 µM D_4CA. The cellular volume of a hepatocyte is estimated to be between 4 and 20 pL (19-24). Assuming 20 pL as the volume of a rat hepatocyte, we estimated that the peak intracellular concentration of D_4TCA and D_4GCA were approximately 200 µM and 400 µM, respectively, while D_4CA levels were in the range of the concentrations in the medium. The intracellular accumulation of conjugated bile salts is transient, peaks at 3 h exposure and then declines. This suggests that export of D_4TCA and D_4GCA is limiting and cannot keep up with the production of conjugated bile salts. In our model with

peroxisomal BAAT, transport of TCA and GCA occurs across the peroxisomal membrane and the plasma membrane (see Fig. 7).

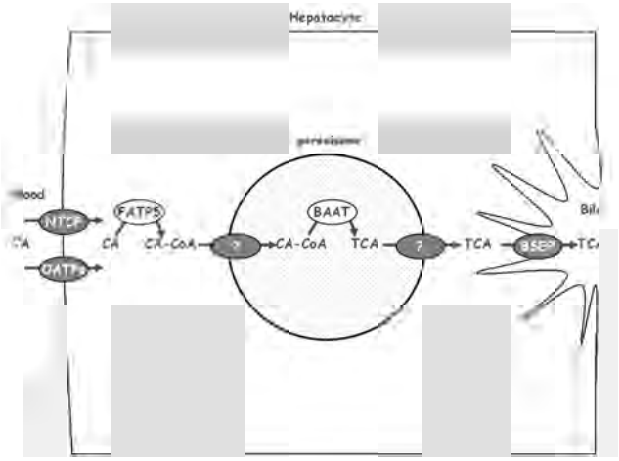

Figure 7. The enterohepatic circulation of unconjugated bile salts includes their transit through hepatocyte peroxisomes. Conjugated and unconjugated bile salts are taken up into hepatocytes by NTCP and/or OATPs (36). Unconjugated bile salts are CoA-activated by FATP5 (6, 7), after which they are transported into peroxisomes by a yet unidentified transporter. Inside peroxisomes, bile salts are conjugated by BAAT, followed by their export by a currently unknown transport protein. Conjugated bile salts are exported into the bile by BSEP.

Digitonin permeabilization and cell fractionation experiments indicate the presence of a peroxisomal and a cytosolic pool of D_4TCA. This suggest that transport of D_4TCA is a limiting factor at both the peroxisomal membrane and the plasma membrane. Only small amounts of D_4TCA were detected in peroxisomes. This may be expected as D_4TCA only transiently resides in peroxisomes. Moreover, D_4TCA may disappear from the peroxisomal fraction during their isolation due to 1) mechanical rupture of the peroxisomal membrane and 2) maintained export of D_4TCA without new production in peroxisomes. However, at present we are not able to discriminate between tauro/glyco-CA formed in the peroxisomes followed by transport to the cytosol and tauro/glycol-CA that is formed in the cytosol directly. This requires manipulation of the peroxisomal bile salt shuttle, either by inhibiting the to-be-identified-peroxisomal bile salt transporters or manipulating peroxisome biogenesis. It is relevant to note that this is the first report that demonstrates the presence of a specific product of peroxisomal metabolism in the peroxisome-enriched fractions after a full cell fractionation procedure. Mechanical breakage of peroxisomes was kept to a minimum by using optimized protocols that stabilize these organelles (13), which also further reconfirmed the predominant peroxisomal location of BAAT as it remained (almost) undetectable in the cytosol-enriched fractions after Nycodenz gradient centrifugation. Remarkably, significant amounts of BAAT, catalase and PMP70 were also detected in low density gradient fractions cofractionating, in part, with mitochondria. In these fractions also D_4TCA was detected. It remains to be determined whether these fractions contain a subpopulation of peroxisomes that may be involved in the bile salt conjugation as well.

To obtain independent evidence for the peroxisomal shuttle we also analyzed the subcellular distribution of several variants of 4-nitrobenzo-2-oxa-1,3-diazole (NBD)-labeled cholic acid (with the NBD group at the 3alpha, 3beta, 7alpha and

7beta position, respectively; see (27)) by fluorescence microscopy. Only 3alpha-NBD-cholate was taurine conjugated and exported to the medium by cultured rat hepatocytes. However, the efficiency of conjugation is much lower (>90%) compared to D_4CA. Interestingly, a clear accumulation of 3alpha-NBD-CA in subcellular structures was detected at early time points (see Supplementary Fig. S2). Unfortunately, due to technical limitations, we have been unable so far to identify these subcellular structures (see Supplementary data for details). Still the detection of a clear punctuate staining pattern for 3alpha NBD-cholate in hepatocytes supports our data that bile salts (transiently) accumulate in membrane enclosed organelles.

Remarkably, we did not detect D_4GCA in the peroxisomal fractions. Still, BAAT is believed to be responsible for both taurine and glycine-conjugation of bile salts (3). This may indicate that the peroxisomal bile salt exporter in rat hepatocytes has a higher affinity for GCA compared to TCA. Clearly, D_4TCA and D_4GCA also accumulate in the cytosol of hepatocytes, implying that the export of conjugated bile salts from hepatocytes by the bile salt export pump (BSEP) is also a rate-limiting step in our assay. This is most likely the result of a suboptimal location and/or activity of BSEP in cultured hepatocytes.

The identity of the peroxisomal bile salt transporters (importer and exporter) is unknown to date. A possible importer of CoA-activated C_{24} bile salts is the 70-kDa Peroxisomal Membrane Protein (PMP70/*ABCD3*). PMP70 is an ATP-binding cassette transporter that is highly expressed in the liver (28). It has been proposed to transport long chain fatty acids into peroxisomes (29, 30). Recent research suggests that it may also transport bile acid intermediates, though thorough experimental evidence has not been presented yet (31). Importantly, the protein-mediated transport of conjugated bile salts across the peroxisomal membrane has recently been demonstrated in vitro (32). The characteristics of the transport activity, e.g. ATP independent, make it unlikely that PMP70, or another peroxisomal ABC-transporter, is involved in this step.

Zellweger Syndrome patients have no (functional) peroxisomes and accumulate intermediates of bile salt biosynthesis in their serum, variable amounts of which are conjugated (33, 34). This suggests that BAAT is (partially) active in the cytosol of these patients and is able to conjugate the accumulated bile salt intermediates. Recent studies using peroxisome-deficient Pex2-/- mice indeed show that the efficiency of conjugation of both C_{24} bile acids and C27 intermediates is reduced, but not absent, under normal conditions in these mutants. Moreover, bile acid conjugation is further impaired when these animals are fed a cholate-containing diet (35). Thus, reconjugation of bile salts may not strictly depend on the shuttle of bile salts through peroxisomes. Rather, it strongly increases the efficiency of the process.

In summary, we provide evidence that unconjugated bile salts shuttle through peroxisomes for taurine or glycine conjugation. Defects in the shuttle of bile salts through these organelles may lead to yet unrecognized cholestatic disorders.

References

1. Hofmann AF. Biliary secretion and excretion in health and disease: current concepts. Ann Hepatol 2007; 6: 15-27.
2. Russell DW. The enzymes, regulation, and genetics of bile acid synthesis. Annu Rev Biochem 2003; 72: 137-174.
3. Falany CN, Johnson MR, Barnes S, Diasio RB. Glycine and taurine conjugation of bile acids by a single enzyme. Molecular cloning and expression of human liver bile acid CoA:amino acid N-acyltransferase. J Biol Chem 1994; 269: 19375-19379.
4. Garbutt JT, Wilkins RM, Lack L, Tyor MP. Bacterial modification of taurocholate during enterohepatic recirculation in normal man and patients with small intestinal disease. Gastroenterology 1970; 59: 553-566.
5. Gurantz D, Schteingart CD, Hagey LR, Steinbach JH, Grotmol T, Hofmann AF. Hypercholeresis induced by unconjugated bile acid infusion correlates with recovery in bile of unconjugated bile acids. HEPATOLOGY 1991r; 13: 540-550.
6. Mihalik SJ, Steinberg SJ, Pei Z, Park J, Kim DG, Heinzer AK, et al. Participation of two members of the very long-chain acyl-CoA synthetase family in bile acid synthesis and recycling. J Biol Chem 2002; 277: 24771-24779.
7. Doege H, Baillie RA, Ortegon AM, Tsang B, Wu Q, Punreddy S, et al. Targeted deletion of FATP5 reveals multiple functions in liver metabolism: alterations in hepatic lipid homeostasis. Gastroenterology 2006; 130: 1245-1258.
8. He D, Barnes S, Falany CN. Rat liver bile acid CoA:amino acid N-acyltransferase: expression, characterization, and peroxisomal localization. J Lipid Res 2003; 44: 2242-2249.
9. Solaas K, Ulvestad A, Soreide O, Kase BF. Subcellular organization of bile acid amidation in human liver: a key issue in regulating the biosynthesis of bile salts. J Lipid Res 2000; 41: 1154-1162.
10. Solaas K, Kase BF, Pham V, Bamberg K, Hunt MC, Alexson SE. Differential regulation of cytosolic and peroxisomal bile acid amidation by PPAR alpha activation favors the formation of unconjugated bile acids. J Lipid Res 2004; 45: 1051-1060.
11. Pellicoro A, van den Heuvel FA, Geuken M, Moshage H, Jansen PL, Faber KN. Human and rat bile acid-CoA:amino acid N-acyltransferase are liver-specific peroxisomal enzymes: implications for intracellular bile salt transport. HEPATOLOGY 2007; 45: 340-348.
12. Vrenken TE, Buist-Homan M, Kalsbeek AJ, Faber KN, Moshage H. The active metabolite of leflunomide, A77 1726, protects rat hepatocytes against bile acid-induced apoptosis. J Hepatol 2008; 49: 799-809.
13. Antonenkov VD, Sormunen RT, Hiltunen JK. The behavior of peroxisomes in vitro: mammalian peroxisomes are osmotically sensitive particles. Am J Physiol Cell Physiol 2004; 287: C1623-C1635.
14. Verheyden K, Fransen M, Van Veldhoven PP, Mannaerts GP. Presence of small GTP-binding proteins in the peroxisomal membrane. Biochim Biophys Acta 1992; 1109: 48-54.
15. Conde de la RL, Schoemaker MH, Vrenken TE, Buist-Homan M, Havinga R, Jansen PL, et al. Superoxide anions and hydrogen peroxide induce hepatocyte death by different mechanisms: involvement of JNK and ERK MAP kinases. J Hepatol 2006; 44: 918-929.
16. Schoemaker MH, Conde de la RL, Buist-Homan M, Vrenken TE, Havinga R, Poelstra K, et al. Tauroursodeoxycholic acid protects rat hepatocytes from bile acid-induced apoptosis via activation of survival pathways. HEPATOLOGY 2004; 39: 1563-1573.
17. Bergmeyer HU BE Lactate dehydrogenase. In: Methods of Enzymatic Analysis. Bergmeyer HU, ed. 2nd ed., Vol. 2. New York: Verlag Chemie; 1974. p 574-579.
18. Rodrigues CM, Setchell KD. Performance characteristics of reversed-phase bonded silica cartridges for serum bile acid extraction. Biomed Chromatogr 1996; 10: 1-5.
19. Drochmans P, Wanson JC, Mosselmans R. Isolation and subfractionation on ficoll gradients of adult rat hepatocytes. Size, morphology, and biochemical characteristics of cell fractions. J Cell Biol 1975; 66: 1-22.
20. Katayama S, Tateno C, Asahara T, Yoshizato K. Size-dependent in vivo growth potential of adult rat hepatocytes. Am J Pathol 2001; 158: 97-105.
21. Wehner F, Guth D. Electric properties of rat liver cell cultures on gas-permeable membranes. Am J Physiol 1991; 261(3 Pt 1): G407-G416.
22. Wehner F. Cell volume-regulated cation channels. Contrib Nephrol 1998; 123: 8-20.
23. Wehner F, Sauer H, Kinne RK. Hypertonic stress increases the Na+ conductance of rat hepatocytes in primary culture. J Gen Physiol 1995; 105: 507-535.
24. Treijtel N, van HH, Barendregt A, Blaauboer BJ, van Eijkeren JC. The use of sandwich-cultured rat hepatocytes to determine the intrinsic clearance of compounds with different extraction ratios: 7-ethoxycoumarin and warfarin. Drug Metab Dispos 2005; 33: 1325-1332.
25. Schoemaker MH, Gommans WM, Conde de la RL, Homan M, Klok P, Trautwein C, et al. Resistance of rat hepatocytes against bile acid-induced apoptosis in cholestatic liver injury is due to nuclear factor-kappa B activation. J Hepatol 2003; 39: 153-161.
26. Haslewood GA. Bile salt evolution. J Lipid Res 1967; 8: 535-550.
27. Rohacova J, Marin ML, Martinez-Romero A, Diaz L, O'Connor JE, Gomez-Lechon MJ, et al. Fluorescent benzofurazan-cholic acid conjugates for in vitro assessment of bile acid uptake and its modulation by drugs. Chem Med Chem 2009; 4: 466-472.
28. Berger J, Albet S, Bentejac M, Netik A, Holzinger A, Roscher AA, et al. The four murine peroxisomal ABC-transporter genes differ in constitutive, inducible and developmental expression. Eur J Biochem 1999; 265: 719-727.
29. Kemp S, Pujol A, Waterham HR, van Geel BM, Boehm CD, Raymond GV, et al. ABCD1 mutations and the X-linked adrenoleukodystrophy mutation database: role in diagnosis and clinical correlations. Hum Mutat 2001; 18: 499-515.
30. Imanaka T, Aihara K, Takano T, Yamashita A, Sato R, Suzuki Y, et al. Characterization of the 70-kDa peroxisomal membrane protein, an ATP binding cassette transporter. J Biol Chem 1999; 274: 11968-11976.
31. Visser WF, van Roermund CW, Ijlst L, Waterham HR, Wanders RJ. Metabolite transport across the

peroxisomal membrane. Biochem J 2007; 401: 365-375.
32. Visser WF, van Roermund CW, Ijlst L, Waterham HR, Wanders RJ. Demonstration of bile acid transport across the mammalian peroxisomal membrane. Biochem Biophys Res Commun 2007; 357: 335-340.
33. Clayton PT, Lake BD, Hall NA, Shortland DB, Carruthers RA, Lawson AM. Plasma bile acids in patients with peroxisomal dysfunction syndromes: analysis by capillary gas chromatography-mass spectrometry. Eur J Pediatr 1987; 146: 166-173.
34. Bootsma AH, Overmars H, van Rooij A, van Lint AE, Wanders RJ, van Gennip AH, et al. Rapid analysis of conjugated bile acids in plasma using electrospray tandem mass spectrometry: application for selective screening of peroxisomal disorders. J Inherit Metab Dis 1999; 22: 307-310.
35. Keane MH, Overmars H, Wikander TM, Ferdinandusse S, Duran M, Wanders RJ, et al. Bile acid treatment alters hepatic disease and bile acid transport in peroxisome-deficient PEX2 Zellweger mice. HEPATOLOGY 2007; 45: 982-997.
36. Mikkaichi T, Suzuki T, Tanemoto M, Ito S, Abe T. The organic anion transporter (OATP) family. Drug Metab Pharmacokinet 2004; 19: 171-179.

SUPPLEMENTARY TABLE S1

Table S1. Antibody dilutions for western blotting

Antibody	Dilution	Company
Rabbit α-PMP70	1:1,000	Sigma-Aldrich, St. Louis, MO, USA
Rabbit α-Baat	1:2,000	Generous gift of Prof. C. Falany, Birmingham, AL, USA (8)
Rabbit α-catalase	1:2,000	Calbiochem, La Jolla, CA, USA
Mouse α-cytochrome C	1:2,000	BD Biosciences, Franklin Lakes, NJ, USA
Mouse α-Gapdh	1:10,000	Calbiochem, La Jolla, CA, USA

SUPPLEMENTARY MATERIAL AND METHODS

LC/MS/MS analysis of bile salts

LC/MS/MS analysis was performed using a triple quadrupole mass spectrometer API 3000 (Applied Biosystems, Foster City, CA, USA) operating with an ESI ionization source in the negative mode. A capillary voltage of -4500V and a source temperature of 400°C were used. The declustering potentials were -96 V, -101 V and -100 V for (D_4)TCA, (D_4)CA and (D_4)GCA, respectively. Due to the lack of any specific and stable fragment ions, detection of CA and D_4CA was performed using single ion monitoring at m/z 407 and m/z 411, respectively. Detection of GCA, D_4GCA, TCA and D_4TCA was performed using the selected reaction-monitoring mode. The transitions of the deprotonated molecules to their corresponding product ions were recorded at m/z 464.2 → 73.9 (GCA), m/z 468.2 → 73.9 (D_4GCA), m/z 514.1 → 79.9 (TCA) and m/z 518.1 → 79.9 (D_4TCA). The collision energy used was -114 eV for TCA and D_4TCA and -72 eV for GCA and D_4GCA. For the chromatographic separation, two LC-200 HPLC pumps (Perkin-Elmer, Waltham, MA, USA) coupled to a series 200 autosampler (Perkin-Elmer) were used, all of them controlled by the mass spectrometer data system. Chromatography was performed with a Luna C18(2) (Phenomenex, Torrance, CA, USA) analytical column (50x2.0 mm; particle size 3 µm) in combination with a frit filter (Upchurch Scientific Inc, Oak Harbor, WA, USA). Ultra pure water and acetonitrile were used as mobile phases A and B, respectively. The initial mobile phase was ultra pure water:acetonitrile 60:40 v/v %, which was kept constant for 2.5 minutes. Subsequently, the solvent was changed to 30:70 v/v % in 1 minute and was kept constant for 2 minutes. In the next step, the solvent was changed to 10:90 v/v % in 0.5 minute, and kept constant for 2 minutes. Finally, the solvent was changed to the initial composition and was kept constant for 4.5 minutes. Column flow was 0.2 ml/min and was introduced into the mass spectrometer without splitting.

SUPPLEMENTARY FIGURES

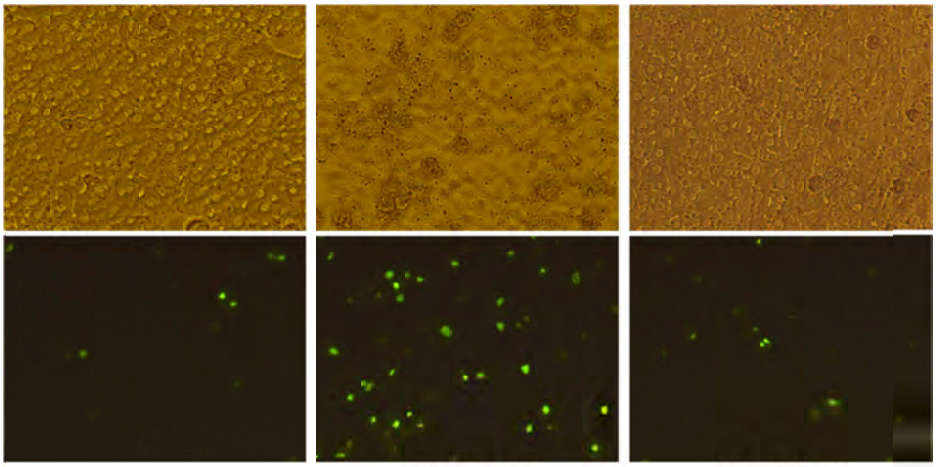

Figure S1. Incubation of rat hepatocytes with 100 µM D_4CA does not induce necrosis. Primary rat hepatocytes were incubated with either 100 µM D_4CA or 50 µM GCDCA for 24 h, followed by Sytox green® staining (In vitrogen; see for protocol Conde de la Rosa *et al*, 2006). Top panels show the bright field images; bottom panels show the fluorescence images. Necrotic cells are visualized by green fluorescent nuclei. GCDCA is a strong inducer of apoptosis (after 3-6 h of exposure). After prolonged incubation (here 24 h) a clear increase in necrotic cells is observed also (middle panels). In contrast, 24 h exposure to 100 µM D_4CA (right panels) does not increase the number of necrotic cells compared to control cells (left panels).

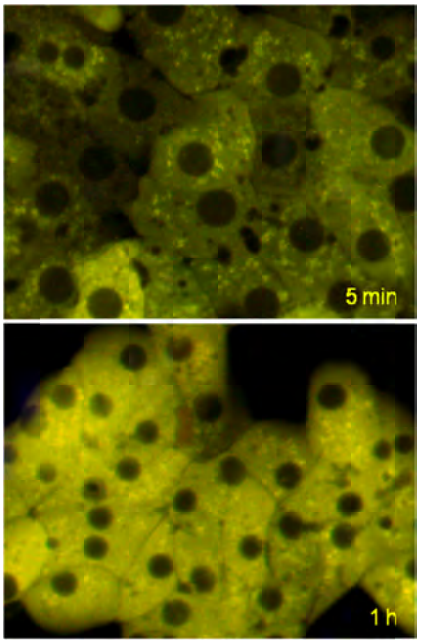

Figure S2: Organellar accumulation of 3α-NBD-CA in rat hepatocytes. Rat hepatocytes were exposed to 0.625 µM 3α-NBD-CA (see for reference Rohacova *et al*, 2009) for 5 minutes (left panel) and 60 minutes (right panel). 3α-NBD-CA is rapidly taken up by hepatocytes and primarily accumulated in dotted structures. Prolonged incubation leads to an increase in cytosolic staining. A more pronounced cytosolic staining was also observed when rat hepatocytes were exposed to high concentrations (25 µM) of 3α-NBD-CA. It is important to note that rat hepatocytes have only very limited capacity to synthesize the taurine conjugate of 3α-NBD-CA, 3α-NBD-TCA.
Unfortunately, we have been unable to identify the 3alpha-NBD-CA-positive structures so far, because the bile salts are lost when cells are prepared for immunofluorescence microscopy (due to the requirement of detergent-mediated permeabilisation and extensive washing to remove non-specific antibodies). Moreover, transient transfection with peroxisomal markers (DsRed-SKL) could not be used, because the cultured hepatocytes rapidly lose their ability to re-conjugate cholate, even before recombinant proteins are produced and properly sorted to peroxisomes.

CHAPTER 3

Involvement of Pmp70 in the intrahepatocyte bile salt shuttle

Krzysztof P. Rembacz[1], Jannes Woudenberg[1], Zhengyu Du[1], Fiona A.J. van den Heuvel[1], Elles Z. Jonkers[2], Frans Stellaard[2], Han Moshage[1], Klaas Nico Faber[1]

[1]Department of Gastroenterology and Hepatology, University Medical Center Groningen, University of Groningen, Groningen, The Netherlands
[2]Department of Laboratory Medicine, University Medical Center Groningen, University of Groningen, Groningen, The Netherlands

In preparation

Involvement of Pmp70 in the intrahepatocyte bile salt shuttle

ABSTRACT

Peroxisomes are organelles highly enriched in the liver, which play a central role in bile salt homeostasis. The final steps of bile salt biosynthesis occur inside peroxisomes, including side chain shortening and conjugation to taurine or glycine, after which they enter the enterohepatic cycle. In this cycle, significant amounts of bile salts are deconjugated in the intestine and after recycling to the liver need to pass through peroxisomes again for reconjugation. In contrast to our knowledge about bile salt transporters in plasmamembranes, very little is known about transport of bile salt (intermediate)s across peroxisomal membranes. Here, we analyzed the putative involvement of the peroxisomal ABC-transporter Pmp70 (*Abcd3*) in this process.

Primary rat hepatocytes were exposed to the PPARα ligand fenofibric acid (FFA) to induce expression of Pmp70. Small interfering RNA was used to prevent FFA-induced expression of Pmp70. FFA- and/or siRNA-treated hepatocytes were exposed for 3 h to deuterium-labeled cholic acid (D_4CA) and conversion to and accumulation of D_4-tauro cholic acid (D_4TCA) in hepatocyes and medium were quantified by LC/MS/MS mass spectrometry.

FFA treatment of rat hepatocytes strongly induced Pmp70 expression (5-10 fold) and increased the accumulation of D_4TCA in the medium (+15%), while reducing the intracellular levels of D_4CA (-44%) and D_4TCA (-15%). SiRNA treatment effectively prevented the FFA-induced expression of Pmp70 in rat hepatocytes and concomitantly increased the intracellular levels of D_4CA and D_4TCA and decreased D_4TCA levels in the medium. FFA did not change the expression of other factors in the conjugation and transport of CA (Fatp5, Baat, Ntcp and Bsep).

These data suggest a role for Pmp70 in the transport of unconjugated bile salts into peroxisomes to become conjugated to taurine and efficiently exported from hepatocytes.

INTRODUCTION

Bile salts are synthesized from cholesterol in the liver and are secreted to bile. Bile allows absorption of fat and fat-soluble vitamins in the intestine. Moreover, bile salt biosynthesis is the main route of cholesterol elimination from the body. In the terminal ileum, 90-95% of bile salts is reabsorbed and transported back to the liver in a process that is called the enterohepatic circulation. Bile salt import and export in hepatocytes and enterocytes are mediated by well-known and characterized transporters, including NTCP, OATP1B1 and BSEP in the liver and ASBT and OSTαβ in the intestine (1).

De novo synthesis in the liver compensates the fecal loss of bile salts. The synthesis involves at least 13 different enzymes localized to different intracellular compartments, including the cytosol, endoplasmic reticulum (ER), mitochondria and peroxisomes. Bile salts are synthesized from cholesterol that undergoes 3 main modifications, e.g. hydroxylation of the steroid nucleus, side chain shortening (□-oxidation) and side chain conjugation (amidation) to taurine or glycine. The last two steps take place in peroxisomes (2). Bile acid-coenzyme A:amino acid N-acyltransferase (BAAT) is responsible for the third (and final) modification step of bile salts (3).

Taurine/glycine conjugating of bile salts remains crucial also during the enterohepatic cycle, since a significant portion of biliary bile salts is deconjugated by intestinal bacteria. Up to one third of bile salts return to the liver in a de-conjugated form (4). The liver has a high capacity to re-conjugates bile salts as exemplified by the 97% efficient conjugation of infused UDCA with glycine or taurine after a single pass through the isolated and perfused rat liver (5).

Unconjugated bile salts entering the hepatocyte are activated with Coenzyme A (CoA) by the fatty acid transport protein 5 (FATP5/ SLC27A5/ ACSVL6 / ACSB / BACS / VLCS-H2 in human or Bal in rat), which is located at the basolateral membrane of hepatocytes (6, 7, 8, 9). Next, C_{24}-bile salt-CoA esters are conjugated to taurine or glycine by BAAT (10). It has been proposed that a cytosolic pool of BAAT is responsible for the reconjugation of bile salts returning from the intestine (11, 12). However, using cell fractionation and microscopical techniques we found that BAAT is predominantly, if not solely, present in peroxisomes of human and rat hepatocytes (13). In support of this, we recently showed that cholic acid shuttles through peroxisomes for taurine conjugation (Rembacz *et al*, 2010 (14)). These observation suggest the existence of yet unidentified transport systems (import and export) for bile salt (intermediate)s in the peroxisomal membrane.

Indeed, experiments with purified peroxisomes reveal the presence of proteins that support transport of taurocholic acid (TCA) (15) and C_{27} bile acid biosynthesis intermediates 3 alpha,7 alpha,12 alpha-trihydroxy-5 beta-cholestanoic acid (THCA) and 3 alpha,7 alpha-dihydroxy-5 beta-cholestanoic acid (DHCA) (16) across peroxisomal membranes. Transport of THCA and DHCA appears to be ATP dependent and is inhibited by compounds that block the activity of ATP-binding cassette (ABC-)transporters, e.g. verapamil, sodium azide and N-ethymaleimide

(16). C_{24} CoA-activated bile salts may use the same transporter to enter peroxisomes. The identity of peroxisomal bile salt importer(s) and exporter(s) is unknown to date.
A likely candidate for the importer of CoA-activated C_{24} and C_{27} bile salts is the peroxisomal membrane protein of 70-kDa (Pmp70/*Abcd3*), an ATP-binding cassette (half-) transporter highly expressed in the liver (17). Pmp70 is suggested to transport long chain fatty acids into peroxisomes, but direct evidence for this activity is not yet available (18, 19).
Pmp70 is a major component of peroxisomal membrane in hepatocytes. Its ATP-binding site faces the cytosol (20), suggesting transport of substrates into peroxisomes. Pmp70 primarily exists as homodimer (21), but the formation of heterodimers between Pmp70 and other peroxisomal ABC half-transporters, such as ALDP, has also been suggested (22, 23). Pmp70 expression is regulated by peroxisome proliferator-activated receptor-alpha (PPARα), a nuclear receptor activated by hypolipidemic agents like clofibrate, bezafibrate, ciprofibrate, fenofibrate or Wy-14,643 (19, 24, 25). In rodents, but not in humans, they dramatically increase the size and number of hepatic and renal peroxisomes as well as their metabolic activities (24, 26, 27).
In this work, we investigated the role of Pmp70 in bile salt shuttling through peroxisomes. We manipulated Pmp70 expression in cultured rat hepatocytes using fenofibric acid and RNA-interference. Subsequently, rat hepatocytes with variable Pmp70 levels were exposed to D_4CA and conversion to and accumulation of D_4TCA in cells and medium were analyzed by LC/MS/MS mass spectrometry (14). Our data demonstrate for the first time the involvement of Pmp70 in bile salt metabolism in hepatocytes.

MATERIALS AND METHODS

Animals
Specified pathogen-free male Wistar rats (220–250 g) were purchased from Charles River Laboratories Inc. (Wilmington, MA, USA). Rats were housed under standard laboratory conditions with free access to standard laboratory chow and water. Experiments were performed following the guidelines of the local Committee for Care and Use of Laboratory Animals.

Hepatocyte isolation and culture conditions
Hepatocytes were isolated and cultured in William's E as described previously (28). Cells were cultured in a humidified incubator at 37 °C and 5% CO_2. Hepatocyte viability and purity were always more than 90%.

siRNA-mediated knock down of Pmp70
Small interfering RNA duplexes specific for *Abcd3*/Pmp70 knock down were designed (sense 5'-GAGACAGGGUACUUCAUAdTdT-3'; antisense 5'-UAU GUUGUACCCUGUCUCdTdT-3') and purchased from Eurogentec (Maastricht,

The Netherlands). Human MRP1 complexes (sense 5'-GGAGUGGAACCCCUCUCU-3'; antisense 5'-AGAGAGGGGUUCCACUCCdTdT-3') were used as siRNA control. For transfection experiments, siRNA duplexes were complexed with Lipofectamin 2000 according to manufacturer's instructions (Invitrogen, Breda, The Netherlands). Hepatocytes were transfected with siRNA/Lipofectamin complexes in a suspension and let attach in 6-well collagen-coated plates in a concentration of 8×10^5 cells/well.

Fenofibric acid (FFA) treatment
Four hours after attachment, primary rat hepatocytes were treated with 5-250 µM fenofibric acid (Sigma, Zwijndrecht, The Netherlands) for variable time periods as specified in the result section. SiRNA treated hepatocytes were exposed to FFA 8 hours after transfection.

SDS-PAGE and Western blotting.
Protein samples were separated by SDS-PAGE and analyzed by Western blotting according to established procedures (13). Protein concentrations were determined using the Bio-Rad Protein Assay system (Bio-Rad Hercules, CA, USA) using bovine serum albumin as standard. Primary antibody dilutions are summarized in Table 1. Proteins signals were detected and quantified using a ChemiDoc XRS system (Bio-Rad, Hercules, CA, USA). Protein band intensities were quantified using Quantity One software (Bio-Rad).

Table 1. Antibody dilutions for western blotting

Antibody	Dilution	Company
Rabbit α-PMP70	1:1,000	Sigma-Aldrich, St. Louis, MO, USA
Rabbit α-Baat	1:2,000	Generous gift of dr C. Falany, Birmingham, AL, USA (10)
Rabbit α-catalase	1:2,000	Calbiochem, La Jolla, CA, USA
Mouse α-cytochrome C	1:2,000	BD Biosciences, Franklin Lakes, NJ, USA
Mouse α-Gapdh	1:10,000	Calbiochem, La Jolla, CA, USA

Uptake and conversion of deuterated cholic acid (D_4CA) by primary rat hepatocytes
Primary rat hepatocytes were plated at a density of 1.0×10^5 cells/cm^2. After a 24 hour attachment period, cells were incubated with 100 µM [2,2,4,4-D]Cholic acid (D_4CA; isotopic purity 98%, ISOTEC, Miamisburg, OH, USA) for 3 hours. Cells and media were harvested and levels of D_4CA and D_4TCA were quantified by LC/MS/MS according to a recently established procedure (14).

RNA isolation and Q-PCR
Total RNA was isolated from hepatocytes with Tri Reagent (Sigma, St Louis, MO), according to manufacturer's instructions. Messenger RNA levels of selected genes were quantified using the ABI PRISM 7700 (Applied Biosystems, California, USA).

Q-PCR conditions were as described (29). Details about primers and probes are shown in Table 2.
The expression of each gene of interest was normalized with respect to the endogenous control, 18S using the ΔΔCt method. The data are given as fold-induction versus 18S as the mean of three independent measurements +/- SD.

Table 2. Primers and probes used for qPCR gene expression level measurements

Gene	Forward primer	Reverse primer	FAM -probe-TAMRA
18S	CGGCTACCACATCCAAGGA	CCAATTACAGGGCCTCGAAA	CGCGCAAATTACCCATCCCGA
Pmp70	CTGGTGCTGGAGAAATCATCAAT	CCAGATCGAACTTCAAAACTAAGGT	TGATCATGTTCCTTTAGCAACACCAAATGG
Baat	TGTAGAGTTTCTCCTGAGACATCCTAA	GTCCAATCTCTGCTCCAATGC	TGCCAACCCCTGGGCCCAG
HMG-CoAs	TGGTGGATGGGAAGCTGTCTA	CTGCGGTAAGCTGCATAGCAT	CCAAGGCCCGCAGGTAGCACTG
Pex11α	GCCCGCCACTACTACTATTTCCT	TCTGTCGCGTGCAACTTGTC	CATATGCAGCAAGACCTCATACAGATCCCG
Aldp	CATCTGGCCTGCTCATGGTA	TTCATGGCTTCTGAGTCTGACTCT	CCCCATCATCACAGCCACTGGCT
Acox1	GCCACGGAACTCATCTTCGA	CCAGGCCACCACTTAATGGA	CCACTGCCACATATGACCCCAAGACCC
Fatp5/Bal	GTGCTGATTGTGGATCCAGAC	GAATGTTCTCAGCTAGCAGCTTG	CCAGGAGAACCTGGAAGAAGTCCTTCC

Subcellular fractionation and peroxisomal isolation
The subcellular fractionation and isolation of peroxisomes from rat liver was performed essentially as described (30) using PEG1500-containing homogenization buffer (isolation medium-3). Peroxisomes were purified from the 500g supernatant (postnuclear supernatant [PNS]) using Nycodenz density gradient centrifugation according to the method described by Verheyden *et al*., (31). Twelve mL PNS was loaded on top of a discontinuous Nycodenz gradient (2 mL 56%, 3 mL 45%, 15 mL 30%, and 5 mL 18%) and centrifuged in a vertical rotor (Sorvall, SV288, Thermo Fisher Scientific, Waltham, MA) at 20,000 rpm for 2 hours at 4°C in a slow acceleration/deceleration mode. Equal volumes of all supernatants, pellets and gradient fractions were analyzed by Western blotting or were further purified for mass spectrometry as described previously (14).

Differential membrane permeabilisation assays using digitonin
Digitonin assays were performed as previously described (14). Equal volumes of supernatant and pellet fractions were analyzed by Western blotting or further processed for mass spectrometry essentially as described (14).

(Immunofluorescence) Microscopy
Cells were cultured on coverslips coated with collagen and after specified time of stimulation with FFA fixed with 4% paraformaldehyde. The rabbit pAb against Pmp70 was used in a 1:500 dilution followed by a secondary mAb carrying the FITC fluorophore. Images were taken with a confocal scanning laser microscope (TCS 4D; Leica, Heidelberg, Germany) equipped with argon/krypton laser and coupled to a Leitz DM IRB (Leica, Heidelberg, Germany) inverted microscope.

Purification of bile salts for mass spectrometry
Media and cell samples for deuterated bile salt LC/MS/MS analysis were purified with C-18 columns in the presence of unlabeled internal standards essentially as described (14).

LC/MS/MS analysis of bile salts
D_4CA and D_4TCA were quantified by LC/MS/MS as previously described (14). In short, LC/MS/MS analysis was performed using a triple quadrupole mass spectrometer API 3000 (Applied Biosystems, Foster City, CA) using ESI ionization in the negative mode. CA and D_4CA were detected using single ion monitoring at m/z 407 and m/z 411, respectively. Detection of TCA, and D_4TCA was performed using the selected reaction-monitoring mode. Two LC-200 HPLC pumps (Perkin-Elmer, Waltham, MA) coupled to a series 200 autosampler (Perkin-Elmer) were used. Chromatography was performed with a Luna C18(2) (Phenomenex, Torrance, CA) analytical column (50 × 2.0 mm; particle size 3 µm).

Statistics
The peak area's for the D_4-labeled bile salts were determined and related to the corresponding unlabeled bile salts added as internal standards (IS). This ratio was corrected for the natural ^{13}C isotope abundance of the IS.
The data are reported as percentage change to control hepatocytes and presented as mean of three independent experiments ± SEM. Student's t-test and Kruskal-Wallis H-test (one-way ANOVA test by ranks) were used to evaluate significance of differences among independent groups of variables. Significance was defined at $p<0.05$.

RESULTS

Small interfering RNA efficiently reduces *Abcd3* transcript levels in cultured primary rat hepatocytes, but not Pmp70 protein.
To analyse the putative involvement of Pmp70 in bile salt transport through peroxisomal membranes, we aimed to repress its expression in cultured rat hepatocytes through transient transfection with *Abcd3*-selective siRNA duplexes, following the procedure we successfully used for caveolin-1 (Woudenberg *et al.*, 2010 (32)). *Abcd3* mRNA levels were significantly reduced by siRNA treatment already after 16 h (70% reduction) and further declined up to 32 h (90% reduction; Fig. 1A). Strongly reduced *Abcd3* levels were maintained up to 72 h after transfection. Unfortunately, Pmp70 protein levels did not mirror the strong reduction in *Abcd3* mRNA levels (Fig. 1B).

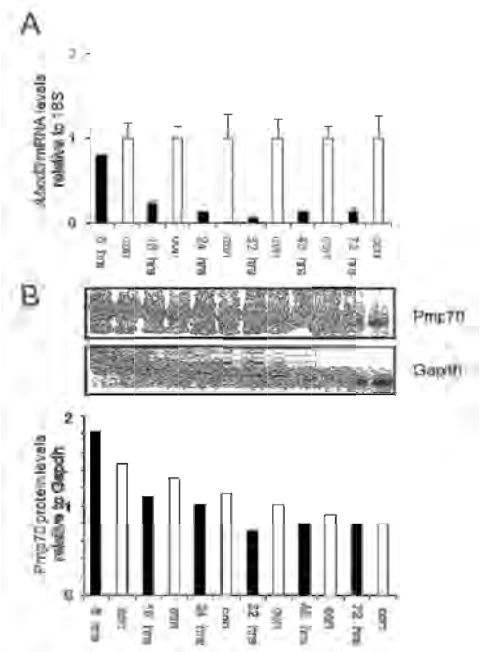

Figure 1: Small interfering RNA efficiently reduces *Abcd3* mRNA levels

(A) Efficient reduction of *Abcd3* mRNA levels after treatment with *Abcd3*-siRNA. Already at 24-hour time-point a 70% reduction is achieved when compared to untreated rat hepatocytes. Values are presented as fold reduction related to controll hepatocytes related to 18S.
(B) Western blot analysis demonstrates ineffective Pmp70 protein reduction. Only a maximum of 30% reduction is observed in *Abcd3*-siRNA treated hepatocytes. The graph represents western blot quantification normalized to Gapdh where black bars depict treated hepatocytes and white bars represent controls.

Pmp70 protein levels dropped slowly, but persistently in untreated rat hepatocytes to approximately 50% after 72 hours in culture. At all time points tested, siRNA treatment lead to only a minor (max. 30%) reduction in Pmp70 protein levels compared to control cells. These data suggest that cultured rat hepatocytes produce only limited amounts of Pmp70 *de novo* and that Pmp70 has a relatively long half life.

Fenofibric acid-mediated induction of Pmp70 expression in cultured rat hepatocytes.

As an alternative approach, we aimed to selectively induce the expression of Pmp70 and analyze its effect on bile salt metabolism. Fenofibric acid (FFA) is a potent agonist of Pparα and induces expression of several peroxisomal proteins, including Pmp70, as well as several other proteins involved in lipid metabolism. Primary rat hepatocytes were exposed for 24 and 48 h to 50 µM FFA and mRNA levels of *Abcd3* and several control genes were determined by Q-PCR (Fig. 2). Expression of well-known Pparα target genes, e.g. mitochondrial HMG-CoA, peroxisomal Acox1 and Pex11a as well as *Abcd3*/Pmp70 were strongly induced by FFA. *Abcd3* levels were elevated 8-fold after 24 h FFA treatment, which remained stable for the next 24 h. The increase in *Abcd3* mRNA coincided with a significant increase in Pmp70 protein levels (Fig. 2G). In contrast, expression of the Pmp70 homolog Aldp (*Abcd1*) was not affected by FFA-exposure and remained stable over a time frame of 48 hours (Figure 2 E). In addition, mRNA levels of the bile salt-conjugation enzyme Baat were unaltered after 24 h incubation with FFA (Fig. 2F).

After 48 h a 2-fold increase in Baat mRNA levels were detected, but this is probably not a direct result of Pparα-mediated transcription.

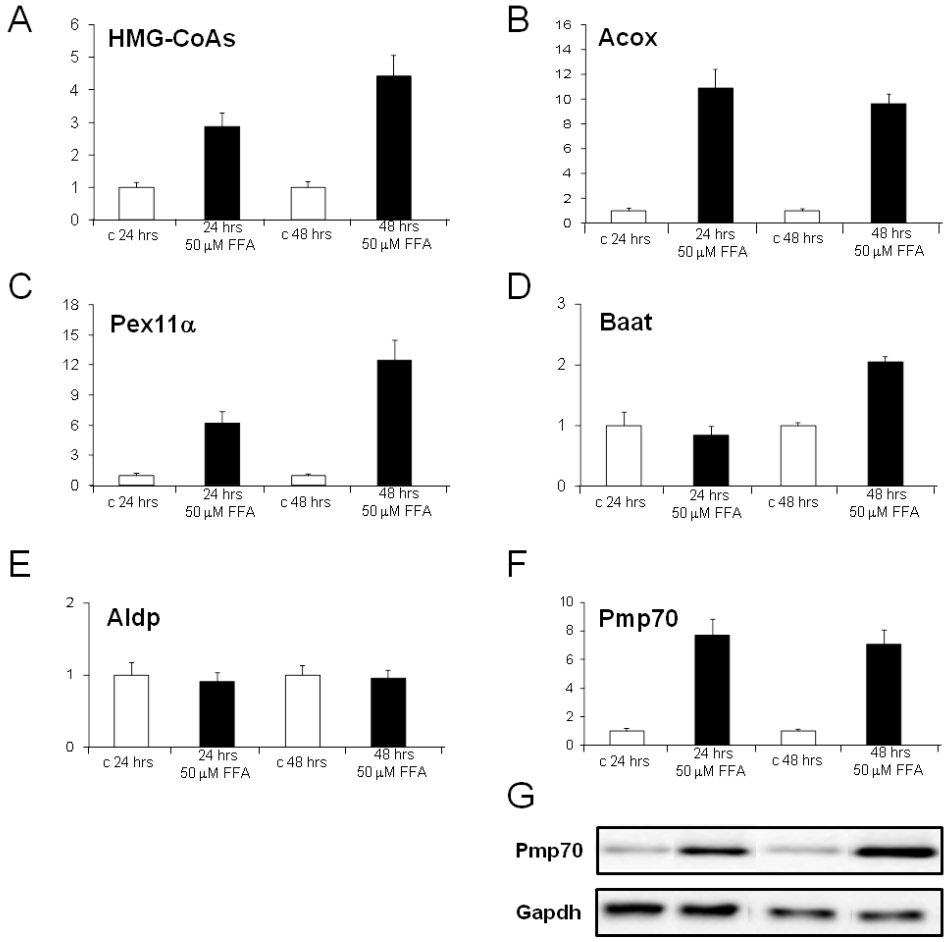

Figure 2: Genes responding to Pparα stimulation with fenofibric acid (FFA)

Pparα target genes: mitochondrial 3-hydroxy-3-methylglutaryl-Coenzyme A synthase 2 (A), peroxisomal acyl-Coenzyme A oxidase 1 (B), and Pex11α (C) are upregulated directly upon Pparα stimulation with FFA, already after 24 hours.
Bile acid CoA: amino acid N-acyltransferase (Baat) does not respond to Pparα stimulation within the first 24 hours (D).
The peroxisomal ABC half-transporters Aldp and Pmp70 are differentially regulated by Pparα. *Abcd1*/Aldp (E) expression is not altered upon FFA treatment of isolated rat hepatocytes. *Abcd3*/Pmp70 (F) is a Pparα target gene and is directly upregulated in response Pparα stimulation already after 24 hours. Western blot analysis revealed a strong Pmp70 protein induction in total cell lysates of hepatocytes treated with 50μM FFA after 24 and 48 hours compared to untreated rat hepatocytes (G).

Dose-dependent upregulation of Abcd3 by FFA in cultured hepatocytes.
Since Abcd3/Pmp70 in rat hepatocytes appeared to respond directly to Pparα agonist (FFA) stimulation, we determined the FFA concentration for maximal Abcd3 induction. FFA dose-dependently increased Abcd3 mRNA and Pmp70 protein levels with a maximum induction at 50 µM FFA after 24 h exposure (Fig. 3). FFA exposure did not significantly change the Baat protein levels, which is in line with the unchanged Baat mRNA levels after 24 h (Fig. 2F). All following experiments were performed with 50 µM FFA unless specified differently.

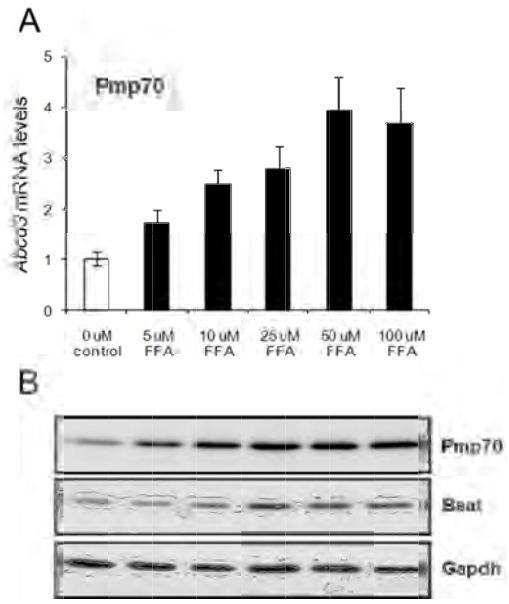

Figure 3: Dose-dependent induction of *Abcd3*/Pmp70 in FFA treated rat hepatocytes.

Abcd3 mRNA levels (A) and Pmp70 protein levels (B) in hepatocytes treated with increasing concentration (0-100 µM) the Pparα agonist FFA. Baat levels are not significantly changed during a 24 hours FFA treatment. Gapdh was used as loading control.

FFA treatment does not lead to an aberrant subcellular location of increased levels of peroxisomal proteins in cultured rat hepatocytes.
It has been reported that Pparα activation in mice results in a relative increase in Baat and catalase protein levels in the cytosol (12). We therefore determined whether FFA-treatment of rat hepatocytes had similar effects, which may directly modulate the conjugation and subcellular transport of bile salts through hepatocytes. Cultured rat hepatocytes were treated for 24 hours with 50 µM of FFA and were analyzed by immunofluorescence microscopy for the subcellular location of Pmp70 (Fig 4A and B). Pmp70 was readily detected in distinct dots throughout the cytoplasm of control rat hepatocytes. In 24 h FFA-treated hepatocytes a similar dotted staining pattern was detected, but with a strongly increased fluorescence staining intensity, as shown by CLSM with a fixed laser intensity (compare Fig. 4 A and B). Fractionation of a post nuclear supernatant from untreated and FFA-treated rat hepatocytes by Nycodenz density gradient centrifugation revealed no significant differences in the subcellular distribution of Pmp70 and Baat in control and FFA-treated rat hepatocytes (Fig. 4 C and D). Baat was predominantly detected

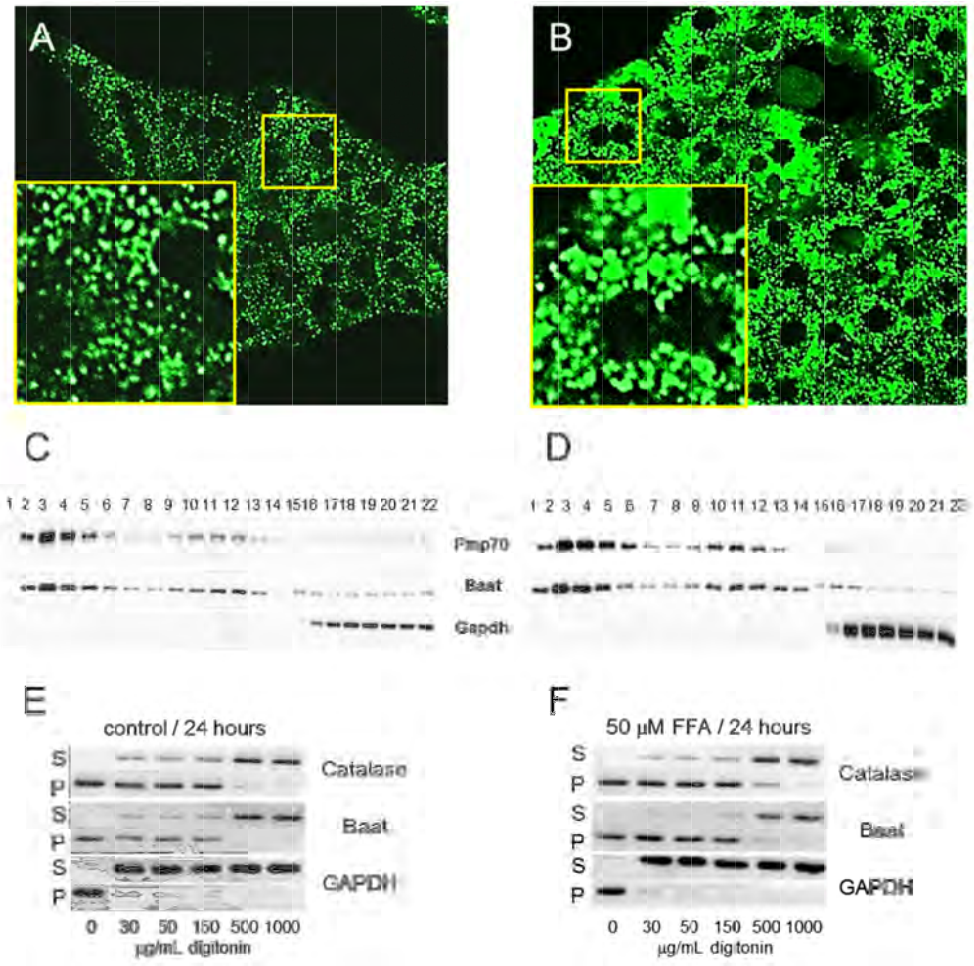

Figure 4. FFA treatment induces PMP70 expression without affecting its intracellular distribution or that of the peroxisomal matrix proteins Baat and catalase.

A and B) Immunostaining for Pmp70 reveals a strong increase of punctuated Pmp70 signal in rat hepatocytes treated with 50µM FFA for 24 hours (B) when compared to untreated hepatocytes (A).
C and D) Western blot analysis of Nycodenz gradient fraction after separation of post-nuclear supernatants (PNS) from control (C) and FFA-treated (D) rat hepatocytes. Fractions 16-22 represent the zone where the PNS was loaded. Gapdh (cytosolic marker) remains in the top fractions after centrifugation. PMP70 and Baat migrate to high density fractions peaking at fractions 2-5 where typically mature peroxisomes are detected. The nature of the organelles containing Baat and Pmp70 in fractions 9-13 is unclear to date, but is routinely observed after Nycodenz density gradient centrifugation. These may represent immature peroxisomes. Important is that Pmp70 and Baat show a similar fractionation patterns in control and FFA-treated hepatocytes.
E and F) Western blot analysis of supernatant (S) and pellet (P) fractions after extraction of control (E) and FFA-treated (F) hepatocytes with increasing concentrations of digitonin. Gapdh (cytosolic marker) is completely extracted at low concentrations digitonin (30 µg/mL), whereas catalase and Baat are only effectively extracted at high digitonin concentrations (500 µg/mL). The extraction profile is the same for control and FFA-treated hepatocytes.

in high density fractions (fractions 2-6) and co-fractionated with Pmp70 in both conditions. Besides the typical high-density peroxisomes, also a second peak enriched in Pmp70 and Baat (fractions 9-13) was detected, which may present a specific subpopulation of peroxisomes. This second peak was detected in both control and FFA-treated cells. Only minor amounts of Baat and Pmp70 were detected on top of the Nycodenz gradient in fractions containing cytosolic proteins (Gapdh; fractions 16-22)). To obtain independent evidence that FFA treatment did not alter the subcellular location of peroxisomal matrix proteins, we performed digitonin permeabilisation experiments on control and FFA-treated rat hepatocytes (Fig. 4 E and F) (Pellicoro *et al.*, 2008 (13); Rembacz *et al.*, 2010 (14)). Exposure of control rat hepatocytes to 30 µg digitonin leads to the complete release of the cytosolic marker Gapdh from the cells. Catalase and Baat remain largely present in the cellular fraction representative of a peroxisomal location. Only at 500 µg digitonin, catalase and Baat are fully extracted from the cells (Fig. 4E). An identical digitonin-extraction profile of Gapdh, catalase and Baat was observed for FFA-treated rat hepatocytes (Fig. 4F).

FFA does not affect expression of plasma membrane bile salt transporters.

Bile salt fluxes through hepatocytes are largely controlled by the bile salt transporters Ntcp (Slc10a1) and Bsep (Abcb11). We analyzed whether FFA-treatment caused any changes in the levels of these two proteins and found that they remained unaffected by FFA concentrations ranging from 25 to 250 µM (Fig. 5).

Collectively, these data show that FFA treatment of cultured hepatocytes leads to a strong increase in peroxisomal Pmp70, without affecting key bile salts transporters in the plasmamembrane or the capacity to conjugate bile salts with taurine and/or glycine.

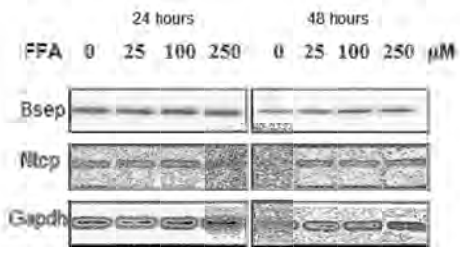

Figure 5: FFA treatment does not change the expression levels of BSEP and NTCP

Cultured rat hepatocytes were treated with 25, 100, and 250 µM FFA for 24 and 48 hours and analyzed by Western blotting. FFA treatment does not change the protein levels of the bile salt export pump (Bsep) and the sodium-taurocholate cotransporting polypeptide (Ntcp) compared to untreated hepatocytes. Gapdh was used as a loading control.

Increased CA to TCA conversion by FFA-treated rat hepatocytes.

Next, we analyzed whether FFA treatment modulates transcellular transport and conjugation of bile salts by exposing rat hepatocytes to deuterium-labeled cholic acid (D_4CA) and analyzing the cellular and extracellular appearance of taurine-conjugated cholic acid (D_4TCA) by mass spectrometry (Fig. 6). FFA treatment lead to a significant decrease in cellular D_4CA compared to control rat hepatocytes (-44%). Similarly, cellular D_4TCA levels were reduced (-15%). In contrast, D_4TCA

levels were slightly, but significantly increased in the medium of FFA-treated rat hepatocytes (+15%). As most of the added D_4CA was still unprocessed after 3 h exposure, high levels of D_4CA were detected in the medium of both control and FFA-treated cells. These data show that FFA treatment increases the conjugation- and transcellular transport rate of D_4CA towards D_4TCA.

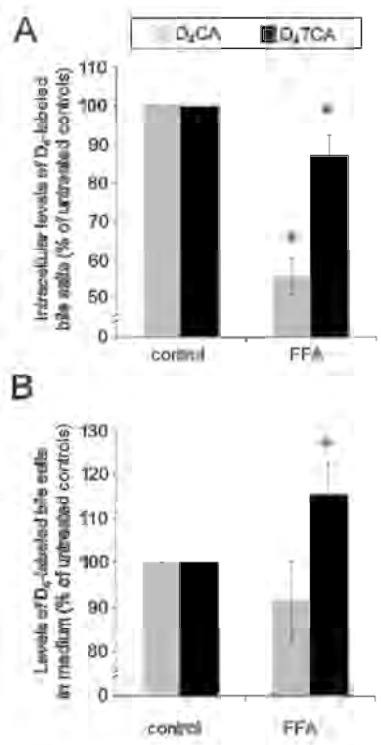

Figure 6. FFA treatment increases D_4CA to D_4TCA conversion by rat hepatocytes

Intracellular levels (A) and medium concentrations (B) of D_4CA (grey bars) and D_4TCA (black bars) 3 h after adding 100 µM D_4CA to the culture medium of control and FFA-treated hepatocytes. Data are presented as relative concentrations compared to control cells. Intracellular levels of both D_4CA and D_4CA are significantly reduced in FFA-treated hepatocytes, while D_4TCA levels in the medium of FFA-treated hepatocytes are significantly increased. The increased D_4TCA concentrations in the medium of FFA treated hepatocytes indicate a higher conjugation and transport rate of taurine conjugated cholate compared to control hepatocytes.
Differences between D_4CA and D_4TCA levels of control and FFA treated hepatocytes were evaluated with a Kruskal-Wallis H-test Differences shown are statistically significant at *$p<0,05$.

siRNA-mediated repression of Pmp70 reverses the FFA-induced CA to TCA conversion.

To determine whether Pmp70 plays a role in this process, we combined the FFA-exposure with *Abcd3*-directed siRNA treatment in order to selectively prevent the induction of Pmp70. Primary rat hepatocytes were transfected with control (Mrp1/*Abcc1*) or Pmp70/*Abcd3*-specific siRNA duplexes followed by a 24 h exposure to 50 µM FFA. FFA-treatment lead to a strong induction of *Abcd3* mRNA and Pmp70 protein levels, which was almost completely suppressed when co-treated with *Abcd3*-siRNA (Fig. 7A). Both FFA-exposure and siRNA-treatment did not change the mRNA levels of Bal and Baat (Fig. 7B). Next, the FFA/siRNA-treated rat hepatocytes were exposed for 3 h to D_4CA after which intracellular and extracellular levels of D_4CA and D_4TCA were determined. As can be seen in Figure 8, *Abcd3*-siRNA treatment (partly) reversed the FFA-induced effect on D_4CA conjugation and transport, leading to increased cellular levels of D_4CA and D_4TCA and decreased levels of D_4TCA in the medium.

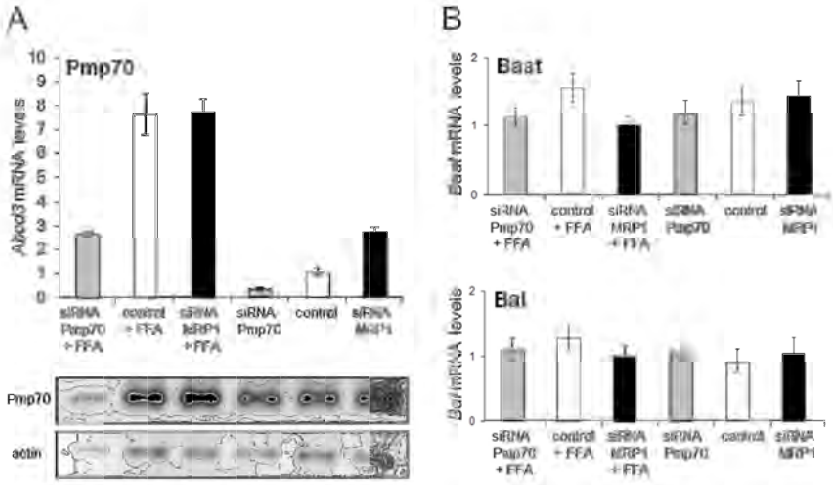

Figure 7. *Abcd3*-targeted siRNA strongly suppresses the FFA-induced expression of Pmp70 in rat hepatocytes without affecting other proteins involved in bile acid (re)conjugation

Cultured rat hepatocytes were co-treated with FFA and *Abcd3*-specific siRNA duplexes leading to a strong suppression of the FFA-induced *Abcd3* mRNA (A, upper panel)) and Pmp70 protein (A, lower panel). *Abcc1* (Mrp1)-specific siRNA duplexes served as controls. B) FFA-treatment and/or siRNA transfections did not significantly affect mRNA levels of Baat and Bal/Fatp5. PCR data are given as fold induction normalized to 18S. b-actin was used as loading control in Western blot analyses.

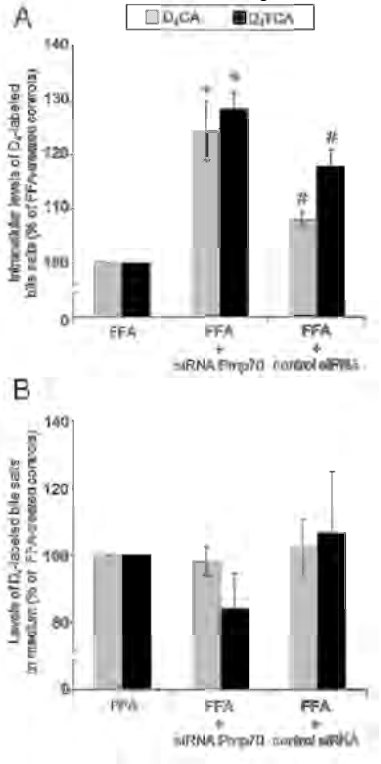

Figure 8. Small interfering RNA-mediated repression of Pmp70 reverses the FFA induced D_4CA to D_4TCA conversion.

Intracellular levels (A) and medium concentrations (B) of D_4CA (grey bars) and D_4TCA (black bars) 3 h after adding 100 µM D_4CA to the culture medium of FFA-treated hepatocytes with and without co-treatment with *Abcd3*-specific siRNA (Pmp70) or *Abcc1*-specific siRNA (control). Data are presented as relative concentrations compared to FFA-treated hepatocytes. Intracellular levels of both D_4CA and D_4CA are significantly increased in FFA/*Abcd3*-siRNA treated hepatocytes compared to FFA- and FFA-*Abcc1* siRNA-treated hepatocytes (A). Medium concentrations of D_4TCA are reduced in FFA/*Abcd3*-siRNA treated hepatocytes compared to FFA- and FFA-*Abcc1* siRNA-treated hepatocytes, though not statistically significant (p=0,13 and 0,44 respectively). D_4CA and D_4TCA levels of the FFA treated group were compared to *Abcd3*-siRNA/FFA treated cells with Student's t-test. Differences between these two groups are statistically significant with *p<0,05.
The FFA/control siRNA group also shows an increase in intracellular D_4-bile salt levels, it is however significantly lower from the *Abcd3*-siRNA/FFA hepatocytes (Student's t-test, #p<0,05).
In combination with data presented in Fig. 7, these results show that selective repression of Pmp70 expression leads to the accumulation of D_4CA and D_4TCA in hepatocytes, while it reduces the levels of D_4TCA excreted to the medium.

DISCUSSION

In this study, we examined the putative role of Pmp70 in glycine/taurine conjugation and/or transhepatocyte transport of externally added cholic acid (CA) by primary rat hepatocytes. Induction of Pmp70 by the PPARα ligand fenofibric acid (FFA) lead to increased conversion of CA to TCA, while simultaneous inhibition of Pmp70 expression through RNA interference suppressed the conversion of TCA leading to reduced concentrations of TCA in de medium. In addition, intracellular levels of CA and TCA decreased in FFA-treated rat hepatocytes, which were increased again when co-treated with Pmp70-specific RNA interference. These data suggest the involvement of Pmp70 in transcellular bile salt transport and/or conjugation to taurine.

Peroxisomes house the enzymes for the final steps in bile salt synthesis. This includes bile acid-coenzyme A:amino acid N-acyltransferase (Baat) that conjugates taurine or glycine to *de novo* synthesized chenodeoxycholic acid (CDCA) and cholic acid (CA). Baat is also essential for reconjugation of bile salts that are deconjugated by intestinal bacteria and return to the liver. Thus, for the efficient taurine/glycine conjugation, bile salt (-intermediates) are transported in and out peroxisomes. Protein-mediated transport of the C_{27} bile acid biosynthesis intermediates 3 alpha,7 alpha,12 alpha-trihydroxy-5 beta-cholestanoic acid (THCA) and 3 alpha,7 alpha-dihydroxy-5 beta-cholestanoic acid (DHCA) across peroxisomal membranes, as well as the primary bile salts GCA and TCA, has been previously demonstrated (15, 16). Transport of THCA and DHCA, especially their CoA-activated forms, was shown to be stimulated by ATP, while transport of GCA and TCA was not. Moreover, transport of THCA-CoA was inhibited by N-ethymaleimide, sodium azide and verapamil, known inhibitors of ABC-transporters. Irrespective of the biochemical characteristics of the putative peroxisomal bile salt transporters, the identity of the peroxisomal bile salt transporters remains elusive so far.

Pmp70 is a likely candidate to act as importer for bile salt (-intermediates) into peroxisomes. It is highly expressed in hepatocyte peroxisomes and its topology suggests it to transport substrates into peroxisomes. It is an ABC transporter requiring ATP to efficiently transport substrates, even against steep concentration gradients. Indeed, unpublished studies have been reported that suggest a role for Pmp70 in the transport of bile acid intermediates, however, no experimental data are publicly available yet to firmly support this claim (33, 34). More solid evidence is available to show that Pmp70 translocates CoA-activated long chain fatty acids into peroxisomes (18, 19), but this does not exclude a possible involvement of Pmp70 in transport of bile salt intermediates, as many ABC transporters have a broad substrate specificity.

Here, we analyzed the putative role of Pmp70 in the process of bile acid re-conjugation of C_{24} bile salts that reside in the pool of enterohepatic cycling bile salts. (see figure 9).

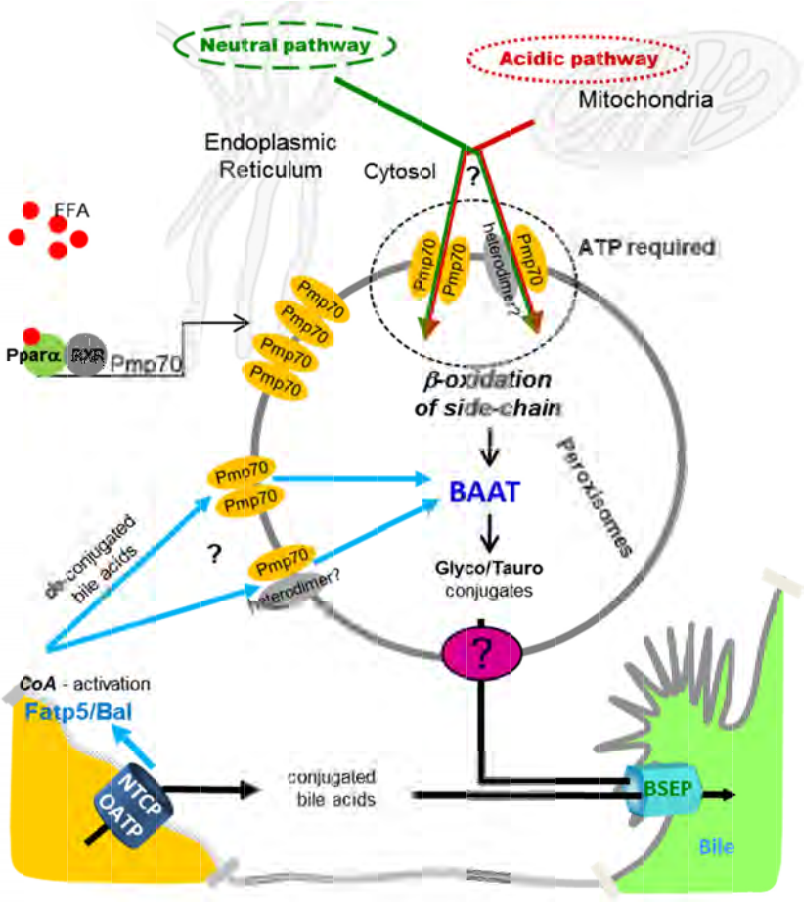

Figure 9. Putative role of Pmp70 in peroxisomal import of CoA-activated de-conjugated bile acids.

A model where Pmp70 plays a general role in (putative) import of both bile acid intermediates and de-conjugated bile salts returning from enterohepatic circulation for their conjugation inside peroxisomes.
Fenofibric acid (FFA-red dots) activates Pparα, which heterodimerizes with Rxr. Pparα/Rxr heterodimer binds to PPRE located in the Pmp70 promoter, which results in Pmp70 upregulation. Pparα activation does not result in Aldp upregulation (Aldp and other possible heterodimerizing partners are shown in grey oval) - one of possible heterodimerizing partners of Pmp70 (ALDPR and P70R). Pmp70 (putative) heterodimerization is proposed since different substrates (originating from *de novo* synthesis bile salt intermediates and de-conjugated bile acids) are expected to be imported into peroxisomes for their further processing. It is possible however, that Pmp70 might facilitate their import as a homodimer. It has been established that peroxisomal import of bile acid-intermediates (green and red arrows) is ATP-dependent (dotted circle). The bile salt peroxisomal export has been found to be ATP-independent (pink oval).

Pmp70 expression was manipulated by treatment of primary rat hepatocytes with fenofibric acid (FFA) with or without co-treatment with Pmp70-specific siRNA. Unfortunately, Pmp70 protein expression could not be significantly reduced in control hepatocytes using siRNA. Even though mRNA levels of *Abcd3* were strongly reduced 16 h after transfection, Pmp70 protein levels remain comparable to control-transfected rat hepatocytes. This suggests that Pmp70 is a relatively stable protein in primary rat hepatocytes. Using the same experimental setup, we have been able to effectively reduce protein levels of caveolin-1 in primary rat hepatocytes (32). Successful siRNA-mediated Pmp70 silencing has been reported for C6 rat glial cells (35). These cells are highly proliferative in culture, while primary rat hepatocytes are not, which may be the main reason why Pmp70 protein reduction was not detected in the later cells.

Consequently, we needed to design an alternative approach to manipulate Pmp70 levels in rat hepatocytes. We aimed to increase the Pmp70 expression level by treating rat hepatocytes with FFA and analyze the effect on taurine conjugation and transcellular transport of D_4CA. As FFA activates PPARα and will change expression of multiple genes (24, 26, 36, 37), we determined Pmp70-specific effects on CA conjugation and transport by preventing induction of Pmp70 through FFA by co-treatment with siRNA.

FFA rapidly induced *Abcd3* mRNA levels in culture rat hepatocytes, which was mirrored by a rapid (within 24 h) and strong (5-10 fold) induction of Pmp70 protein. FFA-treated rat hepatocytes exposed for 3 h to 100 μM D_4CA showed a clear reduction in intracellular accumulation of D_4CA and D_4TCA in conjunction with a small, but significant increase in D_4TCA in the medium. Importantly, expression of other genes/proteins in the D_4CA conjugation and transport cascade, e.g. Ntcp(*Slc10a1*), Bal/Fatp5, Baat and Bsep (*Abcb11*), was not significantly changed by the 24 h treatment with FFA.

Although reduced levels of Baat have been reported in livers of mice fed with PPARα agonists (12), we did not observe this in short-term FFA-exposed primary rat hepatocytes. Reduced Baat expression *in vivo* may thus be caused by secondary factors (e.g. long-term dietary effect) unrelated to transcriptional regulation by PPARα.

To establish a direct effect of Pmp70 in the D_4CA conjugation and transport process, we combined the FFA exposure with *Abcd3*-targeted siRNA treatment. Indeed, the FFA-induced expression of Pmp70 was strongly suppressed by the co-treatment with siRNA. These cells showed increased intracellular levels of D_4CA and D_4TCA again with reduced accumulation of D_4TCA in the medium. Taken together, these data suggest a direct role for Pmp70 in taurine conjugation and/or transcellular transport of CA in hepatocytes and thus plays a role in maintaining high levels of conjugated bile salts in the pool that cycle between the liver and intestine.

A limitation of our study is the relative small effect that is observed on CA conjugation and transport in relation to the strong changes in Pmp70 expression. Rat hepatocytes contain high amounts of Pmp70, which may be involved in

transport of a variety of different substrates, including bile salt (intermediate)s. The Pmp70 levels in control cells may therefore be largely sufficient to accommodate the flux of CA-metabolites in our *in vitro* assay. Still, FFA-induction of Pmp70 and RNAi-mediated inhibition of Pmp70 showed consistent effects on CA conjugation and transcellular transport, implying a role for this protein in this process. Obviously, a full knock down of Pmp70 expression, either *in vitro* or *in vivo*, may definitely establish the role of Pmp70 in transport of bile salt (intermediates) into the peroxisome. In this respect, it is encouraging that unpublished data suggest that bile salt intermediates accumulate in the *Abcd3* knock out mouse. On the other hand, bile salt conjugation may not be completely blocked in the absence of Pmp70 as peroxisomes treated with proteinase K still show uptake of THCA and THCA-CoA (16). Thus, also passive diffusion may partly compensate for the absence of transporter-mediated import of bile salt (intermediates) into peroxisomes. Pmp70 deficiency may therefore not result in a strong phenotype as observed for patients with genetic defects in bile salt biosynthesis, transport or in patients with peroxisome biogenesis disorders (1, 2, 34, 38-42). On the other hand, it appears likely that Pmp70 is also involved in transport of other substrates, like long chain fatty acids, as it is broadly expressed in many tissues, e.g. not restricted to digestive organs that metabolize and transport bile salts.

It seems likely that one transporter is responsible for both the import of C_{27} (*de novo* synthesis) and C_{24} (enterohepatic cycling) of bile salt (intermediates) into peroxisomes. However, two separate transporters with high substrate specificity cannot be excluded at this moment. Alternatively, Pmp70 may form heterodimers with other peroxisomal ABC transporters, like ALDP (*Abcd1*) or ALDPR (*Abcd2*) and thereby form transporters with specific affinities for selected substrates. This could be a potent regulatory mechanism for peroxisomal bile salt transport activities. Peroxisomal transport would then be an extremely flexible and efficient process: when necessary, new transporter formulations could be formed in an immediate response to changing substrate demands (see Figure 9). ALDP-deficiency in adrenoleukodystrophy, however, is not associated with changes in the bile salt profile, thus it is not an obligate partner for Pmp70 in transport of bile salt (intermediates) (43).

In conclusion, our data provide first experimental evidence that Pmp70 is involved in the import of bile salt intermediates into hepatocyte peroxisomes. Future experiments with whole body- or liver-specific knock-down of Pmp70 in mice need to reveal its effect on bile salt homeostasis *in vivo* to establish if defects in peroxisomal bile salt transport machinery may contribute to cholestatic disorders.

References

1. Hofmann AF. Biliary secretion and excretion in health and disease: current concepts. Ann Hepatol 2007;6:15-27.
2. Russell DW. The enzymes, regulation, and genetics of bile acid synthesis. Annu Rev Biochem 2003;72:137-174.
3. Falany CN, Johnson MR, Barnes S, Diasio RB. Glycine and taurine conjugation of bile acids by a single enzyme. Molecular cloning and expression of human liver bile acid CoA:amino acid N-acyltransferase. J Biol Chem 1994;269:19375-19379.
4. Garbutt JT, Wilkins RM, Lack L, Tyor MP. Bacterial modification of taurocholate during enterohepatic recirculation in normal man and patients with small intestinal disease. Gastroenterology 1970;59: 553-566.
5. Gurantz D, Schteingart CD, Hagey LR, Steinbach JH, Grotmol T, Hofmann AF. Hypercholeresis induced by unconjugated bile acid infusion correlates with recovery in bile of unconjugated bile acids. Hepatology, 1991;13:540-550.
6. Inoue Y, Yu AM, Inoue J, Gonzalez FJ. Hepatocyte nuclear factor 4alpha is a central regulator of bile acid conjugation. J Biol Chem. 2004 Jan 23;279(4):2480-9.
7. Watkins PA. Very-long-chain acyl-CoA synthetases. J Biol Chem. 2008 Jan 25;283(4):1773-7.
8. Mihalik SJ, Steinberg SJ, Pei Z, Park J, Kim DG, Heinzer AK, et al. Participation of two members of the very long-chain acyl-CoA synthetase family in bile acid synthesis and recycling. J Biol Chem 2002;277: 24771-24779.
9. Doege H, Baillie RA, Ortegon AM, Tsang B, Wu Q, Punreddy S, et al. Targeted deletion of FATP5 reveals multiple functions in liver metabolism: alterations in hepatic lipid homeostasis. Gastroenterology 2006;130:1245-1258.
10. He D, Barnes S, Falany CN. Rat liver bile acid CoA:amino acid Nacyltransferase: expression, characterization, and peroxisomal localization. J Lipid Res 2003;44:2242-2249.
11. Solaas K, Ulvestad A, Soreide O, Kase BF. Subcellular organization of bile acid amidation in human liver: a key issue in regulating the biosynthesis of bile salts. J Lipid Res 2000;41:1154-1162.
12. Solaas K, Kase BF, Pham V, Bamberg K, Hunt MC, Alexson SE. Differential regulation of cytosolic and peroxisomal bile acid amidation by PPAR alpha activation favors the formation of unconjugated bile acids. J Lipid Res 2004;45:1051-1060.
13. Pellicoro A, van den Heuvel FA, Geuken M, Moshage H, Jansen PL, Faber KN. Human and rat bile acid-CoA:amino acid N-acyltransferase are liver-specific peroxisomal enzymes: implications for intracellular bile salt transport. Hepatology 2007;45:340-348.
14. Rembacz KP, Woudenberg J, Hoekstra M, Jonkers EZ, van den Heuvel FA, Buist-Homan M, Woudenberg-Vrenken TE, Rohacova J, Marin ML, Miranda MA, Moshage H, Stellaard F, Faber KN. Unconjugated bile salts shuttle through hepatocyte peroxisomes for taurine conjugation. Hepatology. 2010 Dec;52(6):2167-76.
15. Visser W.F., van Roermund C.W., Ijlst L., Waterham H.R., Wanders R.J.: Demonstration of bile acid transport across the mammalian pe¬roxisomal membrane. Biochem. Biophys. Res. Commun., 2007; 357: 335–340
16. Une M, Iguchi Y, Sakamoto T, Tomita T, Suzuki Y, Morita M, Imanaka T. ATP-dependent transport of bile acid intermediates across rat liver peroxisomal membranes. J Biochem. 2003 Aug;134(2):225-30
17. Berger J, Albet S, Bentejac M, Netik A, Holzinger A, Roscher AA, et al. The four murine peroxisomal ABC-transporter genes differ in constitutive, inducible and developmental expression. Eur J Biochem 1999;265:719-727.
18. Kemp S, Pujol A, Waterham HR, van Geel BM, Boehm CD, Raymond GV, et al. ABCD1 mutations and the X-linked adrenoleukodystrophy mutation database: role in diagnosis and clinical correlations. Hum Mutat 2001;18:499-515.
19. Imanaka T, Aihara K, Takano T, Yamashita A, Sato R, Suzuki Y, et al. Characterization of the 70-kDa peroxisomal membrane protein, an ATP binding cassette transporter. J Biol Chem 1999;274:11968-11976.
20. Kamijo K, Taketani S, Yokota S, Osumi T, Hashimoto T The 70-kDa peroxisomal membrane protein is a member of the Mdr (P-glycoprotein)-related ATP-binding protein superfamily. J Biol Chem. 1990; 265:4534–4540.
21. Kashiwayama Y., Morita M., Kamijo K., Imanaka T. Nucleotide-induced conformational changes of PMP70, an ATP binding cassette transporter on rat liver peroxisomal membranes. Biochem Biophys Res Commun 2002 291:1245–1251
22. Liu LX, Janvier K, Berteaux-Lecellier V, Cartier N, Benarous R, Aubourg P. Homo- and heterodimerization of peroxisomal ATP-binding cassette half-transporters. J Biol Chem. 1999 Nov 12;274(46):32738-43.
23. Hillebrand M, Verrier SE, Ohlenbusch A, Schäfer A, Söling HD, Wouters FS, Gärtner J. Live cell FRET microscopy: homo- and heterodimerization of two human peroxisomal ABC transporters, the adrenoleukodystrophy protein (ALDP, ABCD1) and PMP70 (ABCD3). J Biol Chem. 2007 Sep 14;282(37):26997-7005.
24. Sinal CJ, Yoon M, Gonzalez FJ. Antagonism of the actions of peroxisome proliferator-activated receptor-alpha by bile acids. J Biol Chem. 2001 Dec 14;276(50):47154-62
25. Hunt MC, Yang YZ, Eggertsen G, Carneheim CM, Gåfvels M, Einarsson C, Alexson SE. The peroxisome proliferator-activated receptor alpha (PPARalpha) regulates bile acid biosynthesis. J Biol Chem. 2000 Sep 15;275(37):28947-53.
26. Forman BM, Chen J, Evans RM. The peroxisome proliferator-activated receptors: ligands and activators. Ann N Y Acad Sci. 1996 Dec 27;804:266-75.
27. Issemann, I. & Green, S. Activation of a member of the steroid hormone receptor superfamily by peroxisome proliferators. Nature 347, 645-650 (1990).
28. Vrenken TE, Buist-Homan M, Kalsbeek AJ, Faber KN, Moshage H. The active metabolite of leflunomide, A77 1726, protects rat hepatocytes against bile acid-induced apoptosis. J Hepatol 2008;49:799-809.
29. Blokzijl H, Vander Borght S, Bok LIH, Libbrecht L, Geuken M, Van den Heuvel FAJ, Dijkstra G, Roskams TA, Moshage H, Jansen PL, Faber KN. Decreased P-glycoprotein (P-gp/MDR1) expression in inflamed human intestinal epithelium is independent of PXR protein levels. Inflamm Bowel Dis 2007;13:710-720.

30. Antonenkov VD, Sormunen RT, Hiltunen JK. The behavior of peroxisomes in vitro: mammalian peroxisomes are osmotically sensitive particles. Am J Physiol Cell Physiol 2004;287:C1623-C1635.
31. Verheyden K, Fransen M, Van Veldhoven PP, Mannaerts GP. Presence of small GTP-binding proteins in the peroxisomal membrane. Biochim Biophys Acta 1992;1109:48-54.
32. Woudenberg J, Rembacz KP, van den Heuvel FA, Woudenberg-Vrenken TE, Buist-Homan M, Geuken M, Hoekstra M, Deelman LE, Enrich C, Henning RH, Moshage H, Faber KN. Caveolin-1 is enriched in the peroxisomal membrane of rat hepatocytes. Hepatology. 2010 May;51(5):1744-53.
33. Visser WF, van Roermund CW, Ijlst L, Waterham HR, Wanders RJ. Metabolite transport across the peroxisomal membrane. Biochem J. 2007 Jan 15;401(2):365-75.
34. Wanders RJA, Visser WF, van Roermund CW, Kemp S, Waterham HR. The peroxisomal ABC transporter family. Pflugers Arch. 2007 Feb;453(5):719-34.
35. Di Benedetto R, Denti MA, Salvati S, Sanchez M, Attorri L, David G, Di Biase A. RNAi-mediated silencing of ABCD3 gene expression in rat C6 glial cells: a model system to study PMP70 function. Neurochem Int. 2008 May;52(6):1106-13.
36. Corton, J. C., Lapinskas, P. J. & Gonzalez, F. J. Central role of PPARalpha in the mechanism of action of hepatocarcinogenic peroxisome proliferators. Mutat. Res. 448, 139-151 (2000).
37. Tugwood, J. D. et al. The mouse peroxisome proliferator activated receptor recognizes a response element in the 5' flanking sequence of the rat acyl CoA oxidase gene. EMBO J. 11, 433-439 (1992).
38. Cai SY, Wang L, Ballatori N, Boyer JL. Bile salt export pump is highly conserved during vertebrate evolution and its expression is inhibited by PFIC type II mutations. Am J Physiol Gastrointest Liver Physiol. 2001 Aug;281(2):G316-22.
39. Wang L, Soroka CJ, Boyer JL.The role of bile salt export pump mutations in progressive familial intrahepatic cholestasis type II. J Clin Invest. 2002 Oct;110(7):965-72.
40. Plass JR, Mol O, Heegsma J, Geuken M, de Bruin J, Elling G, Müller M, Faber KN, Jansen PL. A progressive familial intrahepatic cholestasis type 2 mutation causes an unstable, temperaturesensitive bile salt export pump. J Hepatol. 2004 Jan;40(1):24-30.
41 Ferdinandusse S, Denis S, Faust PL, Wanders RJ. Bile acids: the role of peroxisomes. J Lipid Res. 2009 Nov;50(11):2139-47.
42. Kase BF, Pedersen JI, Strandvik B, Björkhem I. In vivo and vitro studies on formation of bile acids in patients with Zellweger syndrome. Evidence that peroxisomes are of importance in the normal biosynthesis of both cholic and chenodeoxycholic acid. J Clin Invest. 1985 Dec;76(6):2393-402.
43. Van Eldere JR, Parmentier GG, Eyssen HJ, Wanders RJ, Schutgens RB, Vamecq J, Van Hoof F, Poll-The BT, Saudubray JM. Bile acids in peroxisomal disorders. Eur J Clin Invest. 1987 Oct;17(5):386-90.

CHAPTER 4

Lipid rafts are essential for peroxisome biogenesis in HepG2 cells.

Jannes Woudenberg[1], Krzysztof P. Rembacz[1], Mark Hoekstra[1], Antonella Pellicoro[1], Fiona A. J. van den Heuvel[1], Janette Heegsma[1], Sven C. D. van IJzendoorn[2], Andreas Holzinger[3], Tsuneo Imanaka[4], Han Moshage[1], Klaas Nico Faber[1]

[1]Department of Gastroenterology and Hepatology and Department of Cell Biology, University Medical Center Groningen, University of Groningen, Groningen, The Netherlands
[2]Section of Membrane Cell Biology, Department of Cell Biology, University Medical Center Groningen, University of Groningen, Groningen, The Netherlands
[3]Department of Neonatology, Dr. von Hauner's Children's Hospital, Ludwig-Maximilians University, Munich, Germany
[4]Department of Biological Chemistry, Graduate School of Medicine and Pharmaceutical Sciences, University of Toyama, Toyama, Japan

Hepatology. 2010 Aug;52(2):623-33.

Lipid Rafts are Essential for Peroxisome Biogenesis in HepG2 cells

ABSTRACT

Introduction: Peroxisomes are particularly abundant in the liver and are involved in bile salt synthesis and fatty acid metabolism. Peroxisomal membrane proteins (PMPs) are required for peroxisome biogenesis, e.g. the interacting partners Pex13p and Pex14p, and its metabolic function, e.g. the ATP-binding cassette (ABC) transporters ALDP and PMP70. Impaired function of PMPs is the underlying cause of Zellweger syndrome and X-linked adrenoleukodystropy (X-ALD). Here, we studied for the first time the putative association of PMPs to cholesterol-enriched lipid rafts and their function in peroxisome biogenesis.
Material and methods: Lipid rafts were isolated from Triton X-100- or Lubrol WX-lyzed HepG2 cells and analyzed for the presence of various PMPs by western blotting. Lovastatin and methyl-β-cyclodextrin were used to deplete cholesterol and disrupt lipid rafts in HepG2 cells, followed by immunofluorescence microscopy to determine the subcellular location of catalase and PMPs. Cycloheximide was used to inhibit protein synthesis. GFP-tagged fragments of PMP70 and ALDP were analyzed for their lipid raft association.
Results: PMP70 and Pex14p are associated with Triton X-100-resistant rafts, ALDP with Lubrol WX-resistant rafts and Pex13p is not lipid raft associated in HepG2 cells. The minimal peroxisomal targeting signals in ALDP and PMP70 are not sufficient for lipid raft association. Cholesterol depletion leads to dissociation of PMPs from lipid rafts and impaired sorting of newly synthesized catalase and ALDP, but not Pex14p and PMP70. Repletion of cholesterol to these cells efficiently reestablished the peroxisomal sorting of catalase, but not for ALDP.
Conclusions: Human PMPs are differentially associated with lipid rafts independent of protein homology and/or their functional interaction. Cholesterol is required for peroxisomal lipid raft assembly and peroxisome biogenesis.

INTRODUCTION

Peroxisomes are single membrane-bound organelles that are especially abundant in the human liver. They are involved in a wide range of metabolic processes, including β-oxidation of fatty acids, bile acid biosynthesis, plasmalogen biosynthesis and the removal of reactive oxygen species that are generated as a consequence of the high peroxisomal metabolic activity (1, 2). Malfunctioning of peroxisomes is associated with life-threatening diseases like Zellweger Syndrome (ZS) and X-linked adrenoleukodystrophy (X-ALD). ZS is caused by mutations in PEX genes and is characterized by impaired bile salt synthesis leading to the accumulation bile salt intermediates (3). PEX genes encode proteins called peroxins, which are required for the normal biogenesis of peroxisomes. 16 different human peroxins have been identified to date. Most of these proteins are associated with the peroxisomal membrane and function in import of peroxisomal matrix proteins, like catalase and bile acid-CoA:amino acid N-acyltransferase. Pex13p and Pex14p (Fig. 1A) are crucial components for the import of peroxisomal matrix proteins. They physically interact with each other suggesting that they act together in the process of peroxisomal matrix protein import (4, 5).

X-ALD is caused by mutations in the ABCD1 gene encoding the adrenoleukodystrophy protein ALDP. X-ALD is characterized by elevated levels of very long chain fatty acids (VLCFAs) in body fluids and reduced VLCFA β-oxidation in peroxisomes (6). ALDP is an ATP-binding cassette (ABC-) transporter that, together with the highly homologous ALDRP/ABCD2, PMP70/ABCD3 and PMP70R/ABCD4 (PMP69), form the ABCD subfamily (2). ALDP expression is detected in most tissues with moderate levels in the liver. PMP70 is highly expressed in the liver (6). ALDP and PMP70 are thought to be involved in the ATP-dependent transport of VLCFAs and LCFAs across the peroxisomal membrane, respectively. The peroxisomal ABC transporters are so-called half transporters. They contain 6 clustered membrane spanning domains and 1 ATP-binding domain (Fig. 1A). Dimerization leads to the formation of functional substrate pumps resembling the prototypical ABC-transporter, P-glycoprotein/Multidrug resistance 1 protein (P-gp/MDR1). Our knowledge about the functions of peroxins and peroxisomal substrate transporters is steadily increasing, but remarkably little is known about the embedding of these peroxisomal membrane proteins (PMPs) in the peroxisomal membrane and their association with specific lipids.

Research on protein-lipid interactions has been especially focused on their coexistence in detergent–resistant lipid microdomains, routinely called lipid rafts (7, 7, 8, 8). Plasma membrane lipid rafts are enriched in cholesterol and (glyco)sphingolipids as well as specific membrane proteins. Biochemically, lipid rafts are characterized by their insolubility in non-ionic detergents (typically Triton X-100) at low temperatures and their subsequent buoyancy in sucrose flotation gradients. They function in protein trafficking, signal transduction, organization of the cytoskeleton, and pathogen internalization (9-11). Moreover, lipid raft-

association may directly regulate the activity of substrate transporters, including that of ABC transporters (12-14).
In this study, we analyzed the association of the PMPs Pex13p, Pex14p, ALDP and PMP70 with peroxisomal lipid rafts. Our data reveal the existence of different types of lipid rafts in the peroxisomal membrane and that impaired lipid raft assembly leads to peroxisome biogenesis defects.

EXPERIMENTAL PROCEDURES

Pre-established cell lines and plasmids (15-17), as well as standard culture conditions and procedures for transient transfection, RNA isolation, quantitative Polymerase Chain Reaction (18), SDS-PAGE, western blotting (19) and immunofluorescence microscopy (19) are described in Supplementary Experimental Procedures.

Isolation of detergent-resistant lipid microdomains (lipid rafts)
Lipid rafts were isolated from 1×107 HepG2 cells as described by Slimane et al. (20) with minor modifications. Cells were washed two times in ice-cold HBSS (Invitrogen BV, Breda, The Netherlands) and lysed in 2.5 mL ice-cold TNE buffer (20 mM Tris-HCl pH 7.4, 150 mM NaCl, 1 mM EDTA, 1% Triton X-100 (Sigma-Aldrich, St. Louis, MO, USA) or 1% Lubrol WX (Lubrol 17A17 Serva, Heidelberg, Germany) in the presence of CompleteTM protease inhibitors (Roche, Basel, Switzerland) and 25U/µL Benzonase® (EMD Biosciences, Inc. La Jolla, CA, USA). The cell lysate was passed ten times through a 22g needle and incubated on ice for 30 min. The lysate was mixed 1:1 with 80% (w/v) sucrose in TNE buffer and 4 ml was transferred to the bottom of a 12 mL centrifuge tube and overlaid with 4 mL 35% (w/v) and 4 mL 5% (w/v) sucrose in TNE buffer. The remainder of the lysate in 40% (w/v) sucrose was used as total protein extract (T). The gradients were centrifuged for 20 h at 36,000 rpm at 4°C in a Beckman SW 41 rotor. Fractions of 1 mL were harvested from the top of the gradient. The pellet was resuspended in 1 mL 35% (w/v) sucrose in TNE buffer and saved as pellet fraction (P).

Cholesterol depletion and repletion of HepG2 cells and use of cycloheximide
In order to deplete cholesterol from cellular membranes in vitro, the Lubrol WX-extraction protocol described above was performed in the presence of 10 mM methyl-β-cyclodextrin (m-β-CD; Sigma-Aldrich, St. Louis, MO, USA), followed by flotation gradient centrifugation.
Growing HepG2 cells were depleted from cholesterol (in vivo depletion), by incubating them for 24 h at 37oC in DMEM (without FBS) in the presence of 10 µM lovastatin (Sigma-Aldrich, St. Louis, MO, USA) and/or 2 mM m-β-CD. In selected experiments, HepG2 cells were co-treated with 0.02 mg/mL cycloheximide to inhibit protein synthesis. In order to restore cellular cholesterol levels, 24 h lovastatin/m-β-CD-treated cells were subsequently incubated with preformed

m- β-CD/cholesterol complexes (400 µg/mL cholesterol) in serum free DMEM, essentially as described before (20, 21).

Cholesterol isolation and concentration measurements
Cholesterol was isolated from total cell extracts using the Bligh-Dyer method (22). Cholesterol concentrations were determined spectrophotometrically by a cholesterol oxidase/peroxidase assay (23) and normalized against protein concentrations.

RESULTS

Pex13p, Pex14p, PMP70 and ALDP are differentially associated with lipid rafts.
To determine whether PMPs are associated with detergent-resistant lipid microdomains/lipid rafts, we performed the standard lipid raft-extraction protocol on liver-derived human HepG2 cells using Triton X-100 or Lubrol WX, followed by flotation gradient centrifugation. Figure 1D shows that cytosolic proteins (GAPDH, actin) and the peroxisomal matrix protein catalase were solely detected in the bottom fractions (8-12) of the gradient after Triton X-100 extraction, whereas significant amounts of lipid raft markers (c-Src, flotillin) were detected in fraction 4 and 5. PMP70 and Pex14p showed a similar gradient distribution as c-Src, suggesting that these proteins are, at least partly, associated with lipid rafts (quantification shown in supplementary Fig. S1A). In contrast, ALDP and Pex13p were only detected in the bottom (solubilized protein) fractions of the gradient. To detect less stringent association to lipid rafts, HepG2 cells were also extracted by Lubrol WX (Fig. 1C and E). The distribution of marker proteins (GAPDH, actin, catalase, flotillin and c-Src) shows that cellular membranes are efficiently disrupted by Lubrol WX and that lipid rafts float to fractions 4 to 6. Total protein concentrations were slightly higher in fractions 4-6 after Lubrol WX-extraction (Fig. 1C) compared to Triton X-100 (Fig. 1B), confirming the lower stringency of the detergent. As expected, PMP70 and Pex14p were predominantly present in fractions 4 to 6 after Lubrol WX extraction (Fig. 1E). In addition, peak fractions of ALDP were also observed in these fractions, while Pex13p was solely detected in the bottom gradient fractions (Figs. 1E and S1B).
These data show that PMPs have differential extractability by Triton X-100 and Lubrol WX, implying a different environment of these proteins in the peroxisomal lipid bilayer.

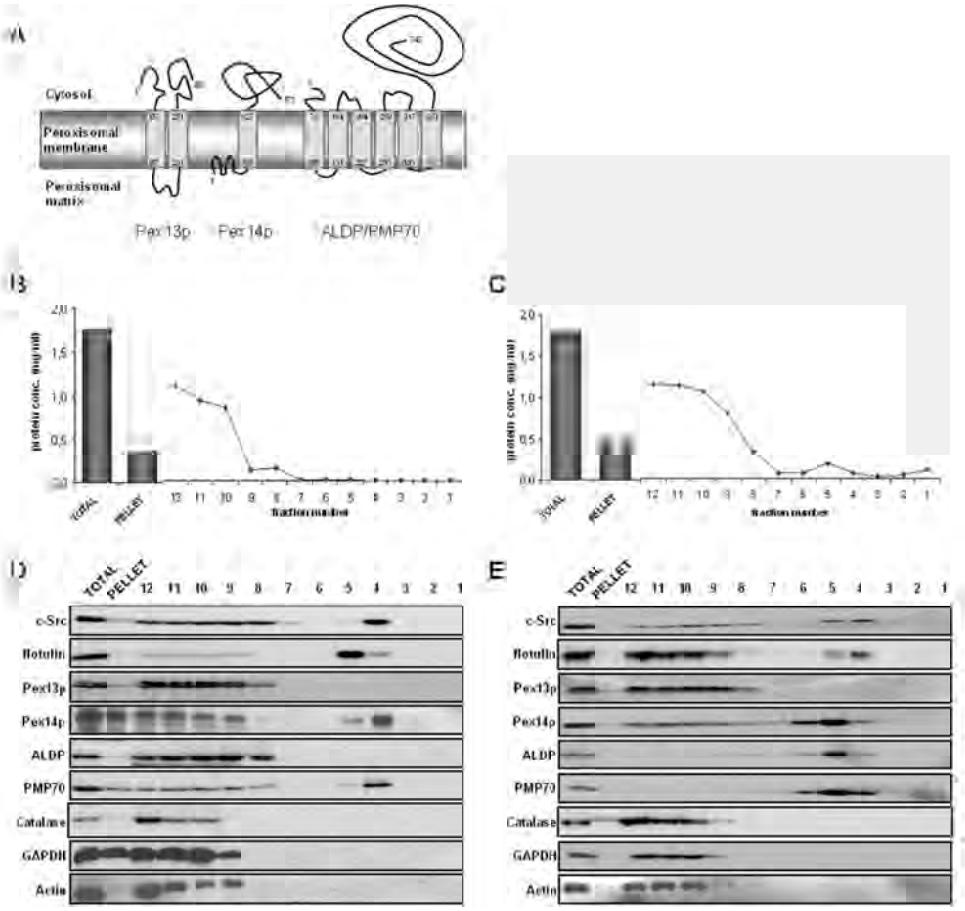

Figure 1. Membrane topology of the human PMPs analyzed in this study and their association with Triton X-100- and Lubrol WX-resistant lipid rafts in HepG2 cells. (A) Schematic representation of the most accepted models for the membrane topology of the human PEX13p, PEX14p, ALDP and PMP70. Numbers indicate amino acid positions. ALDP and PMP70 are highly homologous proteins with comparable membrane topology. The amino acid positions for ALDP are indicated. Human HepG2 cells were lysed in the presence of 1% Triton X-100 (B,D) or 1% Lubrol WX (C,D) followed by flotation gradient centrifugation. One (1) ml fractions (in total 12) were collected from the top and analyzed for protein concentration (B,C) and for western blot analysis (D,E). Equal volumes from the gradient fractions were analyzed using specific antibodies against the lipid raft markers c-Src and flotillin, the non-lipid raft markers β-actin and GAPDH, the peroxisomal matrix protein catalase and peroxisomal membrane proteins Pex13p, Pex14p, ALDP and PMP70 (D,E). Equal volumes of the unfractionated total protein lysate (T) as well as the pellet fraction after flotation gradient centrifugation (P) were also analyzed. Quantification of 3 independent extraction experiments is show in supplementary Figure 1S.

PMPs dissociate from Lubrol WX-lipid rafts after cholesterol depletion of HepG2 membranes in vitro.

Proteins dissociate from lipid rafts when the membrane cholesterol content is reduced (24). To analyze the cholesterol requirement for PMP lipid raft association, HepG2 cells were extracted with Lubrol WX in the presence of 10 mM methyl-β-cyclodextrin (m-β-CD) followed by flotation gradient centrifugation. Figure 2 shows that this results in a shift of peak fractions of c-Src and all lipid raft-associated PMPs from fractions 4-6 to the lower fractions of the gradient. Notably, c-Src is detected in fraction 9 to 12 after m-β-CD treatment, while peak levels of ALDP, PMP70 and Pex14p were detected in fractions 8 and 9 at the interface of the 40% and 35% sucrose layers in the gradient. This suggests that the PMPs remain associated with lipids, but with altered flotation behavior compared to cholesterol-containing lipid rafts.

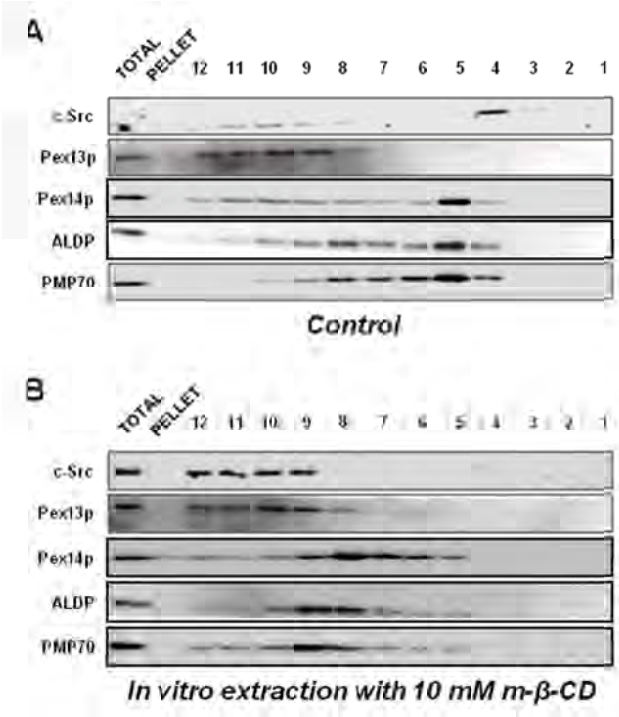

Figure 2. Human PMPs dissociate from Lubrol WX-resistant lipid rafts after *in vitro* cholesterol depletion of HepG2 membranes. Human HepG2 cells were lysed in the presence of 1% Lubrol WX in the absence (A) and presence (B) of 10 mM methyl-β-cyclodextrin followed by flotation gradient centrifugation. Fractions collected from these gradients were analyzed as described in the legend of Figure 1.

PMPs dissociate from Lubrol WX-lipid rafts after cholesterol depletion of HepG2 membranes in vivo.

Next, we aimed to analyze the effect of peroxisomal lipid raft depletion in growing HepG2 cells. Standard protocols that deplete the plasma membrane from cholesterol did not disrupt the raft association of PMPs in HepG2 cells (Fig. S2). Therefore, we optimized the conditions to obtain sufficient depletion of total

cellular cholesterol, including that at intracellular sites. Co-treatment of HepG2 cells with lovastatin (10 µM, cholesterol synthesis inhibitor) and m-β-CD (2 mM) lead to a reduction of over 90% of cellular cholesterol levels (Fig. 3A), which is required to disrupt lipid rafts (25). The larger portion of these cells remained viable as indicated by unchanged transcript and protein expression levels of peroxisomal marker proteins (Fig. 3B and C), no induction of apoptotic markers (caspase-3 activity; Fig. S3A), minor amounts of necrosis (LDH leakage; Fig. S3B) and an active endocytosis pathway (Fig. S3F-H).

Lubrol WX-extraction of lovastatin/m-β-CD treated HepG2 cells revealed that c-Src, PMP70, ALDP and Pex14p were largely absent from the raft-containing fractions 4 and 5 (Fig. 3E, compared to control cells in Fig. 3D). Pex14p and c-Src appeared in fractions 8 to 12, indicating that they were solubilized upon Lubrol WX extraction. In contrast, peak levels of PMP70 and ALDP were detected in fractions 7 and 8 at the 35%-40% sucrose interface similar to the in vitro extraction experiments (Fig. 2). In addition, significant amounts of PMP70, ALDP and Pex14p were detected in the pellet fraction, which may result from aggregation of these PMPs in cholesterol-depleted HepG2 cells either before or during the Lubrol WX-extraction procedure.

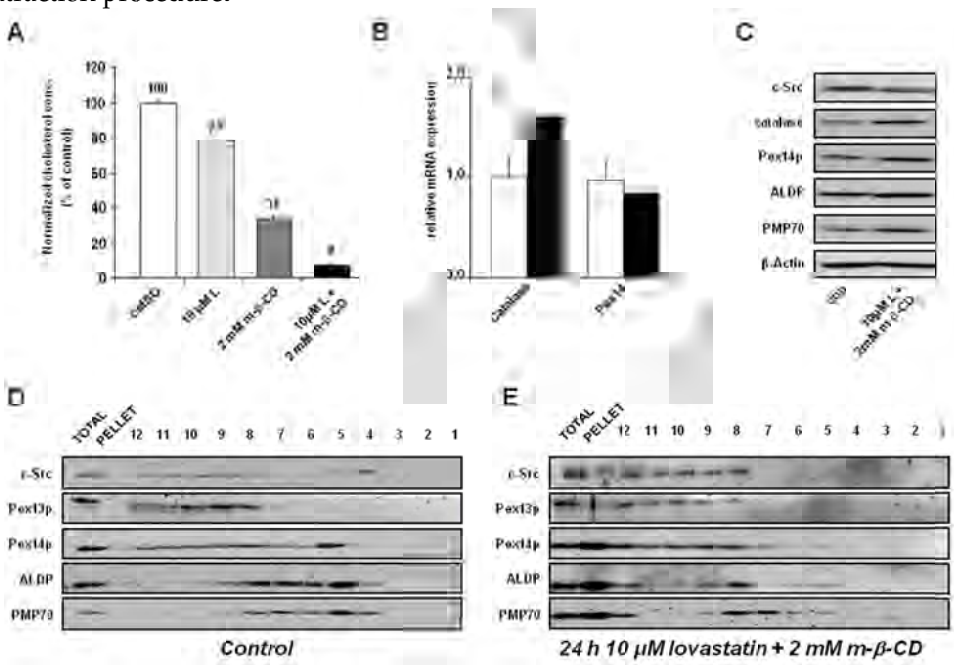

Figure 3. PMPs dissociate from Lubrol WX-resistant lipid rafts after *in vivo* cholesterol depletion of HepG2 membranes. Human HepG2 cells were cultured for 24 h in the presence of 10 µM lovastatin (L), 2 mM methyl-β-cyclodextrin (m-β-CD) or a combination of these 2 compounds. Treatment with 0.1% DMSO (solvent for m-β-CD) served as control. Total cellular cholesterol of treated cells was determined (A). Levels of selected mRNA's (B) and proteins (C) were determined in HepG2 cells treated with a combination of 10 µM lovastatin and 2 mM m-β-CD. Control (D) and L/m-β-CD-treated cells (E) were lysed in the presence of 1% Lubrol WX, followed by flotation gradient centrifugation and gradient fractions were analyzed as described in the legend of Figure 1.

Effect of cellular cholesterol depletion on sorting of PMPs and catalase.
To determine whether cellular cholesterol depletion affects peroxisome biogenesis, we analyzed the subcellular location of PMP70, ALDP, Pex14p and the peroxisomal matrix enzyme catalase in lovastatin/m-β-CD-treated HepG2 cells by immunofluorescence microscopy (Figs. 4, 5 and S4).

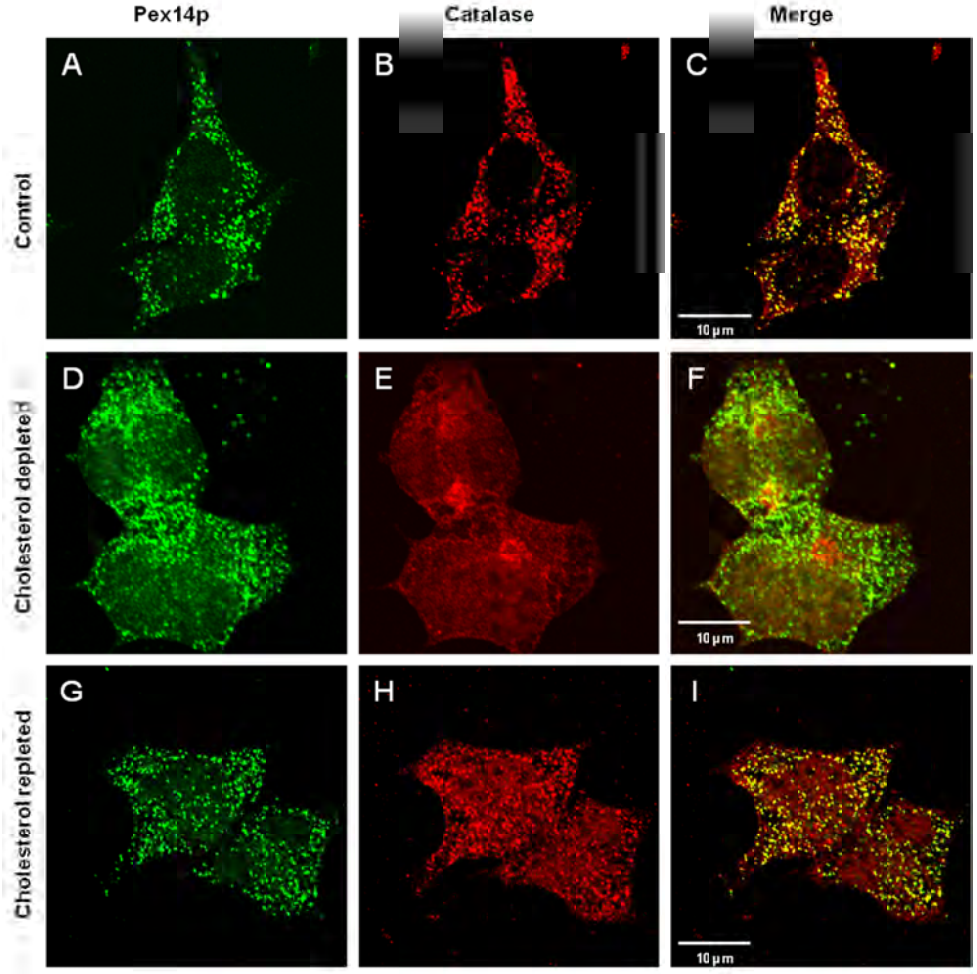

Figure 4. Effect of cholesterol depletion and repletion on the subcellular location of Pex14p and catalase. Human HepG2 cells were cultured for 24 h in the absence (A-C) or presence (D-F) of 10 µM lovastatin and 2 mM methyl-β-cyclodextrin followed by immunofluorescence microscopy to determine the subcellular location of Pex14p (A,D) and catalase (B,E) (merged images in C and F). Cholesterol-depleted HepG2 cells (D-F) were subsequently cultured for 24 h in the presence of exogenously added cholesterol (G-I) and the subcellular location of Pex14p (G) and catalase (H) determined (merged images in I).

A peroxisomal location for all these proteins is detected in untreated HepG2 cells (panels A-C in Figs. 4, 5 and S4). The 24 h lovastatin/m-β-CD treatment lead to the

appearance of a diffuse subcellular location of catalase and ALDP while Pex14p and PMP70 remained localized in peroxisomes (Figs. 4, 5 and S4 panels D-F). The extend of cytosolic staining for catalase was somewhat variable (compare Figs. 4E, 6E, S3F and S4E). The peroxisomal volume in HepG2 cells is approximately 1% of the total cellular volume. As a consequence, catalase is diluted 100-fold in the cytoplasm compared to its peroxisomal location. Any (slight) staining of catalase outside peroxisomes therefore indicates a significant missorting of the protein in (cholesterol-depleted) HepG2 cells. Subsequently, the cholesterol-depleted HepG2 cells were resupplemented with cholesterol and analyzed by immunofluorescence microscopy again after 24 h (Figs. 4, 5 and S4; G-I).

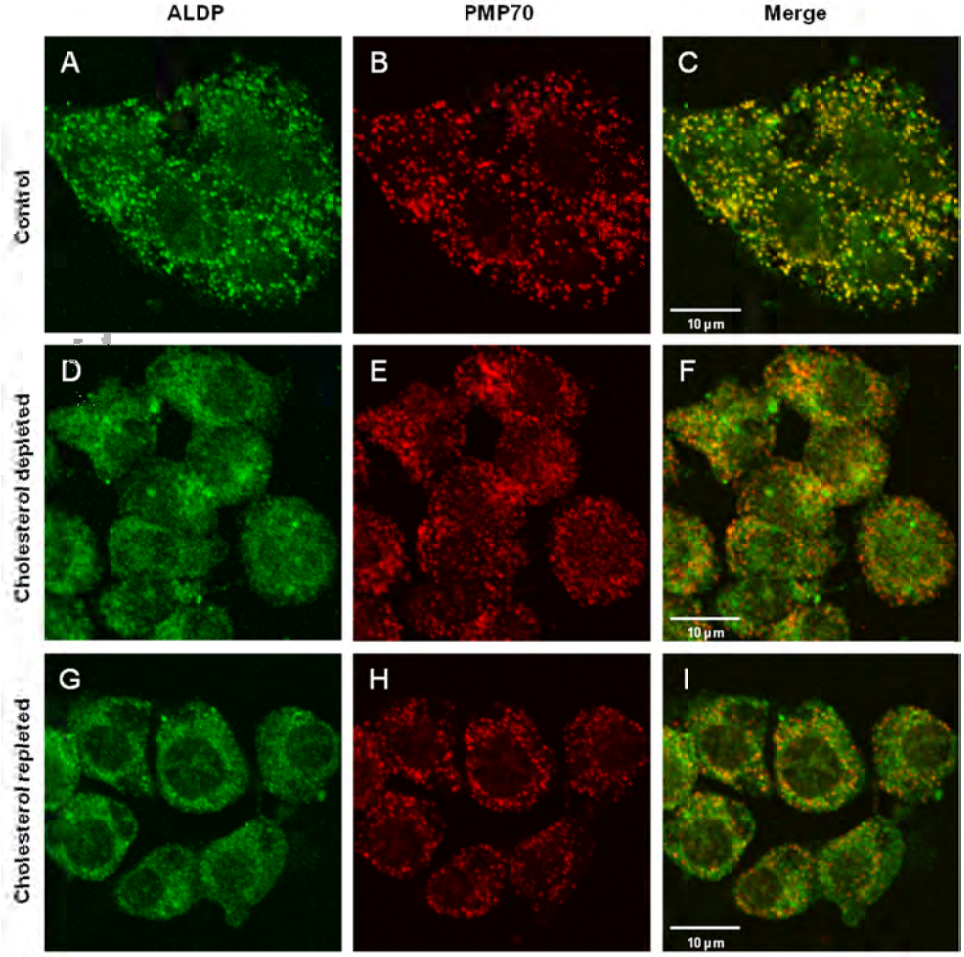

Figure 5. Effect of cholesterol depletion and repletion on the subcellular location of ALDP and PMP70. Human HepG2 cells were cultured for 24 h in the absence (A-C) or presence (D-F) of 10 µM lovastatin and 2 mM methyl-β-cyclodextrin followed by immunofluorescence microscopy to determine the subcellular location of ALDP (A,D) and PMP70 (B,E) (merged images in C and F). Cholesterol-depleted HepG2 cells (D-F) were subsequently cultured for 24 h in the presence of exogenously added cholesterol (G-I) and the subcellular location of ALDP (G) and PMP70 (H) determined (merged images in I).

Catalase staining re-appeared in peroxisomes of cholesterol-repleted HepG2 cells, showing a clear co-localization with Pex14p (Fig. 4; G-I). ALDP staining appeared more heterogeneous after cholesterol repletion. Some dotted colocalization of ALDP with PMP70 and catalase was detected, but mostly a diffuse staining for ALDP was observed (Figs. 5 and S4 respectively; G-I). Importantly, peroxisomal catalase was detected in cells with a diffuse ALDP staining, confirming the recovery of these cells after cholesterol depletion (Figs. S4, lower panels).

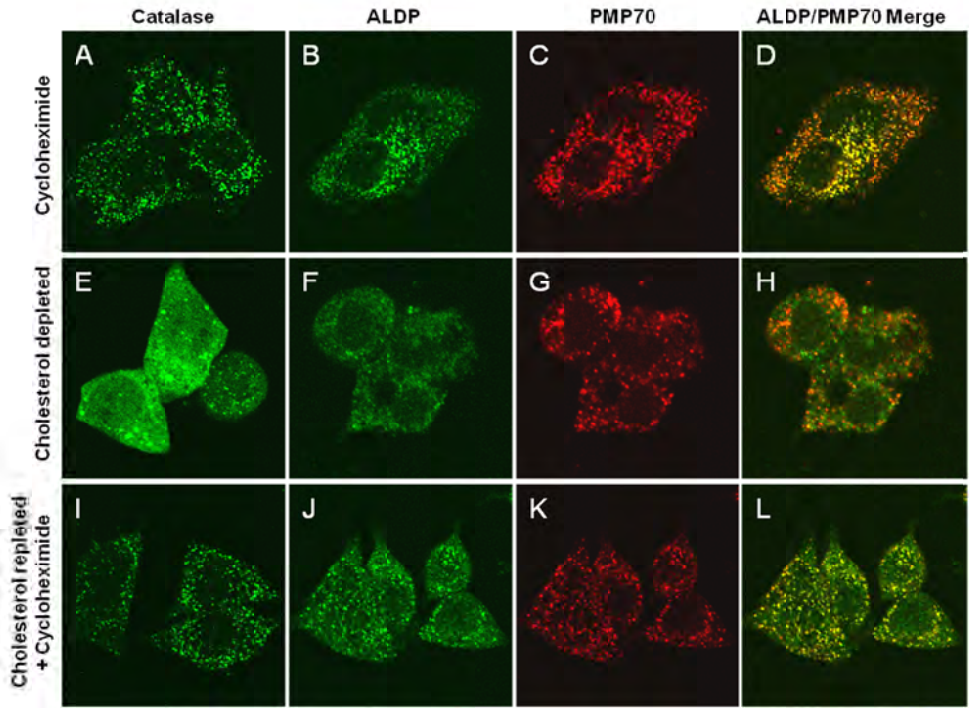

Fig. 6. Impaired sorting of newly synthesized catalase and ALDP in cholesterol-depleted HepG2 cells. Human HepG2 cells were cultured for 24 h in the absence (A-D) or presence (E-L) of 10 µM lovastatin and 2 mM methyl-β-cyclodextrin. Protein synthesis was inhibited during the 24 h period by adding cycloheximide to control cells (A-D) or L/m-β-CD-tread cells (I-L). Immunofluorescence microscopy was used to determine the subcellular location of catalase (A, E, I), ALDP (B, F, J) and PMP70 (C, G, K) (merged images of ALDP and {PMP70 in D, H, L).

To analyze whether the abnormal cellular location of catalase and ALDP in cholesterol-depleted cells is a result of mistargeting of newly synthesized protein or caused by dissociation of existing protein from damaged peroxisomes, we performed the lovastatin/m-β-CD treatment in the absence and presence of the protein synthesis inhibitor cycloheximide (Fig. 6). While a diffuse staining for catalase and ALDP became readily detectable in the absence of cycloheximide (Fig. 6E and F), a predominant peroxisomal staining was detected in lovastatin/m-β-CD/cycloheximide co-treated HepG2 cells (Fig. 6I and J). These data show that cholesterol depletion leads to impaired sorting of newly synthesized catalase and ALDP.

Protein sequences that define lipid raft-association of PMP70 and ALDP

Finally, we determined whether the sequences in PMP70 and ALDP that are required for sorting to the peroxisomal membrane (mPTSs) are also sufficient for lipid raft-association. Previously, it was shown that the N-terminal regions containing the first 2 transmembrane domains (TMDs) of PMP70 (aa1-144) or ALDP (aa1-110 and aa67-164) are sufficient for peroxisomal targeting (16, 17). We transiently expressed these and various other fragments of PMP70 and ALDP fused to GFP or YFP in HepG2 cells, confirmed their peroxisomal targeting in HepG2 cells (data not shown) and performed Lubrol WX extraction to analyze their lipid raft association (Fig. 7). G/YFP-tagged full-length PMP70 and ALDP were detected in gradient fraction 4 and 5, indicating that these hybrid proteins, at least partly, associate with lipid rafts. In contrast, hybrid proteins consisting of GFP and the minimal mPTS-containing regions of PMP70 (aa1-144) or ALDP (aa1-110, aa1-164 and aa67-164) were not detected in the lipid raft-containing fraction 4 and 5. The N-terminal fragments containing the first 4 TMDs of ALDP (aa1-281) or the 6 TMDs of PMP70 (aa1-375) were detected in fractions 4 and 5, indicating that sequences outside the minimal mPTS of PMP70 and ALDP are required for lipid rafts association. For the PMP70-derived hybrid proteins similar results were obtained after Triton X-100 extraction (data not shown).

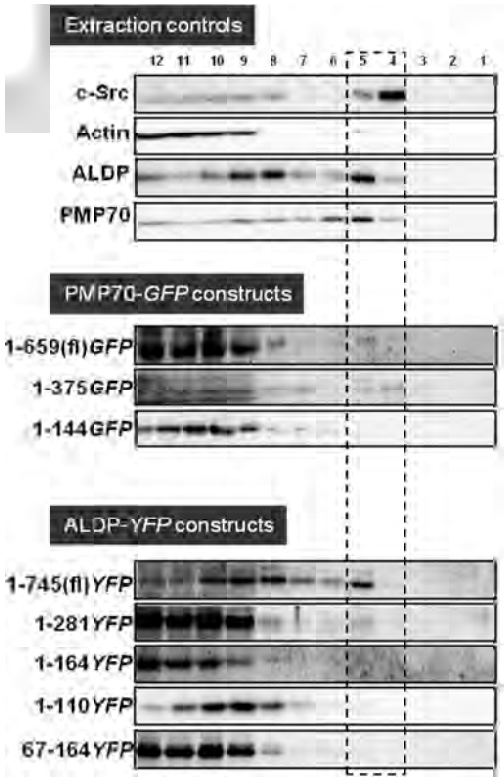

Fig. 7. The peroxisomal targeting signals of PMP70 and ALDP do not drive lipid-raft association. HepG2 cell were transiently transfected with the indicated Y/GFP-tagged fragments of PMP70 and ALDP. 48 h post-transfection, cells were lysed in the presence of 1% Lubrol WX followed by flotation gradient centrifugation. Gradient fractions were analyzed by western blotting as detailed in Figure 1 by using antibodies against GFP and extraction marker proteins c-Src, actin, PMP70 and ALDP. The white star indicates the presence of a non-specific protein cross-reacting with the α-GFP antibody in fractions 9-12.

DISCUSSION

In this study, we show that human peroxisomal membrane proteins are differentially associated with lipid rafts and that sequences other than the peroxisomal membrane targeting signal (mPTS) are required for lipid raft-association. Cholesterol depletion leads to missorting of catalase and ALDP, but not of Pex14p and PMP70. Peroxisomal sorting of catalase is effectively restored upon cholesterol repletion. Thus, cholesterol is required for the assembly of peroxisomal lipid rafts and for efficient peroxisome biogenesis.

Lipid rafts have been detected in plasma membranes and various organellar membranes, but this is the first report that they also exist in mammalian peroxisomal membranes. A clear hierarchy appears to exist in the lipid raft-association of PMPs. The ABC-transporter PMP70 and the peroxin Pex14p show the strongest lipid raft-association of the PMPs studied here. In contrast, the PMP70-homologue, ALDP, is effectively extracted by Triton X-100, but resists Lubrol WX solubilisation. The significance of the behavior of membrane proteins after Lubrol WX extraction, or any other mild detergent, is a matter of debate (26-28). However, the fact that the integral PMP Pex13p is completely extracted by both detergents strongly suggests that ALDP is embedded in a lipid environment different from PMP70, Pex14p and Pex13p.

Pex13p and Pex14p physically interact with each other and with Pex5p, the cycling receptor crucial for targeting of peroxisomal matrix proteins (29-32). Studies with the yeast orthologs showed that the relative amounts of Pex13p and Pex14p must be tightly balanced for normal peroxisome biogenesis (33). In rat liver, however, Pex13p and Pex14p were detected in separate protein complexes in the peroxisomal membrane (34). Our observation that Pex14p and Pex13p show different lipid raft-association characteristics is in line with the existence of separate Pex13p- and Pex14p-containing protein complexes and suggests that their transient interaction is crucial for peroxisome biogenesis.

The cholesterol content in the peroxisomal membrane is low (35). Still, it appears to serve a crucial role in peroxisomal lipid raft assembly and sorting of peroxisomal matrix and membrane proteins. In cholesterol-depleted HepG2 cells, Pex14p and PMP70 become Triton X-100-extractable, but sorting to the peroxisomes is not disturbed for these proteins. In contrast, targeting of catalase and ALDP is impaired under these conditions. This implies that cholesterol depletion leads to selective effects on the sorting of peroxisomal proteins, which is most likely a direct effect of the disruption of peroxisomal lipid rafts. If there would be a basal requirement for cholesterol for peroxisome biogenesis, than a generalized effect on sorting of peroxisomal proteins would be expected when cholesterol levels were insufficient. The peroxisomal sorting of catalase is efficiently re-established when cholesterol is supplied to the cholesterol-depleted HepG2 cells. This is most likely the result of the reestablishment of the lipid raft association of PMPs involved in matrix protein import and the ability of the import machinery to transport fully-

folded and oligomeric proteins (36). Thus, both newly-synthesized catalase and cytosol-accumulated catalase are targeted to peroxisomes when the import machinery is restored. Importantly, cholesterol-depletion does not induce leakage of resident proteins from peroxisomes as shown by cycloheximide co-treatment. Interestingly, cholesterol-repletion did not efficiently restore the peroxisomal location of ALDP. This indicates that missorted ALDP is incompetent to return to peroxisomes of cholesterol-repleted HepG2 cells and that effective targeting of newly-synthesized ALDP is only slowly established in these cells.

To date, the only other report about lipid microdomains in peroxisomal membranes is on ergosterol/ceramide-rich (ECR) domains in peroxisomes of the yeast Yarrowia lipolytica (37). These ECR domains play a role in a complex transition of pre-peroxisomal structures to mature peroxisomes, but it is unclear whether similar mechanisms are involved in human peroxisome biogenesis. Therefore, it remains to be determined whether a functional relationship exists between the human peroxisomal rafts and the Y. lipolytica ECR domains.

The distinct detergent-extractability of ALDP and PMP70 indicate that the lipid environment of these two highly homologous ABC-transporters in the peroxisomal membrane is different. Whether they exist in spatially separated lipid rafts or that different extractability is a result of a heterogeneous lipid distribution within one raft remains to be determined, as for rafts occurring in other cellular membranes (28). Several other ABC transporters, (MDR1/Pgp/ABCB1, MRP1/ABCC1, BCRP/ABCG2) have been shown to reside in lipid rafts and their substrate transporting activity is regulated by their lipid environment (13, 14, 38-41). It is therefore likely that also the activity of PMP70 and ALDP is controlled by their association to specific lipids. The protein-lipid interaction is not (solely) determined by the mPTSs of ALDP and PMP70, since correctly sorted GFP-tagged fragments of ALDP and PMP70 appear not to be lipid raft associated. It is interesting to note that significant amounts of ALDP and PMP70 appear to remain associated with lipids after Lubrol WX-extraction of cholesterol-depleted HepG2 cells, as indicated by their accumulation at the 40%-35% sucrose interphase after flotation gradient centrifugation. Pex14p and c-Src, in contrast, are fully solubilized under these conditions. This may indicate that ALDP and PMP70 are associated with other lipids that reside in the peroxisomal membrane. The slight, but highly reproducible difference in peak fractions of raft-associated c-Src versus PMPs after flotation gradient centrifugation of Lubrol WX-extracted HepG2 cells may be a result of this peroxisome-specific lipid environment.

It is relevant to note that many X-ALD patients are treated with cholesterol lowering drugs like lovastatin and simvastatin (42, 43) aimed to reduce VLCFA levels. In X-ALD patients with residual ALDP protein-activity, cholesterol reduction could theoretically effect the subcellular location of ALDP thereby further reducing its function and aggravating X-ALD disease symptoms. In our HepG2 cells, treatment with lovastatin alone reduced the cellular cholesterol levels to maximally 50% compared to control cells. This reduction did not affect the raft

association of ALDP, nor PMP70 or Pex14p (supplementary Fig. S5). It is therefore unlikely that lovastatin treatment alone will be harmful due to effects on peroxisome biogenesis.

In summary, our data show that PMPs are differentially associated with detergent-resistant lipid rafts. Cholesterol depletion leads to disruption of the lipid raft association and peroxisome biogenesis defects. The role of peroxisomal lipid rafts in diseases where peroxisomes are malfunctioning, e.g. Zellweger Syndrome and X-ALD, needs further analysis.

ACKNOWLEDGEMENTS

Dr. J.W. Kok (Department of Cell Biology, UMCG, Groningen, The Netherlands) is kindly acknowledged for his help and suggestions during this project.

References

1. Wanders RJ, Waterham HR. Biochemistry of mammalian peroxisomes revisited. Annu Rev Biochem 2006;75:295-332.
2. Theodoulou FL, Holdsworth M, Baker A. Peroxisomal ABC transporters. FEBS Lett 2006;580(4):1139-1155.
3. Sundaram SS, Bove KE, Lovell MA, Sokol RJ. Mechanisms of disease: Inborn errors of bile acid synthesis. Nat Clin Pract Gastroenterol Hepatol 2008;5(8):456-468.
4. Williams C, Distel B. Pex13p: docking or cargo handling protein? Biochim Biophys Acta 2006;1763(12):1585-1591.
5. Azevedo JE, Schliebs W. Pex14p, more than just a docking protein. Biochim Biophys Acta 2006;1763(12):1574-1584.
6. Berger J, Albet S, Bentejac M, Netik A, Holzinger A, Roscher AA, et al. The four murine peroxisomal ABC-transporter genes differ in constitutive, inducible and developmental expression. Eur J Biochem 1999;265(2):719-727.
7. Simons K, Ikonen E. Functional rafts in cell membranes. Nature 1997;387(6633):569-572.
8. Brown DA. Lipid rafts, detergent-resistant membranes, and raft targeting signals. Physiology 2006;21:430-439.
9. Brown DA, London E. Functions of lipid rafts in biological membranes. Annual Review of Cell and Developmental Biology 1998;14:111-136.
10. Simons K, Toomre D. Lipid rafts and signal transduction. Nature Reviews Molecular Cell Biology 2000;1(1):31-39.
11. Rajendran L, Simons K. Lipid rafts and membrane dynamics. J Cell Sci 2005;118(Pt 6):1099-1102.
12. Troost J, Lindenmaier H, Haefeli WE, Weiss J. Modulation of cellular cholesterol alters P-glycoprotein activity in multidrug-resistant cells. Molecular Pharmacology 2004;66(5):1332-1339.
13. Dos Santos SM, Weber CC, Franke C, Muller WE, Eckert GP. Cholesterol: Coupling between membrane microenvironment and ABC transporter activity. Biochem Biophys Res Commun 2007;354(1):216-221.
14. Storch CH, Ehehalt R, Haefeli WE, Weiss J. Localization of the human breast cancer resistance protein (BCRP/ABCG2) in lipid rafts/caveolae and modulation of its activity by cholesterol in vitro. J Pharmacol Exp Ther 2007;323(1):257-264.
15. Kashiwayama Y, Asahina K, Shibata H, Morita M, Muntau AC, Roscher AA, et al. Role of Pex19p in the targeting of PMP70 to peroxisome. Biochim Biophys Acta 2005;1746(2):116-128.
16. Kashiwayama Y, Asahina K, Morita M, Imanaka T. Hydrophobic regions adjacent to transmembrane domains 1 and 5 are important for the targeting of the 70-kDa peroxisomal membrane protein. J Biol Chem 2007;282(46):33831-33844.
17. Landgraf P, Mayerhofer PU, Polanetz R, Roscher AA, Holzinger A. Targeting of the human adrenoleukodystrophy protein to the peroxisomal membrane by an internal region containing a highly conserved motif. Eur J Cell Biol 2003;82(8):401-410.
18. Blokzijl H, Vander Borght S, Bok LIH, Libbrecht L, Geuken M, Van den Heuvel FAJ, et al. Decreased P-glycoprotein (P-gp/MDR1) expression in inflamed human intestinal epithelium is independent of PXR protein levels. Inflammatory Bowel Diseases 2007;13(6):710-720.
19. Pellicoro A, van den Heuvel FA, Geuken M, Moshage H, Jansen PL, Faber KN. Human and rat bile acid-CoA:amino acid N-acyltransferase are liver-specific peroxisomal enzymes: implications for intracellular bile salt transport. Hepatology 2007;45(2):340-348.
20. Slimane TA, Trugnan G, van Ijzendoorn SCD, Hoekstra D. Raft-mediated trafficking of apical resident proteins occurs in both direct and transcytotic pathways in polarized hepatic cells: Role of distinct lipid microdomains. Molecular Biology of the Cell 2003;14(2):611-624.
21. Klein U, Gimpl G, Fahrenholz F. Alteration of the myometrial plasma membrane cholesterol content with beta-cyclodextrin modulates the binding affinity of the oxytocin receptor. Biochemistry 1995;34(42):13784-13793.
22. Bligh EG, Dyer WJ. A Rapid Method of Total Lipid Extraction and Purification. Canadian Journal of Biochemistry and Physiology 1959;37(8):911-917.
23. Gamble W, Vaughan M, Kruth HS, Avigan J. Procedure for Determination of Free and Total Cholesterol in Microgram Or Nanogram Amounts

Suitable for Studies with Cultured-Cells. Journal of Lipid Research 1978;19(8):1068-1070.
24. Laliberte JP, McGinnes LW, Peeples ME, Morrison TG. Integrity of membrane lipid rafts is necessary for the ordered assembly and release of infectious newcastle disease virus particles. Journal of Virology 2006;80(21):10652-10662.
25. Foster LJ, De Hoog CL, Mann M. Unbiased quantitative proteomics of lipid rafts reveals high specificity for signaling factors. Proc Natl Acad Sci U S A 2003;100(10):5813-5818.
26. Shogomori H, Brown DA. Use of detergents to study membrane rafts: the good, the bad, and the ugly. Biol Chem 2003;384(9):1259-1263.
27. Chamberlain LH. Detergents as tools for the purification and classification of lipid rafts. FEBS Lett 2004;559(1-3):1-5.
28. Pike LJ. Lipid rafts: heterogeneity on the high seas. Biochem J 2004;378(Pt 2):281-292.
29. Albertini M, Rehling P, Erdmann R, Girzalsky W, Kiel JA, Veenhuis M, et al. Pex14p, a peroxisomal membrane protein binding both receptors of the two PTS-dependent import pathways. Cell 1997;89(1):83-92.
30. Fransen M, Terlecky SR, Subramani S. Identification of a human PTS1 receptor docking protein directly required for peroxisomal protein import. Proceedings of the National Academy of Sciences of the United States of America 1998;95(14):8087-8092.
31. Schliebs W, Saidowsky J, Agianian B, Dodt G, Herberg FW, Kunau WH. Recombinant human peroxisomal targeting signal receptor PEX5. Structural basis for interaction of PEX5 with PEX14. J Biol Chem 1999;274(9):5666-5673.
32. Otera H, Harano T, Honsho M, Ghaedi K, Mukai S, Tanaka A, et al. The mammalian peroxin Pex5pL, the longer isoform of the mobile peroxisome targeting signal (PTS) type 1 transporter, translocates the Pex7p.PTS2 protein complex into peroxisomes via its initial docking site, Pex14p. J Biol Chem 2000;275(28):21703-21714.
33. Bottger G, Barnett P, Klein AT, Kragt A, Tabak HF, Distel B. Saccharomyces cerevisiae PTS1 receptor Pex5p interacts with the SH3 domain of the peroxisomal membrane protein Pex13p in an unconventional, non-PXXP-related manner. Mol Biol Cell 2000;11(11):3963-3976.
34. Reguenga C, Oliveira ME, Gouveia AM, Sa-Miranda C, Azevedo JE. Characterization of the mammalian peroxisomal import machinery: Pex2p, Pex5p, Pex12p, and Pex14p are subunits of the same protein assembly. J Biol Chem 2001;276(32):29935-29942.
35. Lyons HT, Kharroubi A, Wolins N, Tenner S, Chanderbhan RF, Fiskum G, et al. Elevated cholesterol and decreased sterol carrier protein-2 in peroxisomes from AS-30D hepatoma compared to normal rat liver. Arch Biochem Biophys 1991;285(2):238-245.
36. Platta HW, Erdmann R. Peroxisomal dynamics. Trends Cell Biol 2007;17(10):474-484.
37. Boukh-Viner T, Guo T, Alexandrian A, Cerracchio A, Gregg C, Haile S, et al. Dynamic ergosterol- and ceramide-rich domains in the peroxisomal membrane serve as an organizing platform for peroxisome fusion. J Cell Biol 2005;168(5):761-773.
38. Gayet L, Dayan G, Barakat S, Labialle S, Michaud M, Cogne S, et al. Control of P-glycoprotein activity by membrane cholesterol amounts and their relation to multidrug resistance in human CEM leukemia cells. Biochemistry 2005;44(11):4499-4509.
39. Marbeuf-Gueye C, Stierle V, Sudwan P, Salerno M, Garnier-Suillerot A. Perturbation of membrane microdomains in GLC4 multidrug-resistant lung cancer cells--modification of ABCC1 (MRP1) localization and functionality. FEBS J 2007;274(6):1470-1480.
40. Pal A, Mehn D, Molnar E, Gedey S, Meszaros P, Nagy T, et al. Cholesterol potentiates ABCG2 activity in a heterologous expression system: improved in vitro model to study function of human ABCG2. J Pharmacol Exp Ther 2007;321(3):1085-1094.
41. Telbisz A, Muller M, Ozvegy-Laczka C, Homolya L, Szente L, Varadi A, et al. Membrane cholesterol selectively modulates the activity of the human ABCG2 multidrug transporter. Biochim Biophys Acta 2007;1768(11):2698-2713.
42. Di Biase A., Salvati S, Vari R, Avellino C, Sforza F, Cappa M, et al. Susceptibility to oxidation of plasma low-density lipoprotein in X-linked adrenoleukodystrophy: effects of simvastatin treatment. Mol Genet Metab 2000;71(4):651-655.
43. Pai GS, Khan M, Barbosa E, Key LL, Craver JR, Cure JK, et al. Lovastatin therapy for X-linked adrenoleukodystrophy: clinical and biochemical observations on 12 patients. Mol Genet Metab 2000;69(4):312-322.

SUPPLEMENTARY EXPERIMENTAL PROCEDURES

Cell lines, culture conditions and transient transfection
The human hepatoma cell line HepG2 was cultured in Dulbecco's modified Eagle medium (DMEM), supplemented with GlutaMax-1, 4,500 mg/L D-glucose, sodium pyruvate, pyridoxine and with 10% (v/v) heat-inactivated (56°C, 30 min) fetal bovine serum (FBS), 100 U/mL penicillin G, 100 mg/mL streptomycin and 250 ng/mL fungizone (Invitrogen BV, Breda, the Netherlands). The cell cultures were passaged twice a week. HepG2 cells were transfected using Lipofectamin 2000 (Invitrogen BV, Breda, The Netherlands) at a ratio of 3 µL Lipofectamin 2000 per µg plasmid DNA as recommended by the manufacturer.

Plasmids
Plasmids expressing PMP70(AA.1-659)-GFP, PMP70(AA.1-375)-GFP, PMP70(AA.1-144)-GFP, ALDP(AA.1-745)-YFP, ALDP(AA.1-281)-GFP, ALDP(AA.1-164)-GFP, ALDP(AA.67-164)-GFP have been described before (15-17).

RNA isolation and Quantitative Polymerase Chain Reaction (Q-PCR)
The isolation of total RNA, its conversion to cDNA and its analysis by Q-PCR was carried out as described before (18). Primers and probes used in this study are listed in supplementary Table S1. The expression of each gene of interest was normalized to 18S (ΔΔCt method).

SDS-PAGE and western blotting
Equal volumes of the gradient fractions and the fractions P and T were separated by SDS-PAGE and analyzed by western blotting according to established procedures (19). Protein concentrations were determined using the Bio-Rad Protein Assay system (Bio-Rad Hercules, CA, USA) using bovine serum albumin as standard. All primary antibodies used are listed in supplementary Table S2. Horse radish peroxidase-conjugated secondary antibodies (HRP-conjugated swine-anti rabbit, rabbit anti-goat and rabbit anti-mouse, Dako A/S, Glostrup, Denmark) and the phototope®-HRP Western Blot Detection System (Cell Signaling technology Inc, Danvers, MA) were used for detection according to the manufacturers' protocols. The blots were exposed in a ChemiDoc XRS system (Bio-Rad). Protein band intensities were quantified by the Quantity One software (Bio-Rad, Hercules, CA, USA).

Immunofluorescence microscopy
Control, cholesterol-depleted and cholesterol-repleted HepG2 cells (6x105 cells) were fixed with 4% paraformaldehyde, labeled and analyzed as described previously (19). Primary antibody dilutions are listed in supplementary Table S2.

SUPPLEMENTARY FIGURES

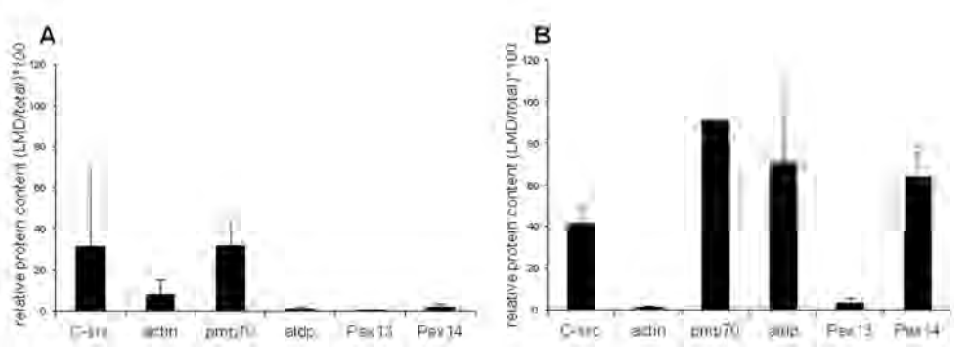

Figure S1. Quantification of western blot signals of flotation gradients after Triton X-100 and Lubrol WX-extraction of HepG2 cells. Westernblot signals of flotation gradients were quantified from 3 independent Triton X-100- (A) and Lubrol WX- (B) extraction experiments of HepG2 cells as described in Figure 1. Protein band intensities were quantified using the Quantity One software (Bio-Rad, Hercules, CA, USA). The cumulative intensity of all 12 fractions was set to 100% and the relative amount present in the raft-containing fractions (4-6) is shown. Since equal volume fractions were loaded, the relative levels indicate the cellular amount of the indicated proteins that are lipid raft-associated under the given experimental conditions. The data show that similar amounts (approximately 30%) of c-Src, PMP70 and Pex14p resist Triton X-100 extraction, whereas over 50% of PMP70, Pex14p and ALDP resist Lubrol WW-extraction

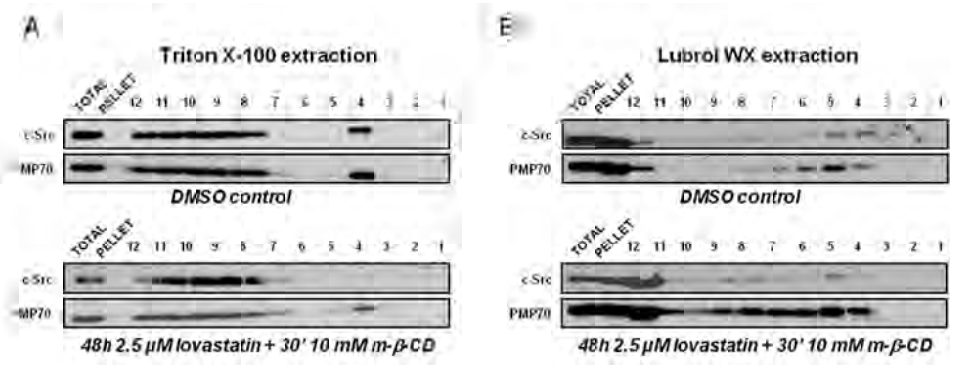

Figure S2. Standard cholesterol depletion protocols do not cause dissociation of PMP70 from organellar lipid rafts in HepG2 cells. Human HepG2 cells were cultured in the presence of 2.5 µM lovastatin (L) for 48 h followed by treatment with 10 mM methyl-β-cyclodextrin (m-β-CD) for 30 minutes. The cells were lysed in the presence of 1% Triton X-100 (A) or 1% Lubrol WX (B), followed by flotation gradient centrifugation. One (1) ml fractions were taken from the top and analyzed by Western blot analysis using antibodies against the lipid raft marker c-Src, and the peroxisomal membrane protein PMP70. Equal volumes of the unfractionated total protein lysate (T) as well as the pellet fraction after flotation gradient centrifugation (P) were also analyzed.

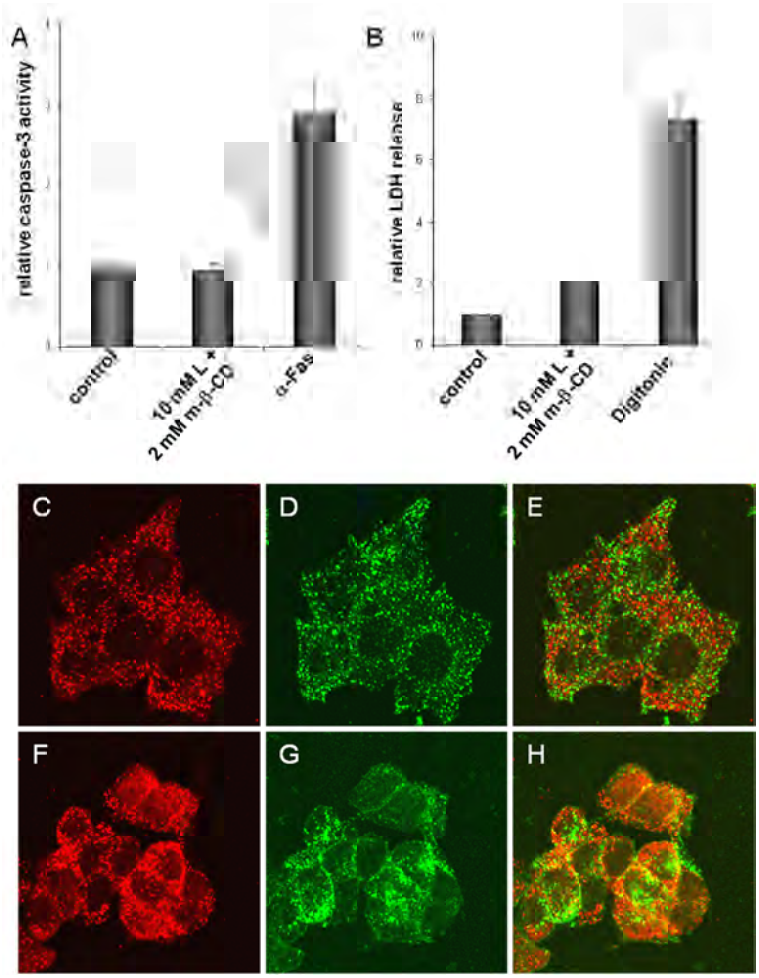

Figure S3. Analysis of necrosis, apoptosis and endocytosis in cholesterol-depleted HepG2 cells. Human HepG2 cells were cultured for 24 h in the absence (control) or presence of 10 µM lovastatin and 2 mM methyl-β-cyclodextrin (10 µM L + 2 mM m-β-CD) followed by (A) measurement of LDH activity in the medium to quantify necrotic cell death (digitonin (50 mg/mL) permeabilisation was used as positive control); (B) caspase-3 activity to quantify apoptotic cell death (α-Fas 91 ug/ml) was used as positive control); (C-H) a 40-minute exposure to FITC-labelled transferrine to analyze endocytosis. Immunofluorescence microscopy was used to determine the subcellular of catalase (C,F) and FITC-transferrin (D,G) (merged images in E, H) in control (C-E) and L /m-β-CD-treated cells (F-H). Note that the level of endocytosis in cholesterol-depleted HepG2 cells (G) seems reduced compared to untreated HepG2 cells (D). Still, cholesterol-depleted HepG2 cells (with missorted catalase, see F and H) are able to endocytose the FITC-labeled transferine (G and H), at least to a certain extend. Thus, catalase missorting in cholesterol-depleted HepG2 cells is not a result of a total/general collapse of cellular functions.

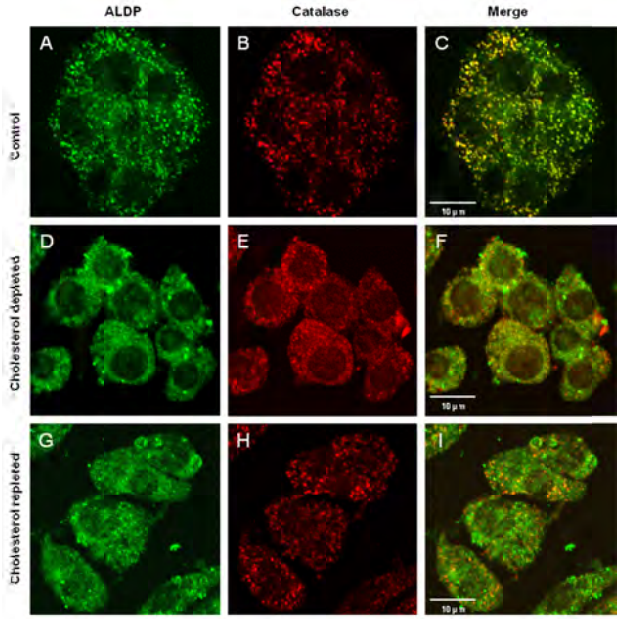

Figure S4. Effect of cholesterol depletion and repletion on the subcellular location of ALDP and catalase.
This figure is added to substantiate the difference in peroxisomal accumulation of catalase and ALDP after repletion of cholesterol in HepG2 cells. Human HepG2 cells were cultured for 24 h in the absence (A-C) or presence (D-F) of 10 µM lovastatin and 2 mM methyl-β-cyclodextrin followed by immunofluorescence microscopy to determine the subcellular location of ALDP (A,D) and catalase (B,E using a rabbit polyclonal antibody against catalase, Calbiochem Novabiochem Corp. La Jolla, CA, USA) (merge images in C and F). Cholesterol-depleted HepG2 cells (D-F) were subsequently cultured for 24 h in the presence of exogenously added cholesterol (G-I) and the subcellular location of ALDP (G) and catalase (H) determined. (merged images in I). In control cells (A-C), ALDP and catalase show a strong colocalisation in peroxisomal dots. Cholesterol-depletion leads to a diffuse staining for ALDP and catalase (D-F). Cholesterol repletion leads to a significant clustering of catalase in dots, while the ALDP staining remains predominantly diffusely localized in the cytoplasm (G-I).

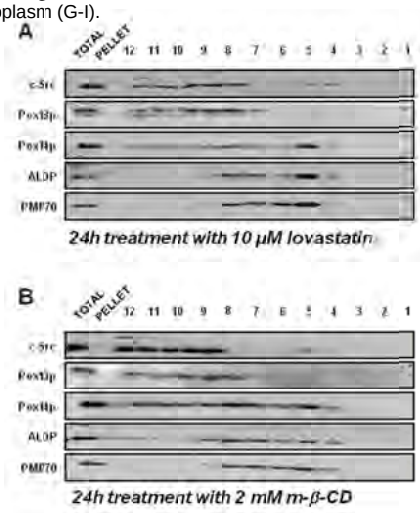

Figure S5. Incubation of HepG2 cells with only 10 µM lovastatin or 2mM methyl-β-cyclodextrin does not lead to the dissociation of PMPs from rafts in HepG2 cells. Human HepG2 cells were cultured in the presence of 10 µM lovastatin (A) or 2 mM methyl-β-cyclodextrin (m-β-CD) (B) for 24 h. The cells were lysed in the presence of 1% Lubrol WX, followed by flotation gradient centrifugation. One (1) ml fractions were taken from the top and analyzed by western blot analysis using antibodies against the lipid raft marker c-Src, and the peroxisomal membrane proteins Pex13p, Pex14p, ALDP and PMP70. Equal volumes of the unfractionated total protein lysate (T) as well as the pellet fraction after flotation gradient centrifugation (P) were also analyzed.

CHAPTER 5

Caveolin-1 is enriched in the peroxisomal membrane of rat hepatocytes.

Jannes Woudenberg[1], Krzysztof P. Rembacz[1], Fiona A. J. van den Heuvel[1], Titia E. Woudenberg-Vrenken[1], Manon Buist-Homan[1], Mariska Geuken[1], Mark Hoekstra[1], Leo E. Deelman[2], Carlos Enrich[3], Rob H. Henning[2], Han Moshage[1], Klaas Nico Faber[1]

[1]Department of Gastroenterology and Hepatology, University Medical Center Groningen, University of Groningen, Groningen, The Netherlands
[2]Department of Clinical Pharmacology, University Medical Center Groningen, University of Groningen, Groningen, The Netherlands
[3]Departament de Biologia Cellular, Immunologia i Neurociències, Institut d'Investigacions Biomèdiques August Pi i Sunyer (IDIBAPS), Facultat de Medicina, Universitat de Barcelona, Casanova 143, 08036-Barcelona, Spain

Hepatology. 2010 May;51(5):1744-53.

Caveolin-1 is Enriched in the Peroxisomal Membrane of Rat Hepatocytes

ABSTRACT

Background: Caveolae are a subtype of cholesterol-enriched lipid microdomains/rafts that are routinely detected as vesicles pinching off from the plasmamembrane. Caveolin-1 is an essential component of caveolae. Hepatic caveolin-1 plays an important role in liver regeneration and lipid metabolism. Expression of caveolin-1 in hepatocytes is relatively low and it has been suggested to reside also at other subcellular locations than the plasmamembrane. Recently, we found that the peroxisomal membrane contains lipid microdomains. Like caveolin-1, hepatic peroxisomes are involved in lipid metabolism. Here, we analyzed the subcellular location of caveolin-1 in rat hepatocytes.

Methods: The subcellular location of rat hepatocyte caveolin-1 was analyzed by cell fractionation procedures, immuno-fluorescence and immuno-electron microscopy. GFP-tagged caveolin-1 was expressed in rat hepatocytes. Lipid rafts were characterized after Triton X-100 or Lubrol WX extraction of purified peroxisomes. Fenofibric acid-dependent regulation of caveolin-1 was analyzed. Peroxisome biogenesis was studied in rat hepatocytes after RNA interference-mediated silencing of caveolin-1 and caveolin-1 knock out mice.

Results: Cell fractionation and microscopical analyses reveal that caveolin-1 colocalizes with peroxisomal marker proteins (catalase, PMP70, ALDP, Pex14p, BAAT) in rat hepatocytes. Artificially expressed GFP-caveolin-1 accumulated in catalase-positive organelles. Peroxisomal caveolin-1 is associated with detergent-resistant microdomains. Caveolin-1 expression is strongly repressed by the PPARα-agonist fenofibric acid. Targeting of peroxisomal matrix proteins, peroxisome number and shape were not altered in rat hepatocytes with 70-80% reduced caveolin-1 levels and in livers of caveolin-1 knock out mice.

Conclusions: Caveolin-1 is enriched in peroxisomes of hepatocytes. Caveolin-1 is not required for peroxisome biogenesis, but this unique subcellular location may determine its important role in hepatocyte proliferation and lipid metabolism.

INTRODUCTION

Caveolae are subtypes of lipid microdomains/rafts that are morphologically recognizable as flask-like invaginations of the plasma membrane. They are particularly involved in signal transduction and endocytosis (1). The characteristic protein component of caveolae are the caveolins that interact strongly with cholesterol (2). Three different caveolins (caveolin-1, caveolin-2 and caveolin-3) have been described. Caveolin-1 is crucial for the formation of caveolae in non-muscle cells (1) and is highly expressed in lung, heart and adipose tissue (3). In accordance with this expression profile, severe pulmonary defects, abnormal cardiac function and lipid disorders have been reported in caveolin-1 knockout mice (4-6).

Caveolin-1 is only moderately expressed in the liver (7, 8), where it has been detected in hepatocytes, Kupffer cells, stellate cells and endothelial cells (8-12). Still, hepatic caveolin-1 is involved in important metabolic pathways like (intracellular) cholesterol trafficking (13) and lipid homeostasis (14). The important function of hepatic caveolin-1 is evident from the impaired liver regeneration and low survival of caveolin-1-/- mice after partial hepatectomy (15). In hepatocytes, caveolin-1 has been detected in the plasmamembrane. However, significant amounts of caveolin-1 have also been detected intracellularly, where it has been reported to localize to lipid droplets, endoplasmic reticulum, Golgi and/or mitochondria (3, 8, 14). We became interested in a putative peroxisomal localisation of caveolin-1 after we detected that the peroxisomal membrane contains lipid microdomains/rafts (Woudenberg, J. et al., Chapter 4).

Peroxisomes are required for important hepatocyte functions like bile acid biosynthesis and β-oxidation of very long chain fatty acids (VLCFAs) (16, 17). Typical marker proteins for peroxisomes are the peroxins that are required for peroxisome biogenesis, the peroxisomal antioxidant enzyme catalase and the peroxisomal ATP-binding cassette (ABC) transporters, the Adrenoleukodystrophy Protein (ALDP, ABCD1) and 70 kDa Peroxisomal Membrane Protein (PMP70) (18, 19). Recently, we found that ALDP, PMP70 and the peroxins Pex13p and Pex14p are differentially associated with lipid rafts in human peroxisomes (Woudenberg, J. et al., Chapter 4). Cellular depletion of cholesterol leads to defective sorting of the peroxisomal enzyme catalase, indicating that lipid rafts are required for peroxisome biogenesis.

As caveolae are a subtype of lipid rafts, we here analyzed the subcellular location of caveolin-1 in rat hepatocytes using biochemical and microscopical techniques. Caveolin-1 was predominantly detected in peroxisomes. Expression of caveolin-1 is strongly reduced after exposure to fenofibric acid, a strong ligand for the peroxisome proliferator activated receptor alpha (PPARα). Peroxisome biogenesis defects were not observed after RNA-mediated silencing of caveolin-1 in rat hepatocytes and in livers of caveolin-1 knock out mice. We discuss these findings in relation to the putative function of caveolin-1 in liver peroxisomes.

EXPERIMENTAL PROCEDURES

Animals

Specified pathogen-free male Wistar rats (220–250 g) were purchased from Charles River Laboratories Inc. (Wilmington, MA, USA). They were housed under standard laboratory conditions with free access to standard laboratory chow and water. Experiments were performed following the guidelines of the local Committee for Care and Use of laboratory animals.

Caveolin-1 knock out and wild type mice (4, 15) were kept under a controlled humidity and lighting schedule with a 12 hours dark period. All animals received human care in compliance with institutional guidelines regulated by the European Community. Food and water were available ad libitum. Male mice were sacrificed at the age of 12 weeks after which livers were removed and processed for western blotting or immunofluorescence microscopy.

Primary cells and culture conditions

Hepatocytes were isolated and cultured in William's E medium as described previously (20). Cells were cultured in a humidified incubator at 37 °C and 5% CO2. Hepatocyte viability and purity were always more than 90% as assessed by trypan blue exclusion.

Plasmids and transient transfection

Full-length mouse caveolin-1 cDNA was obtained from C2C12 myoblast cells by PCR and cloned into pGEM-T-easy (Promega, Leiden, Netherlands). Constructs were sequenced and a clone without errors was selected. BglII and SalI restriction sites were added to the caveolin-1 cDNA by PCR using adapter-primers (For-BglII: 5'-GGACTCAGATCT-ATGTCTGGGGGCAAATACGTGGAC-3', Rev-SalI: 5'-TACAAGAGTCGA-CTGCGAGAGCAACTTGGAATTG-3'). The resulting PCR product was inserted as a BglII-SalI DNA fragment in the corresponding sites of pEGFP-C1 (Clontech, Palo Alto, CA, USA), resulting in an expression vector with caveolin-1 fused to the C-terminus of enhanced green fluorescent protein (EGFP).

Primary rat hepatocytes were transiently transfected with EGFP-caveolin-1 using electroporation, as described previously (21). After 48 h, the expression of the hybrid protein was analyzed by western blotting and the subcellular location of EGFP-caveolin-1 was analyzed using fluorescence microscopy.

Caveolin-1 RNA interference

Primary rat hepatocytes were plated at a density of 1.25 x 105 cells/cm2 in William's E Medium with Glutamax supplemented with 1% heat-inactivated fetal calf serum (Invitrogen) and dexamethasone (Sigma-Aldrich, St. Louis, MO) in the

presence of double-stranded siRNA duplexes (Table 1) aimed to silence caveolin-1 (siRNA-Cav, Invitrogen). Control cells were transfected with oligonucleotides directed against luciferase (siRNA-Luc, Invitrogen). Lipofectamine (Invitrogen) was used as transfection reagent according to the manufacturer's instructions. After 24 h, cells were either fixed for immunofluorescence microscopy or lysed for Q-PCR or western blot analysis.

Table 1. Primers used for caveolin-1 RNA interference

RNA	Sense	Antisense	Company/Reference
luciferase	5'-cuu acg cug agu acu ucg auu-3'	5'-ucg aag uac uca gcg uaa guu-3'	Invitrogen
caveolin-1	5'-aau cuc aau cag gaa gcu cuu -3'	5-gag cuu ccu gau uga gau uuu-3'	Invitrogen, (38)

Fenofibric acid treatments

Primary rat hepatocytes were plated as described previously (20). Four (4) hours after plating, cells were incubated with 50 µM fenofibric acid (Sigma-Aldrich) or 0.1% DMSO (solvent for fenofibric acid) for 24 h. Cells were lysed for Q-PCR or western blot analysis.

RNA isolation and Quantitative Polymerase Chain Reaction (Q-PCR)

The isolation of total RNA, its conversion to cDNA and its analysis by Q-PCR was carried out as described previously (22). Primers and probes used in this study are listed in Table 2. The expression of each gene of interest was normalized with respect to the endogenous control, 18S (ΔΔCt method).

Table 2. Primers and probes

Gene	Sense	Antisense	Probe
18S	5'-cgg cta cca cat cca agg a -3'	5'-cca att aca ggg cct cga aa-3'	5'FAM-cgc gca aat tac cca ctc ccg a-TAMRA3'
caveolin-1	5'-aac cgc gac ccc aag c-3'	5-ccg caa tca cat ctt caa agt c-3'	5'FAM-tct caa cga cga cgt ggt caa gat-TAMRA3'
Pex11p	5´-gcc cgc cac tac tac tat ttc ct-3´	5´-tct gtc gcg tgc aac ttg tc-3´	5´FAM-cat atg cag caa gac ctc ata cag atc ccg -TAMRA3´
PMP70	5'-ctg gtg ctg gag aaa tca tca at-3'	5'-cca gat cga act tca aaa cta agg t-3'	5'FAM-tga tca tgt tcc ttt agc aac acc aaa tgg-TAMRA3'
AOX	5´-gcc acg gaa ctc atc ttc ga-3´	5´-cca ggc cac cac tta atg ga-3´	5´FAM-cca ctg cca cat atg acc cca aga ccc-TAMRA3´
Baat	5´-tgt aga gtt tct cct gag aca tcc taa-3´	5´-gtc caa tct ctg ctc caa tgc-3´	5´FAM-tgc caa ccc ctg ggc cca g-TAMRA3´
catalase	5'-gga tta tgg cct cc gaga tct-3'	5-acc ttg gtc agg tca aat gga t-3'	5'FAM-atg cca tcg cca gtg gca att acc-TAMRA3'

Subcellular fractionation and isolation of peroxisomes

The subcellular fractionation and isolation of peroxisomes from rat liver was performed as described previously by Antonenkov et al. using isolation medium-3 (23). Peroxisomes were further purified from the 17,000 x g pellet by Nycodenz density gradient centrifugation according to established methods (24). For westernblot analysis, pellet fractions were resuspended in the same volume as the corresponding supernatant fractions and equal volumes were loaded

Isolation of detergent-resistant microdomains from peroxisomes
Purified peroxisomal fractions from the Nycodenz gradients were pooled and centrifuged in an SS34 rotor at 17,000 x g. The pellets (1-1.5 mg protein) were subjected to extraction by 1% Triton X-100 (Sigma-Aldrich) or 1% Lubrol WX (Sigma-Aldrich) for the isolation of Triton X-100- or Lubrol WX-resistant rafts, respectively, according to established methods (25). Equal volume fractions of the gradient were analyzed by western blotting.

SDS-PAGE and western blotting
Protein samples were separated by SDS-PAGE and analyzed by western blotting as described before (21). Protein concentrations were determined using the Bio-Rad Protein Assay system (Bio-Rad Hercules, CA, USA) using bovine serum albumin as standard. Primary antibodies used are listed in Table 3. Horse radish peroxidase-conjugated secondary antibodies (HRP-conjugated swine anti-rabbit, rabbit anti-goat and rabbit anti-mouse, Dako A/S, Glostrup, Denmark) and the phototope®-HRP western blot Detection System (Cell Signalling Technology Inc, Danvers, MA, USA) were used for detection according to the manufacturers' protocols. The blots were exposed in a ChemiDoc XRS system (Bio-Rad).

Immunofluorescence microscopy
Immunofluorescence microscopy was performed on 4-µm thick sections from paraffin-embedded mouse liver as well as on paraformaldehyde (4%)-fixed primary rat hepatocytes.

Table 3. Antibody dilutions for protein analysis

Antibody	WB	IF	EM	Company/Reference
Mouse α-ALDP	1:1000	1:100		Clone 1D6, Euromedex, Mundolsheim France
Rabbit α-Baat	1:2000			Generous gift of Prof. C. Falany, USA (39)
Rabbit α-BSEP	1:2000			(40)
Rabbit α-calnexin	1:2000			SPA 860D, Stressgen, MI, USA
Rabbit α-catalase	1:2000	1:200		Calbiochem, La Jolla, CA, USA
Mouse α-catalase	1:2000	1:200	1:200	Sigma-Aldrich, St. Louis, MO, USA
Rabbit α-caveolin-1	1:1000	1:100	1:100	N20, Santa Cruz Inc, CA, USA
Mouse α-cytochrome C	1:2000			BD Biosciences, Franklin Lakes, NJ, USA
Mouse α-Gapdh	1:10.000			Calbiochem, La Jolla, CA, USA
Mouse α-EGFP	1:1000			Roche Diagnostic, Almere, NL
Goat α-Pex13p	1:1000			Abcam, Cambridge, UK
Rabbit α-Pex14p	1:2000			Generous gift of Dr. M. Fransen, BE (41)
Rabbit α-PMP70	1:1000			Sigma-Aldrich, St. Louis, MO, USA
Rabbit α-c-Src	1:500			sc18, Santa Cruz Inc., CA, USA

Sections were deparaffinized in xylene followed by rehydration and antigen retrieval was performed using EDTA buffer. Liver sections and hepatocytes were labelled and analyzed as described previously (21). Primary antibody dilutions are listed in Table 3. Images were captured with a TCS SP2/AOBS confocal laser scanning microscope (Leica, Heidelberg, Germany).
Statistical analysis

All numerical results are reported as the mean of at least 3 independent experiments ± standard error of the mean (S.E.M).

RESULTS

Endogenous caveolin-1 co-localizes with peroxisomal markers in rat hepatocytes.

To study the presence and location of caveolin-1 in rat hepatocytes, we performed immunofluorescence microscopy using specific antibodies against caveolin-1 and the peroxisomal markers catalase and ALDP (Fig. 1).

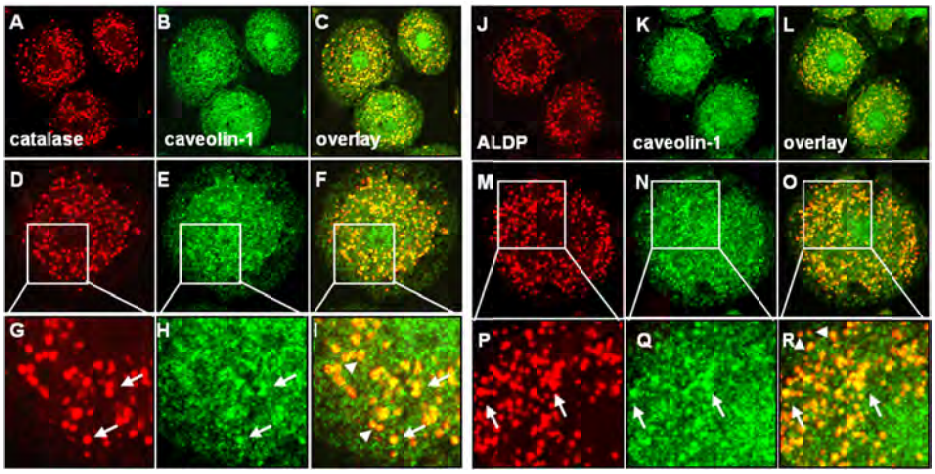

Figure 1. Caveolin-1 co-localizes with peroxisomal markers in rat hepatocytes
Primary rat hepatocytes were analyzed by immunofluorescence microscopy to determine the subcellular location of catalase (A, D, G), ALDP (J, M, P) and caveolin-1 (B, E, H and K, N, Q). The merged images are displayed in C, F, I, L, O and R. The high magnification images in G-I and P-R show strong co-localization between caveolin-1 and catalase and ALDP, respectively (arrows). Some catalase-positive peroxisomes contain little amounts of caveolin-1 (I and R, closed arrowheads). Caveolin-1 is also detected at the plasmamembrane of hepatocytes (B and K, open arrowheads).

The anti-caveolin-1-dependent signal was low, in line with the limited expression of this protein in liver ((8) and supplementary Figure S1). When observing the caveolin-1 staining alone, no distinct localization pattern is evident, with significant dotted intracellular signals, together with nuclear and plasmamembrane signals (Fig. 1B). However, when combined with a specific staining for catalase (Fig. 1, overlay in C, F and I) or ALDP (Fig. 1, overlay in L, O, R) a significant co-localization of caveolin-1 with these peroxisomal markers is evident (Fig. 1, merged images, arrows). Some peroxisomes appeared to be (almost) devoid of caveolin-1, especially those at the rim of hepatocytes (Fig. 1F and O).

Heterologously expressed caveolin-1 partly sorts to hepatocyte peroxisomes.
To obtain further proof for a peroxisomal location of hepatic caveolin-1, we transiently transfected primary rat hepatocytes with an expression plasmid producing Enhanced Green Fluorescent Protein (EGFP)-tagged caveolin-1. Using antibodies against EGFP, a protein band with the expected molecular weight of 49 kDa was readily detected in transfected rat hepatocytes, whereas this band was absent in untransfected cells (Fig. 2A). Fluorescence microscopy revealed that EGFP-caveolin-1 was detected in dotted structures that also contain (endogenous) catalase, as indicated by the yellow stain in the merged images (Fig. 2E-G, arrows). EGFP-caveolin-1 was also detected at other cellular locations, in particular in cells that highly express the hybrid protein (Fig. S2).

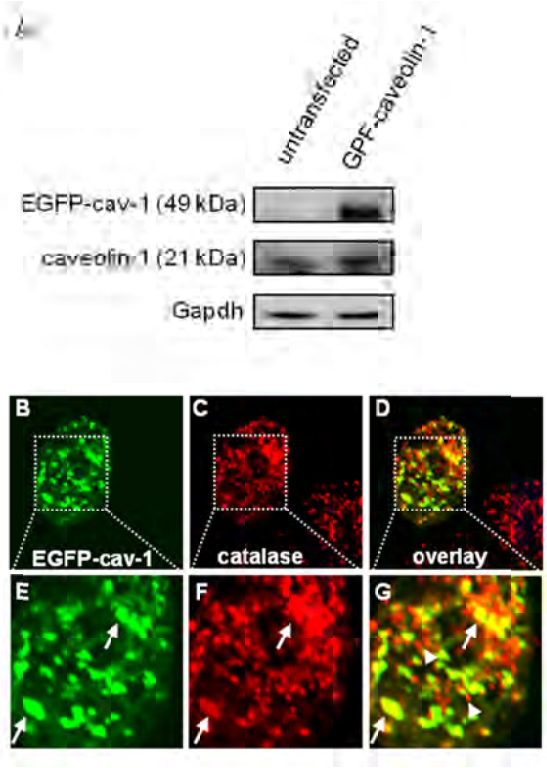

Figure 2. In rat hepatocytes, EGFP-caveolin-1 partly sorts to catalase-positive peroxisomes.
Primary rat hepatocytes were transiently transfected with EGFP-caveolin-1. Forty eight (48) hours after transfection, expression of transfected (EGFP-caveolin-1, 49 kDa) and endogenous caveolin-1 (21 kDa) was analyzed by western blotting. Gapdh expression was analyzed as a marker for equal protein loading (A). EGFP-caveolin-1-transfected hepatocytes were analyzed by immunofluorescence microscopy to determine the subcellular location of EGFP-caveolin-1 (B, E) or catalase (C, F). The merged images are displayed in figure D and G. In the high magnification images, clear co-localization between caveolin-1 and catalase in dotted structures (arrows), can be observed. Some catalase-positive peroxisomes contain little amounts of caveolin-1 (G, arrowheads).

Endogenous caveolin-1 co-fractionates with peroxisomal proteins after subcellular fractionation of rat liver.
To confirm the presence of caveolin-1 in hepatic peroxisomes, we performed cell fractionation studies on rat liver. After differential centrifugation of osmotically-stabilized total liver homogenates, caveolin-1 was almost exclusively detected in the 17,000 x g pellet fraction also containing the markers for peroxisomes, mitochondria ER and plasmamembranes (Fig. 3A). The cytosolic marker Gapdh did not appear in any of the pellet fractions (Fig. 3A). Next, the organelles in the

17,000 x g pellet fraction were separated using Nycodenz density gradient centrifugation. Western blot analyses showed that the peroxisomal markers PMP70, Pex14p, catalase and Baat were enriched in fractions 3-6 (Fig. 3B), the unique high density-location of peroxisomes in these gradients (24). Caveolin-1 was also highly enriched in these fractions and clearly separated away from mitochondria (cytochrome C, fractions 12-14), canalicular membranes (Bsep, fractions 12-15), plasmamembranes (c-Src, fractions 15,16) and the ER (calnexin, fractions 12-15). These data show that caveolin-1 predominantly co-purifies with peroxisomes during cell fractionation studies of rat liver. Only minor amounts may be present in the plasma membrane, mitochondria, ER and/or other organelles not analyzed here.

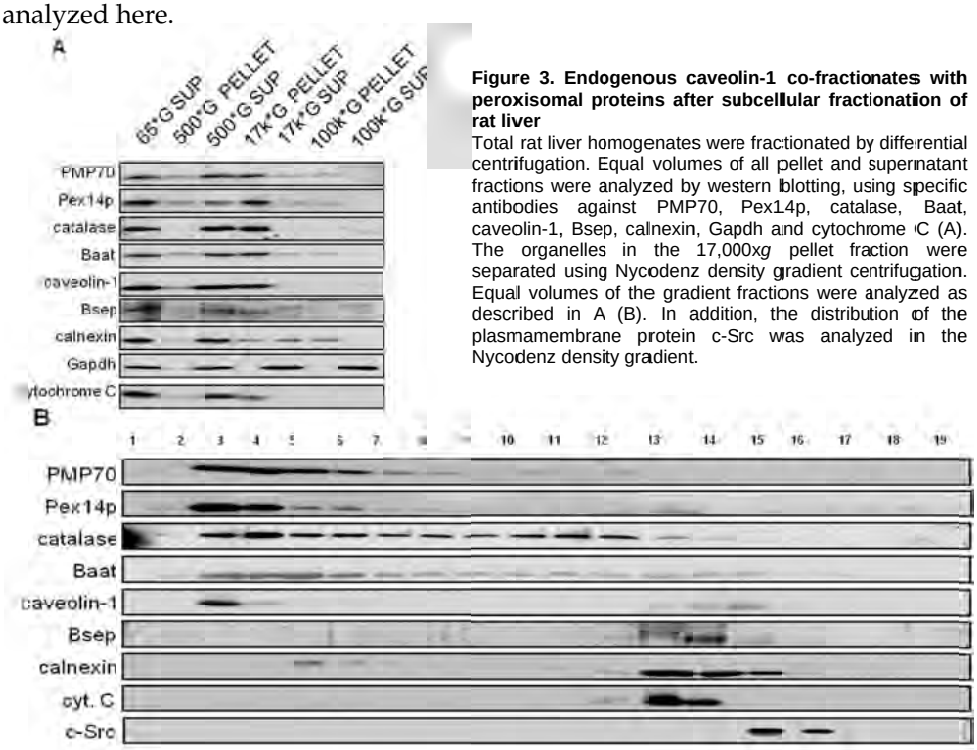

Figure 3. Endogenous caveolin-1 co-fractionates with peroxisomal proteins after subcellular fractionation of rat liver
Total rat liver homogenates were fractionated by differential centrifugation. Equal volumes of all pellet and supernatant fractions were analyzed by western blotting, using specific antibodies against PMP70, Pex14p, catalase, Baat, caveolin-1, Bsep, calnexin, Gapdh and cytochrome C (A). The organelles in the 17,000x*g* pellet fraction were separated using Nycodenz density gradient centrifugation. Equal volumes of the gradient fractions were analyzed as described in A (B). In addition, the distribution of the plasmamembrane protein c-Src was analyzed in the Nycodenz density gradient.

Caveolin-1 is localized to detergent-resistant microdomains in the peroxisomal membrane.

In order to determine whether peroxisomal caveolin-1 is localized to detergent-resistant microdomains, we treated purified rat liver peroxisomes with Triton X-100 or Lubrol WX followed by flotation gradient centrifugation. Equal volumes of the gradient fractions were analyzed by western blotting. Caveolin-1 largely resisted extraction by Triton X-100, as indicated by its flotation to fractions 3-5. All peroxisomal marker proteins analyzed, PMP70, Pex14p, Pex13p, catalase and Baat, were detected in the Triton X-100 solubilized fractions 8 to 12 (Fig. 4A).

Importantly, significant amounts of Pex14p, PMP70 and caveolin-1 resisted Triton X-100 extraction when performed on total hepatocyte cell lysates (Fig. S3A) as reported before in human HepG2 cells (Woudenberg, J. et al, Chapter 4). PMP70 and Pex14p largely resisted Lubrol WX extraction when performed on purified peroxisomes (Fig 4B) and total hepatocyte lysates (Fig. S3B), with a predominant flotation to fractions 4 and 5. As expected, also the majority of peroxisomal caveolin-1 was associated with these Lubrol WX-resistant microdomains. Pex13p, catalase and Baat were detected only in fraction 12, representing the solubilized fraction in this gradient (Fig. 4B). These results demonstrate that peroxisomal caveolin-1 is localized to detergent resistant microdomains distinct from the ones that contain the peroxisomal membrane proteins PMP70 and/or Pex14p.

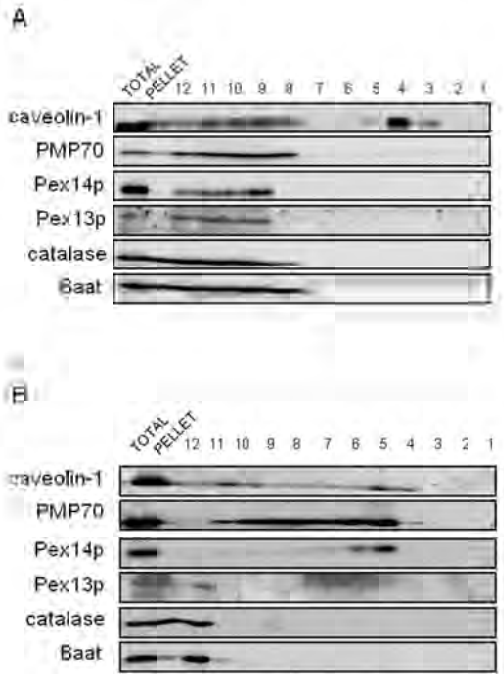

Figure 4. Caveolin-1 is localized to detergent-resistant microdomains in the peroxisomal membrane
Freshly isolated rat liver peroxisomes were lysed in the presence of 1% Triton X-100 or Lubrol WX followed by flotation gradient centrifugation. One (1) ml fractions (in total 12) were collected from the top and analyzed by western blotting (A, Triton X-100 extraction; B, Lubrol WX extraction). Equal volumes from the gradient fractions were analyzed using specific antibodies against caveolin-1, the peroxisomal membrane proteins PMP70, Pex14p, Pex13p and the peroxisomal matrix proteins catalase and Baat. Equal volumes of the unfractionated total protein lysate (T) as well as the pellet fraction after flotation gradient centrifugation (P) were also analyzed.

RNA interference-mediated downregulation of caveolin-1 does not affect the peroxisomal location of Baat in primary rat hepatocytes.
To study whether caveolin-1 may play a direct role in the sorting of peroxisomal enzymes, we inhibited its expression by RNA interference. Transient transfection of primary rat hepatocytes with caveolin-1-specific small interfering RNA duplexes (siRNA-Cav) led to a 70-80% reduction of caveolin-1 mRNA and protein levels (Fig. 5A, C). The mRNA and/or protein expression of the peroxisomal markers Pex11p, PMP70 and Baat were comparable in siRNA-Cav-1-treated and control cells (Fig. 5B, C). Immunofluorescence microscopy analysis showed that the peroxisome-specific staining of caveolin-1 was strongly reduced in siRNA-Cav-treated hepatocytes. Under these conditions, the peroxisomal matrix enzyme Baat

was still predominantly present in dotted structures in the cytoplasm, indistinguishable from the staining pattern in control cells (Fig. 5D-O).

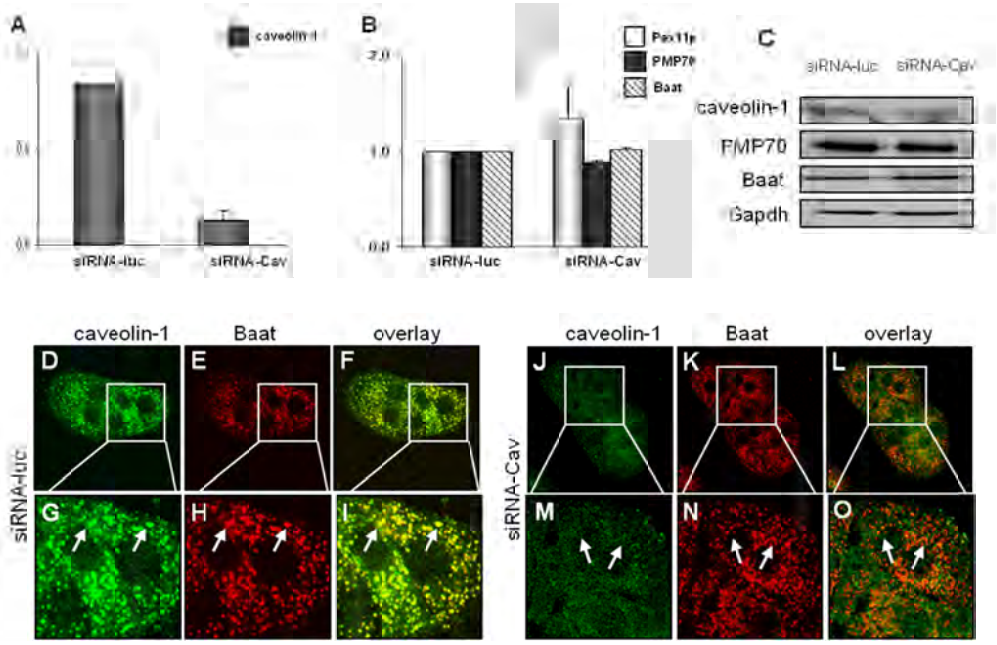

Figure 5. RNA interference-mediated downregulation of caveolin-1 does not affect the peroxisomal location of Baat in primary rat hepatocytes
Primary rat hepatocytes were transiently transfected to silence caveolin-1 expression (siRNA-Cav). Control cells were transfected with oligonucleotides directed against luciferase (siRNA-luc). After 24 h, mRNA levels of caveolin-1 (A) and Pex11p, PMP70, catalase and Baat (B) were analyzed by Q-PCR. Levels of selected proteins were analyzed by western blotting, using antibodies against caveolin-1, PMP70, catalase and Baat. As a loading control, Gapdh expression was analyzed (C). The subcellular location of caveolin-1 (siRNA-luc: D, G; siRNA-Cav: J, M) and the peroxisomal matrix marker Baat (siRNA-luc: E, H; siRNA-Cav: K, N) were analyzed by immunofluorescence microscopy. The merged images are shown in F, I (siRNA-luc) and L, O (siRNA-Cav) respectively, showing clear co-localization of caveolin-1 and Baat in luciferase treated cells (arrows). The subcellular location of Baat is not affected by the downregulation of caveolin-1 (O, arrows).

Catalase sorting, peroxisome number and shape in hepatocytes of caveolin-1 knock out mice.

To obtain conclusive evidence for a putative role of caveolin-1 in peroxisome biogenesis, we analyzed the subcellular location of catalase in liver sections of caveolin-1 knock-out mice compared to wild type controls. The absence of caveolin-1 was confirmed by western blot analysis of total liver protein lysates (Fig. 6A). Catalase staining was detected throughout the liver parenchyma, with a specific dotted pattern in wild type hepatocytes (Fig. 6B) and caveolin-1 deficient hepatocytes (Fig 6C). No significant amount of cytosolic catalase was detected in caveolin-1 deficient hepatocytes, nor was the number or shape of peroxisomes altered compared to wild type hepatocytes.

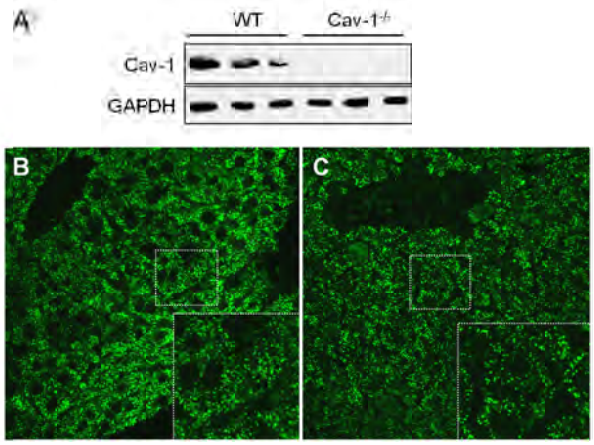

Fig. 6. Catalase sorting, peroxisome number and shape in hepatocytes of caveolin-1 knock out mice
Caveolin-1 expression in the livers of wild type and caveolin-1 knockout mice was analyzed by western blotting. In caveolin-1 knock out mice, caveolin-1 protein expression is undetectable. As a loading control, Gapdh expression was analyzed (A).
The subcellular location of catalase in the livers of wild type (B) and caveolin-1 knock out mice (C) was analyzed by immunofluorescence microscopy. Caveolin-1 deficiency does not affect the sorting of catalase to punctuate dots, representing peroxisomes.

Caveolin-1 is negatively regulated by the PPARα agonist fenofibric acid.
Finally, we determined whether expression of caveolin-1 is co-regulated with genes encoding peroxisomal proteins. Primary rat hepatocytes were treated for 24 h with the ligand for PPARα, fenofibric acid. Typical PPARα target genes, like Pex11, PMP70 and acyl coenzyme A oxidase (AOX) were strongly induced by this compound (Fig. 7A). In contrast, expression of Baat was not responsive to fenofibric acid treatment. Remarkably, fenofibric acid treatment strongly reduced the mRNA levels of caveolin-1 to 20-30% compared to untreated cells (Fig. 7B). These data show that expression of caveolin-1 is regulated by the PPAR ligand fenofibric acid, but that its expression is reduced under conditions were peroxisomes proliferate.

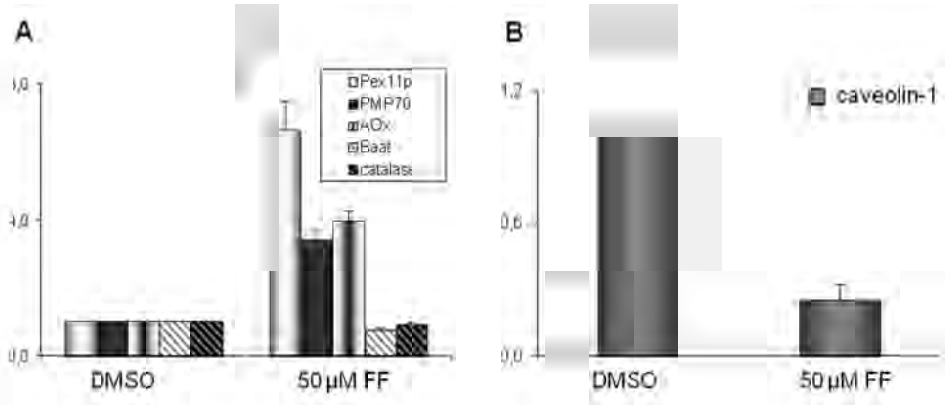

Figure 7. Caveolin-1 is negatively regulated by the PPARα agonist fenofibric acid
Primary rat hepatocytes were incubated with 50 µM fenofibric acid (FF) or 0.1% DMSO (solvent for FF) for 24 h. Pex11p, PMP70, AOX, Baat , catalase (All in A) and caveolin-1 (B) mRNA levels were analyzed by Q-PCR.

DISCUSSION

In this study, we show that caveolin-1 in rat hepatocytes is present in peroxisomes. Peroxisomal caveolin-1 is highly resistant to Triton X-100 extraction, more so than PMP70 and Pex14p that were previously shown to reside in peroxisomal lipid rafts (Woudenberg, J. et al., Chapter 4). Hepatic caveolin-1 is negatively regulated by the PPARα agonist fenofibric acid, which induces peroxisome proliferation. In line with this, peroxisome biogenesis is still intact in the absence of caveolin-1.

Expression of caveolin-1 in the liver is relatively low (7, 8), where it is particularly enriched in endothelial cells and stellate cells (9-11). Still, significant amounts of caveolin-1 are detected in hepatocytes (8, 12, 26). Previous studies have predominantly focused on the role of caveolin-1 in internalization of caveolae from the plasma membrane. However, it has also been noted that caveolin-1 may reside at other subcellular locations, including the endoplasmic reticulum, Golgi apparatus, endosomes, lipid droplets (27) and mitochondria (3, 8, 14). Our observation that significant amounts of caveolin-1 appear to reside in the peroxisomal membrane of hepatocytes therefore came as a surprise. A possible peroxisomal location of caveolin-1 in hepatocytes may, however, been overlooked in previous studies. Caveolin-1 has been shown to co-fractionate with catalase after Nycodenz gradient separation of mouse liver organelles (28), clearly separated from plasma membranes and the Golgi apparatus. Other studies excluded the analysis of peroxisomal marker proteins (29) and caveolin-1 may have been miss-assigned to plasma membranes or the endoplasmic reticulum, as peroxisomes also may co-fractionate with these subcellular fractions (30). In addition, immunofluorescence microscopy studies revealed that caveolin-1 co-localized with PMP70 in peroxisomal structures in the rat hepatoma cell line mcA-RH7777 (31). Our study shows that significant amounts of caveolin-1 co-localize with the peroxisomal markers catalase, Baat, ALDP, PMP70 and Pex14p in rat hepatocytes using both cell fractionation and microscopical techniques. Also, EGFP-tagged caveolin-1 expressed in rat hepatocytes was found to accumulate in cellular structures that contain the peroxisomal marker catalase. Similar to endogenous caveolin-1, EGFP-caveolin-1 also sorted to other subcellular organelles and the plasma membrane, which was especially evident in cells expressing high levels of the hybrid protein (Fig. S2). This may suggest that peroxisomes are the primary subcellular destination of caveolin-1 when the cellular levels of this protein are low. Alternatively, a cell type-specific sorting pathway may exist in hepatocytes that drives the accumulation of caveolin-1 in peroxisomes. A similar hepatocyte-specific sorting pathway has been detected for the enzyme BAAT (21).

In the plasma membrane, caveolin-1 is an integral membrane protein with its hydrophilic N- and C-terminus exposed to the cytosol (32). We found that also in hepatocyte peroxisomes, caveolin-1 is an integral peroxisomal membrane protein with its hydrophilic N- (and most probably also C-) terminus facing the cytosol (Fig. S4). In plasma membranes, caveolin-1 interacts with cholesterol to form

caveolae, which are morphologically characterized by their flask-shaped appearance. Such structures have not yet been described at the peroxisomal surface. The level of caveolin-1 in the peroxisomal membrane may be too low to form caveolae and its function may be unrelated to vesicle traffic to or from this organelle. On the other hand, local concentrations of caveolin-1-specific staining were often observed in immunofluorescence and occasionally in immunoelectron microscopy (Fig. S5), which may suggest local caveolae formation.

Recently, we found that ALDP, PMP70 and Pex14p are associated with peroxisomal lipid rafts and that these microdomains are essential for peroxisome biogenesis in human HepG2 cells (Woudenberg, J. et al., Chapter 4). PMP70 and Pex14p were detected in Triton X-100-resistant lipid rafts, while ALDP was detected in Lubrol WX-resistant lipid rafts. Pex13p, also an integral component of the peroxisomal membrane and interacting partner of Pex14p, appeared not to be associated with either of these biochemically-defined lipid rafts. PMP70 and Pex14p are also detected in Triton X-100-resistant lipid rafts in rat liver extracts, as was caveolin-1 (Fig. S3). All the PMPs were, however, fully solubilized when purified hepatocyte peroxisomes were extracted with Triton X-100 (Fig. 4A). This is most likely due to the very low lipid:protein ratio in purified fractions of peroxisomes compared to total cell extracts. Consequently, peroxisomal membrane(lipid)s are exposed to high detergent concentrations when purified peroxisomes are used in these extraction procedures. It is well-known that lipid raft-associated proteins eventually will be extracted when the detergent:lipid ratio is increased, also in total cell lysates (33). Nevertheless, peroxisomal caveolin-1 resisted Triton X-100 extractions even when performed on purified rat hepatocyte peroxisomes. These data suggest that three biochemically distinguishable lipid rafts exist in the peroxisomal membrane that contain either 1) caveolin-1, 2) PMP70 and/or Pex14p or 3) ALDP (Fig. S6). Pex13p does not seem to associate with either of these peroxisomal microdomains.

The function of peroxisomal caveolin-1-containing lipid rafts is currently unknown. The absence of caveolin-1 did not affect the peroxisomal location of catalase in mouse liver. This suggests that caveolin-1 is not required for peroxisome biogenesis, while other types of peroxisomal lipid rafts are (Woudenberg, J. et al., Chapter 4). Moreover, caveolin-1 expression was strongly reduced by treating rat hepatocytes with the PPARα agonist fenofibric acid, which induces peroxisome proliferation. This observation actually suggests a negative link between caveolin-1 and peroxisome proliferation. Although such a repressive effect of caveolin-1 on peroxisome proliferation is highly speculative, it is in line with the low levels of caveolin-1 and high numbers of peroxisomes in hepatocytes (7, 34). Previously, mouse liver caveolin-1 has been shown to be positively regulated by PPARγ (35). In contrast to PPARα, which is an important regulator of (peroxisomal) fatty acid oxidation, PPARγ stimulates the storage of fatty acids and lipids (35). Caveolae and caveolin-1 are involved in intracellular cholesterol and lipid metabolism. Hepatocyte peroxisomes are involved in the conversion of

cholesterol to bile acids and in β-oxidation of VLCFAs. Peroxisomal caveolin-1 may therefore be involved in transporting substrates for these metabolic activities to or from the peroxisomes. Related to this, caveolin-1 has been suggested to play a role in lipid droplet formation. Hepatocytes accumulate triacylglycerol and cholesteryl esters in these lipid droplets during liver regeneration (15, 36). The levels of hepatic cholesterol and triglycerides increase ten-fold (36) during the first 24 h after partial hepatectomy, which coincides with an increased number of peroxisomes (37). The lipid droplets are usually detected in the vicinity of peroxisomes (15). The number of hepatic lipid droplets is strongly decreased in caveolin1-/- mice and liver regeneration is strongly compromised after partial hepatectomy, resulting in increased mortality.
In conclusion, caveolin-1 resides in the peroxisomal membrane of hepatocytes. It does not seem to play a crucial role in peroxisome biogenesis. Future research needs to establish whether peroxisomal caveolin-1 is required for efficient liver regeneration and/or hepatocyte proliferation.

ACKNOWLEDGEMENTS

The authors would like to thank E.H. Blaauw, F. Dijk and Dr. J.J.L. van der Want for their excellent technical assistance and critical view on the electron microscopy experiments and Dr. L. Conde de la Rosa (Universitat de Barcelona, Spain) for preparing the paraffin-embedded liver sections from caveolin-1 knock out mice.

References

1. Williams TM, Lisanti MP. The caveolin proteins. Genome Biol 2004;5(3):214.
2. Murata M, Peranen J, Schreiner R, Wieland F, Kurzchalia TV, Simons K. VIP21/caveolin is a cholesterol-binding protein. Proc Natl Acad Sci U S A 1995 Oct 24;92(22):10339-10343.
3. Li WP, Liu P, Pilcher BK, Anderson RG. Cell-specific targeting of caveolin-1 to caveolae, secretory vesicles, cytoplasm or mitochondria. J Cell Sci 2001 Apr;114(Pt 7):1397-1408.
4. Drab M, Verkade P, Elger M, Kasper M, Lohn M, Lauterbach B, et al. Loss of caveolae, vascular dysfunction, and pulmonary defects in caveolin-1 gene-disrupted mice. Science 2001 Sep 28;293(5539):2449-2452.
5. Cohen AW, Razani B, Wang XB, Combs TP, Williams TM, Scherer PE, et al. Caveolin-1-deficient mice show insulin resistance and defective insulin receptor protein expression in adipose tissue. Am J Physiol Cell Physiol 2003 Jul;285(1):C222-C235.
6. Razani B, Engelman JA, Wang XB, Schubert W, Zhang XL, Marks CB, et al. Caveolin-1 null mice are viable but show evidence of hyperproliferative and vascular abnormalities. J Biol Chem 2001 Oct 12;276(41):38121-38138.
7. Glenney JR, Jr. The sequence of human caveolin reveals identity with VIP21, a component of transport vesicles. FEBS Lett 1992 Dec 7;314(1):45-48.
8. Pol A, Calvo M, Lu A, Enrich C. The "early-sorting" endocytic compartment of rat hepatocytes is involved in the intracellular pathway of caveolin-1 (VIP-21). Hepatology 1999 Jun;29(6):1848-1857.
9. Ohata M, Ito T. Experimental study on the fine structure of chicken liver parenchyme with special references to extrasinusoidal macrophages and sinusoidal blood cells. Part 1. Sinusoidal cells and macrophages in the normal and India ink-perfused livers. Arch Histol Jpn 1986 Mar;49(1):83-103.
10. Tanuma Y, Ohata M, Ito T. Electron microscopic studies on the sinusoidal cells in the monkey liver. Arch Histol Jpn 1983 Jun;46(3):401-426.
11. Garver WS, Erickson RP, Wilson JM, Colton TL, Hossain GS, Kozloski MA, et al. Altered expression of caveolin-1 and increased cholesterol in detergent insoluble membrane fractions from liver in mice with Niemann-Pick disease type C. Biochim Biophys Acta 1997 Oct 24;1361(3):272-280.
12. Mayoral R, Fernandez-Martinez A, Roy R, Bosca L, Martin-Sanz P. Dispensability and dynamics of caveolin-1 during liver regeneration and in isolated hepatic cells. Hepatology 2007 Sep;46(3):813-822.
13. Smart EJ, Ying Y, Donzell WC, Anderson RG. A role for caveolin in transport of cholesterol from endoplasmic reticulum to plasma membrane. J Biol Chem 1996 Nov 15;271(46):29427-29435.
14. Pol A, Luetterforst R, Lindsay M, Heino S, Ikonen E, Parton RG. A caveolin dominant negative mutant

associates with lipid bodies and induces intracellular cholesterol imbalance. J Cell Biol 2001 Mar 5;152(5):1057-1070.
15. Fernandez MA, Albor C, Ingelmo-Torres M, Nixon SJ, Ferguson C, Kurzchalia T, et al. Caveolin-1 is essential for liver regeneration. Science 2006 Sep 15;313(5793):1628-1632.
16. Lazarow PB. Rat liver peroxisomes catalyze the beta oxidation of fatty acids. J Biol Chem 1978 Mar 10;253(5):1522-1528.
17. Pedersen JI, Gustafsson J. Conversion of 3 alpha, 7 alpha, 12 alpha-trihydroxy-5 beta-cholestanoic acid into cholic acid by rat liver peroxisomes. FEBS Lett 1980 Dec 1;121(2):345-348.
18. Wanders RJ, Waterham HR. Biochemistry of mammalian peroxisomes revisited. Annu Rev Biochem 2006;75:295-332.
19. Heiland I, Erdmann R. Biogenesis of peroxisomes. Topogenesis of the peroxisomal membrane and matrix proteins. FEBS J 2005 May;272(10):2362-2372.
20. Vrenken TE, Buist-Homan M, Kalsbeek AJ, Faber KN, Moshage H. The active metabolite of leflunomide, A77 1726, protects rat hepatocytes against bile acid-induced apoptosis. J Hepatol 2008 Nov;49(5):799-809.
21. Pellicoro A, van den Heuvel FA, Geuken M, Moshage H, Jansen PL, Faber KN. Human and rat bile acid-CoA:amino acid N-acyltransferase are liver-specific peroxisomal enzymes: implications for intracellular bile salt transport. Hepatology 2007 Feb;45(2):340-348.
22. Blokzijl H, Vander Borght S, Bok LIH, Libbrecht L, Geuken M, Van den Heuvel FAJ, et al. Decreased P-glycoprotein (P-gp/MDR1) expression in inflamed human intestinal epithelium is independent of PXR protein levels. Inflammatory Bowel Diseases 2007;13(6):710-720.
23. Antonenkov VD, Sormunen RT, Hiltunen JK. The behavior of peroxisomes in vitro: mammalian peroxisomes are osmotically sensitive particles. Am J Physiol Cell Physiol 2004 Dec;287(6):C1623-C1635.
24. Verheyden K, Fransen M, Van Veldhoven PP, Mannaerts GP. Presence of small GTP-binding proteins in the peroxisomal membrane. Biochim Biophys Acta 1992 Aug 10;1109(1):48-54.
25. Slimane TA, Trugnan G, van IJzendoorn SC, Hoekstra D. Raft-mediated trafficking of apical resident proteins occurs in both direct and transcytotic pathways in polarized hepatic cells: role of distinct lipid microdomains. Mol Biol Cell 2003 Feb;14(2):611-624.
26. Calvo M, Tebar F, Lopez-Iglesias C, Enrich C. Morphologic and functional characterization of caveolae in rat liver hepatocytes. Hepatology 2001 May;33(5):1259-1269.
27. Pol A, Martin S, Fernandez MA, Ferguson C, Carozzi A, Luetterforst R, et al. Dynamic and regulated association of caveolin with lipid bodies: modulation of lipid body motility and function by a dominant negative mutant. Mol Biol Cell 2004 Jan;15(1):99-110.
28. Garver WS, Heidenreich RA, Erickson RP, Thomas MA, Wilson JM. Localization of the murine Niemann-Pick C1 protein to two distinct intracellular compartments. J Lipid Res 2000 May;41(5):673-687.
29. Balbis A, Baquiran G, Mounier C, Posner BI. Effect of insulin on caveolin-enriched membrane domains in rat liver. J Biol Chem 2004 Sep 17;279(38):39348-39357.
30. Appelkvist EL, Brunk U, Dallner G. Isolation of peroxisomes from rat liver using sucrose and Percoll gradients. J Biochem Biophys Methods 1981 Oct;5(4):203-217.
31. Zhou M, Parr RD, Petrescu AD, Payne HR, Atshaves BP, Kier AB, et al. Sterol carrier protein-2 directly interacts with caveolin-1 in vitro and in vivo. Biochemistry 2004 Jun 15;43(23):7288-7306.
32. Li S, Song KS, Lisanti MP. Expression and characterization of recombinant caveolin. Purification by polyhistidine tagging and cholesterol-dependent incorporation into defined lipid membranes. J Biol Chem 1996 Jan 5;271(1):568-573.
33. Chamberlain LH, Gould GW. The vesicle- and target-SNARE proteins that mediate Glut4 vesicle fusion are localized in detergent-insoluble lipid rafts present on distinct intracellular membranes. J Biol Chem 2002 Dec 20;277(51):49750-49754.
34. Goldfischer S, Essner E. Further observations on the peroxidatic activities of microbodies (Peroxisomes). J Histochem Cytochem 1969 Oct;17(10):681-685.
35. Yu S, Matsusue K, Kashireddy P, Cao WQ, Yeldandi V, Yeldandi AV, et al. Adipocyte-specific gene expression and adipogenic steatosis in the mouse liver due to peroxisome proliferator-activated receptor gamma1 (PPARgamma1) overexpression. J Biol Chem 2003 Jan 3;278(1):498-505.
36. Glende EA, Jr., Morgan WS. Alteration in liver lipid and lipid fatty acid composition after partial hepatectomy in the rat. Exp Mol Pathol 1968 Apr;8(2):190-200.
37. Ferri D, Moro L, Mastrodonato M, Capuano F, Marra E, Liquori GE, et al. Ultrastructural zonal heterogeneity of hepatocytes and mitochondria within the hepatic acinus during liver regeneration after partial hepatectomy. Biol Cell 2005 Apr;97(4):277-288.
38. Beardsley A, Fang K, Mertz H, Castranova V, Friend S, Liu J. Loss of caveolin-1 polarity impedes endothelial cell polarization and directional movement. J Biol Chem 2005 Feb 4;280(5):3541-3547.
39. He D, Barnes S, Falany CN. Rat liver bile acid CoA:amino acid N-acyltransferase: expression, characterization, and peroxisomal localization. J Lipid Res 2003 Dec;44(12):2242-2249.
40. Vos TA, Hooiveld GJ, Koning H, Childs S, Meijer DK, Moshage H, et al. Up-regulation of the multidrug resistance genes, Mrp1 and Mdr1b, and down-regulation of the organic anion transporter, Mrp2, and the bile salt transporter, Spgp, in endotoxemic rat liver. Hepatology 1998 Dec;28(6):1637-1644.
41. Fransen M, Terlecky SR, Subramani S. Identification of a human PTS1 receptor docking protein directly required for peroxisomal protein import. Proceedings of the National Academy of Sciences of the United States of America 1998;95(14):8087-8

SUPPLEMENTARY EXPERIMENTAL PROCEDURES

Extraction of peroxisomal membrane proteins

The extraction of peroxisomal membrane proteins (PMPs) was performed according to established methods (1) with some adaptations. Three (3) fractions of ~250 µg purified peroxisomes were pelleted at 100,000 x g in a Beckman TLA-100.3 rotor (Beckman, Fullerton, CA, USA). The pellets were resuspended in 1 mL of either 100 mM Tris-HCl, pH 8.0, or 1 M NaCl in 100 mM Tris-HCl, pH 8.5, or 0.1 M Na2CO3, pH 11.0 and incubated on ice for 15 minutes. Insoluble materials were pelleted by centrifugation for 15 minutes at 200,000 × g at 4 °C in a Beckman TLA-100.3 rotor (Beckman). Pellet fractions were resuspended in the appropriate buffer as described above. Equal volume fractions were analyzed by western blotting.

Proteinase K protection assay

Aliquots of purified peroxisomes (approximately 100 µg) were subjected to proteolysis by proteinase K as described previously (2). These aliquots were incubated with either 0 or 0.2 mg/ml proteinase K (Invitrogen) in the presence or absence of 0.1% Triton X-100 (Sigma-Aldrich) for 30 minutes at 4ºC. The proteinase K digestion was terminated by the precipitation of each sample with 12.5% trichloroacetic acid (TCA, Sigma-Aldrich), followed by TCA protein precipitation (3). Equal volumes of all protein samples were analyzed by western blotting.

Immunogold labeling and electron microscopy

Ten million freshly isolated hepatocytes were pelleted and fixed with 2% glutaraldehyde (Sigma-Aldrich) at 4ºC for 30 minutes and further processed according to the method described by van der Wel et al. (4). Briefly, cryo-sections were prepared according to Tokuyashu (5) followed by immunogold labeling (6). Primary antibodies (Table 3) were visualized using gold conjugated secondary antibodies (5 nm gold-conjugated goat-anti mouse and 15 nm gold-conjugated goat-anti rabbit, BB International, Cardiff UK). Images were captured on a FEI CM100 Bio (FEI Co., Hillsboro, OR). Digital pictures were taken at 80kV accelerating voltage.

1. Wiemer EA, Luers GH, Faber KN, Wenzel T, Veenhuis M, Subramani S. Isolation and characterization of Pas2p, a peroxisomal membrane protein essential for peroxisome biogenesis in the methylotrophic yeast Pichia pastoris. J Biol Chem 1996 Aug 2;271(31):18973-18980.
2. Hohfeld J, Veenhuis M, Kunau WH. PAS3, a Saccharomyces cerevisiae gene encoding a peroxisomal integral membrane protein essential for peroxisome biogenesis. J Cell Biol 1991 Sep;114(6):1167-1178.
3. Hohfeld J, Veenhuis M, Kunau WH. PAS3, a Saccharomyces cerevisiae gene encoding a peroxisomal integral membrane protein essential for peroxisome biogenesis. J Cell Biol 1991 Sep;114(6):1167-1178.
4. van der Wel NN, Fluitsma DM, Dascher CC, Brenner MB, Peters PJ. Subcellular localization of mycobacteria in tissues and detection of lipid antigens in organelles using cryo-techniques for light and electron microscopy. Curr Opin Microbiol 2005 Jun;8(3):323-330.
5. Tokuyasu KT. A technique for ultracryotomy of cell suspensions and tissues. J Cell Biol 1973 May;57(2):551-565.
6. Painter RG, Tokuyasu KT, Singer SJ. Immunoferritin localization of intracellular antigens: the use of ultracryotomy to obtain ultrathin sections suitable for direct immunoferritin staining. Proc Natl Acad Sci U S A 1973 Jun;70(6):1649-1653.

SUPPLEMENTARY FIGURES

Figure S1. Expression of caveolin-1 in rat liver
Total protein extracts from rat lung and liver were analyzed by western blotting using a specific antibody against caveolin-1 and Gapdh. The left panel shows results when equal amounts of extracts (20 µg) were loaded of both organs. In the right panel, the total protein extract from rat lung was 100-fold diluted to obtain comparable signal intensities for caveolin-1.

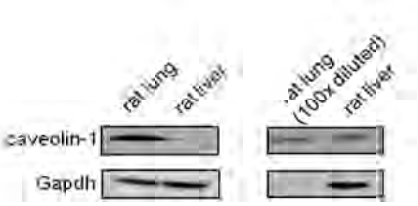

Figure S2. EGFP-caveolin-1 accumulates at various subcellular locations when highly expressed in rat hepatocytes.
Primary rat hepatocytes were transiently transfected and analyzed as described in Figure 2. Hepatocytes with high levels of EGFP-caveolin-1 (right panel) show accumulation of the heterologous hybrid protein at multiple cellular locations, including the plasmamembrane (arrows). Immunodetection of catalase (left panel) is shown for comparison.

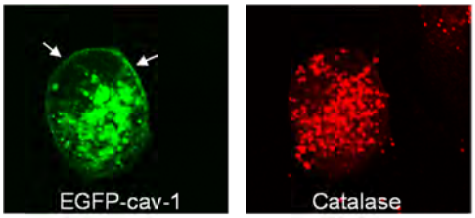

Figure S3. Triton X-100 and Lubrol WX extractions on rat hepatocytes
Primary rat hepatocytes were lysed in the presence of 1% Triton X-100 or Lubrol XW followed by flotation gradient centrifugation. One (1) ml fractions (in total 12) were collected from the top and analyzed by western blotting (A, Triton X-100 extraction; B, Lubrol WX extraction). For western blot analysis, equal volumes from the gradient fractions were analyzed using specific antibodies against caveolin-1, the peroxisomal membrane proteins ALDP, PMP70, Pex14p, Pex13p and the cytosolic proteins β-actin and Gapdh. Equal volumes of the unfractionated total protein lysate (T) as well as the pellet fraction after flotation gradient centrifugation (P) were also analyzed.

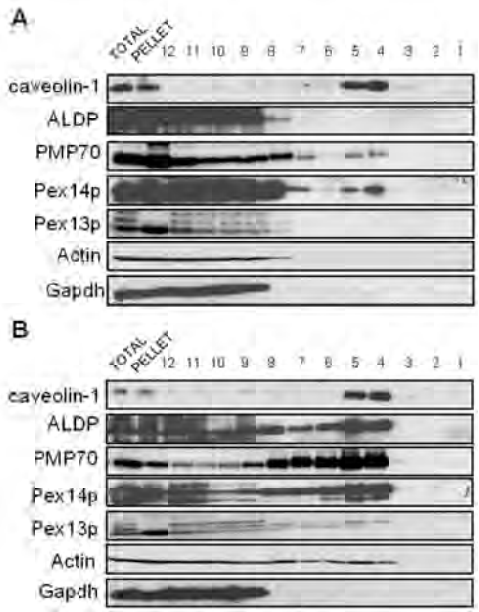

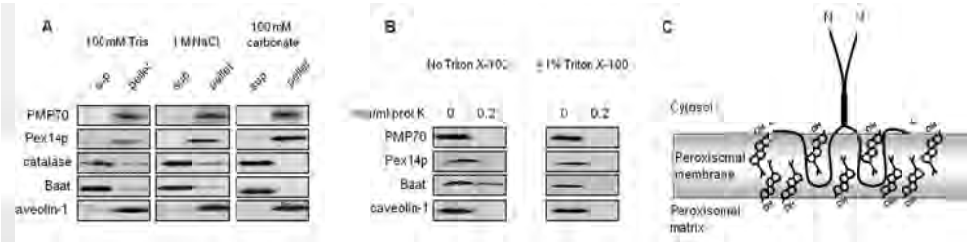

Figure S4. Caveolin-1 is an integral peroxisomal membrane protein with its N-terminus exposed to the cytosol

Freshly isolated rat liver peroxisomes were lysed in buffers containing 1 M sodium chloride or 100 mM sodium bicarbonate (pH 11) and compared to hypertonic lysis of peroxisomes (100 mM Tris HCl). Insoluble materials were pelleted by centrifugation. Equal volume fractions of pellets and supernatants were analyzed by western blotting using antibodies against PMP70, Pex14p, catalase, Baat and caveolin-1 (A). Freshly isolated rat liver peroxisomes were subjected to proteinase K digestion (0,2 mg/ml proteinase K) in the absence or presence of 1% Triton X-100. Equal volumes of all protein samples were analyzed by western blotting using antibodies against PMP70, Pex14p, Baat and caveolin-1 (B).

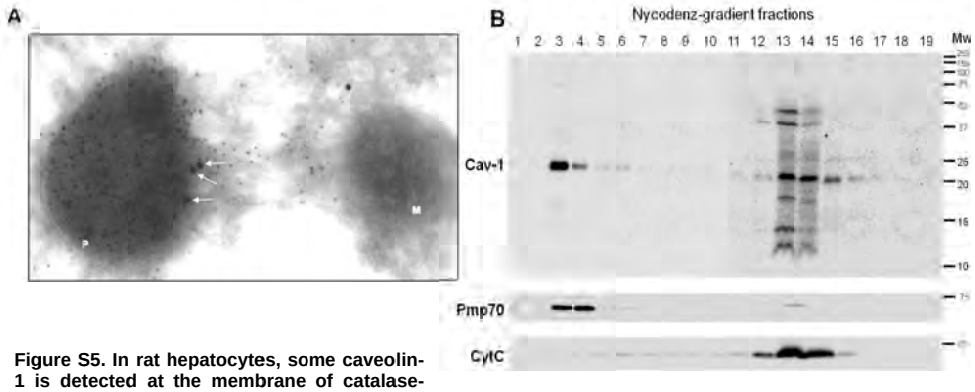

Figure S5. In rat hepatocytes, some caveolin-1 is detected at the membrane of catalase-positive peroxisomes

(A) Primary rat hepatocytes were analyzed by immuno-electron microscopy to determine the subcellular location of catalase and caveolin-1. Catalase and caveolin-1 were detected using specific primary antibodies that were recognized by secondary antibodies conjugated to 5 nm gold and 15 nm gold (arrows), respectively. Gold-labeled catalase and caveolin-1 were clearly present in peroxisomes (P) but not in mitochondria (M). The specific detection of caveolin-1 in the peroxisomal peak fraction (fractions 3 and 4) after Nycodenz gradient centrifugation is shown in (B). Besides caveolin-1 (at 21 kDa), no other peroxisomal protein between 10 and 250 kDa shows significant cross reaction with the anti-caveolin-1 antibody.

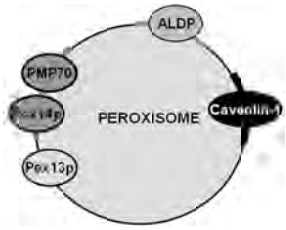

Figure S6. Co-existence of caveolin-1 with other lipid rafts in the peroxisomal membrane. Caveolin-1 is embedded in a different lipid environment than the peroxisomal membrane proteins (PMPs) Pex13p, Pex14p, ALDP and PMP70. Pex13p is not raft-associated, while ALDP is associated with Lubrol-resistant rafts (gray). Pex14p and PMP70 are embedded in Triton X-100 resistant rafts (dark gray). Caveolin-1 even resists Triton X-100 extraction under very stringent conditions, in which PMP70 and Pex14p are solubilized. Therefore, caveolin-1 is embedded in a different lipid environment than the other PMPs (black).

CHAPTER 6

General discussion & future perspectives

General discussion and future perspectives

In this thesis, we have studied various aspects of peroxisome biogenesis and functions in bile salt homeostasis. We have demonstrated for the first time that bile acids in the enterohepatic cycle shuttle through peroxisomes to become (re-) conjugated to taurine or glycine. The 70-kDa peroxisomal membrane protein (PMP70/Pmp70) is the most dominant proteinaceous component of the membrane of liver peroxisomes and manipulation of PMP70 expression in rat hepatocytes directly affects bile acid conjugation and transport by rat hepatocytes. PMP70 appears to be associated with peroxisomal lipid rafts, which are small detergent-resistant microdomains in cellular membranes, but had not been found in mammalian peroxisomes before. In fact, peroxisomal membrane proteins show distinct lipid-raft association characteristics, suggesting the presence of at least 3 different types of lipid rafts in mammalian peroxisomes. Remarkably, hepatocyte peroxisomes appeared to contain most of the cellular amount of caveolin-1, a protein that is involved in lipid transport and in most other cell types is characteristically detected in endocytotic pits at the plasmamembrane. We show that peroxisomal lipid rafts are required for peroxisome biogenesis. Their putative role in bile salts and/or lipid transport remains to be determined.

Detailed information is available about transporters that are involved in bile salt shuttling between liver and the intestine. Little is known, however, how bile salts are transported inside hepatocytes and enterocytes. This is especially relevant for bile salts that lost their taurine or glycine moiety in the intestine, since they need to be re-conjugated in the liver. Earlier studies showed that the enzyme responsible for bile salt reconjugation, bile acid CoA:amino acid:N-acyltransferase (BAAT), resides predominantly (if not solely) in peroxisomes (1), however, direct evidence for bile salt transport in and/or out of peroxisomes has not been demonstrated by others.
In chapter 2, we show that deuterium-labeled cholic acid (D_4CA) shuttles through peroxisomes to become conjugated to taurine in cultured rat hepatocytes. We propose a model where unconjugated bile acids that return to the liver are taken up by Oatps (or Ntcp) and subsequently activated to CoA-esters by Fatp5/Bal, which resides at the basolateral membrane. CoA-activated bile acids enter peroxisomes where they are conjugated to taurine or glycine. We developed an assay that shows a time-dependent conversion of D_4CA and intracellular accumulation of newly-formed conjugates (D_4TCA and D_4GCA). We observe that the strongest accumulation occurs at the three-hour time point of incubation with D_4CA and speculate that this effect is most likely caused by retention of conjugates inside peroxisomes, which is demonstrated by digitonin permeabilization assays.

The fact that bile acids need to enter peroxisomes for conjugations is in line with our previous work that revealed that BAAT is predominantly, if not solely, present in peroxisomes. The intracellular localization of BAAT has been a topic of various studies, with variable outcomes. Some authors reported that this enzyme resides in the cytosol (O'Byrne J. *et al*., 2003 (2)), while others detected it both in peroxisomes and in the cytosol (He D. *et al*., 2003 (3) and Solaas K. *et al*., 2000 (4)). In some experiments, 75% of BAAT activity was found in cytosolic fractions (Styles NA. *et al*., 2007 (5)). Other authors have suggested that there are two forms of this enzyme, one residing in peroxisomes and the other in the cytoplasm (Solaas K. *et al*., 2004 (6)). Mutations in the gene encoding BAAT lead to a bile salt pool that is completely uncojugated (7, 8). This indicates that there is only one enzyme able to perform glycine/taurine conjugation of bile salts, at least in human. The combination of immunofluorescence microscopy and digitonin permeabilization assays on rat and human hepatocytes revealed a typical peroxisomal location for BAAT (Pellicoro A. *et al*., 2007 (1)). With the detection of conjugated D_4TCA in peroxisomes isolated from hepatocytes that were exposed to D_4CA, the studies in this thesis now also provide direct evidence that unconjugated bile acids shuttle through peroxisomes.

For the proper interpretation of the subcellular accumulation of D_4-conjugates, it was crucial to exclude the possibility that they may also accumulate in a canalicular network formed between polarized rat hepatocytes in culture. Such canalicular networks are, however, formed at later time points (48-72 hours after attachment) in rat hepatocyte cultures. In our study, the hepatocytes were used within 24 hours after attachment. Moreover, the hepatocytes were washed with Ca^{2+}-free HBSS, which disrupts tight junctions and thereby the interaction between hepatocytes that is required to maintain canalicular vacuoles and/or network. Finally, the canalicular is rich in cholesterol and is permeabilized at low (30 ug/ml) concentrations digitonin. In contrast, D_4TCA was only completely released at high (500 ug/ml) concentrations digitonin, indicating that it is present in organelles with membranes with low cholesterol content. The peroxisomal membrane is relatively low in cholesterol content.

Peroxisomes are fragile organelles that easily get damaged and lose (part of) their content during cell fractionation experiments (9, 10) This is probably the main reason why in many experiments significant amounts of Baat were detected in fractions that represent the cytosol. We used an optimized protocol for isolation of peroxisomes to minimize the leakage of matrix proteins, such as Baat and catalase (Antonenkov *et al*., 2004 (9)). Polyethylene glycol 1500 is added to buffers to stabilize organellar membranes during the isolation procedure This lead to a strong reduction of peroxisomal damage during the hepatocyte homogenization step and allowed the separation of the various organelles and cytosol from a postnuclear supernatant (PNS) fraction using a discontinuous Nycodenz® gradient (11). Previously, this was only done by loading an organelle-enriched high-speed

centrifugation pellet fraction. Direct loading of a PNS fraction onto the Nycodenz® gradient minimized the osmotic damage to peroxisomes and provided additional evidence for a predominant peroxisomal localization of BAAT.

The separation of a PNS by Nycodenz® density gradient centrifugation additionally allowed the detection of solutes/metabolites in peroxisome-enriched fractions from the gradient, which has not been documented before. After exposing hepatocytes for 3 h to D_4CA we were able to detect the conjugation product D_4TCA in the peroxisomal peak fraction. The D_4TCA peak intensity was relatively low, but its distribution in the high-density fraction of the Nycodenz gradient followed exactly that of peroxisomal marker proteins. The low amounts of D_4TCA in these fractions may be a result of a very efficient export process of conjugated bile acids from the peroxisome or release of these bile acids during the isolation procedure. Indeed, most of D_4TCA was detected on the top of the Nycodenz gradient where cytosolic compounds are present. Cytosolic D_4TCA could also be a result of potential reuptake of previously produced and secreted D_4TCA (12). Because it is already conjugated, it will not travel through peroxisomes again, but add to the cytosolic concentration of this bile salt. When studying the overall dynamics of D_4CA conjugation to either taurine or glycine, it is clear that the potential reuptake of D_4TCA does not give rise to a strong cytosolic accumulation in rat hepatocytes. This is supported by the observation that cellular concentrations of conjugated bile salts is low after twenty-four hours of incubation, while their concentration in the medium is high. Moreover, organelle isolations were performed 3 h after exposing hepatocytes to D_4CA and at that time point, the amounts of extracellular D_4TCA and D_4GCA were still relatively low.

All treatments with D_4CA were performed with hepatocytes no longer than 24 hours in culture to avoid yet another limitation, namely the progressive loss of the capacity to take up bile salts of cultured hepatocytes (12). We additionally kept rat hepatocytes attached to collagen-coated plates/flasks, as those in suspension demonstrate reduced bile salt efflux kinetics (12).

The Nycodenz® gradient of post-nuclear supernatant (Chapters 2 and 3) revealed two distinct peroxisomal populations: one migrating as high-density peroxisomes at fractions 2-5 and the other migrating together with (light) mitochondria in factions 10-11. Similar data have been obtained by others (13, 14). Remarkably, high amounts of D_4TCA were detected in fractions that contain the low-density peroxisomes (see Chapter 2, figure 6). It has been described that peroxisomes in the liver exist as a mixed population of organelles at several biogenesis stages (13, 14, 15), which is manifested by heterogeneous uricase and homogenous catalase staining (16) among peroxisomes in the hepatocyte. At present, only the high density peroxisomal population has been successfully isolated as a fraction of almost 95% purity (17, 18). Early studies suggest that the “low density” peroxisomes contain predominantly the newly-synthesized peroxisomal proteins. Pulse-chase experiments revealed that Acox first localizes to the low density peroxisomes compartment after which it appears in the high-density peroxisomes (19). In line with this, Pmp70 transits from the “light” to the “heavy” peroxisomal

fraction during peroxisomal biogenesis after partial hepatectomy. Consequently, these two peroxisomal populations may differ in membrane protein composition and metabolic activity. The heterogeneity is transient and it most probably reflects the incompetence of mature peroxisomes to incorporate new proteins (20, 21).

The amount of D_4TCA detected in the low density peroxisomes seems to correlate better with the digitonin latency analyses. The latter suggest that a significant amount of cellular D_4TCA is present in peroxisome-like organelles surrounded by membranes with low cholesterol content. The very small amounts of D_4TCA cannot account for this. It may be that almost all D_4TCA is lost from the high density peroxisomes during the isolation procedure (either by transport or leakage). However, the alternative possibility is that most of the D_4TCA is actually trapped in the low-density peroxisomes. This could be a result of a heterogeneous distribution of bile salt transporters among the light and heavy fraction during peroxisomal biogenesis. In this scenario, the peroxisomal bile salt exporter may not be optimally localized/expressed in the light fraction compared to "heavy" peroxisomes.
As indicated before, peroxisomes are fragile organelles *in vitro* and easily rupture in cell fractionation experiments. The level of organelle damage is difficult to determine as some proteins leak out easily (e.g. catalase) while others remain well associated to peroxisome-enriched fractions (e.g. isocitrate dehydrogenase) (22). The phenomenon of peroxisomal leakiness *in vitro* has not been explained so far. Recently, however, the existence of peroxisomal channel formed by Pxmp2 has been described (23). This diffusion pore is responsible for the peroxisomal membrane permeability to small solutes, but does not seem to allow free passage of bulky compounds like bile salts and proteins. On the other hand, the peroxisomal membrane contains large (9 nm) pores that allows the translocation of large, fully folded, oligomeric peroxisomal matrix proteins (like catalase) (24). These pores may become permeable *in vitro* when losing their cellular environment during isolation and lead to the observed leakage of (even complex) compounds.
Peroxisomal enzymes are made on polysomes in the cytosol and post-translationally imported into the target organelle. Thus, even if BAAT activity is restricted to peroxisomes, some BAAT protein will be present in the cytosol and on its way to peroxisomes. A clear cytosolic pool of BAAT was observed when it was overexpressed in a fusion with the Green Fluorescent Protein (GFP-BAAT) in human fibroblasts (1). However, this fusion protein was efficiently sorted to peroxisomes when expressed in hepatocytes (1), suggesting the existence of cell-type specific factors that enhance peroxisomal sorting of BAAT.
In summary, we propose that under normal physiological conditions both C_{27}- and recycled C_{24}-bile salts are conjugated by BAAT in peroxisomes. Future research should establish the physiological relevance of the peroxisomal location of BAAT for bile salt homeostasis. The first step may be to try to identify the proteins that transport bile salts in and out peroxisomes.

In chapter 3, we studied the putative role of the peroxisomal membrane transporter Pmp70 in the bile salt re-conjugation process. Pmp70 is the most dominant peroxisomal membrane protein in rat liver, still very little is known about its function and which substrates it transports. Its ATP-binding site faces the cytosol, which suggests that it transports substrates into peroxisomes. Our data suggest that this peroxisomal ABC-half transporter is involved in bile acid re-conjugation and transhepatocyte transport of cholic acid in isolated rat hepatocytes. Pmp70 expression was increased by the peroxisome proliferator-activated receptor-alpha (PPARα) ligand fenofibric acid (FFA) and lead to increased conversion of CA to TCA in isolated rat hepatocytes. Simultaneous inhibition of Pmp70 expression through RNA interference (*Abcd3*-siRNA) suppressed the conversion of TCA leading to reduced concentrations of TCA in de medium. In addition, intracellular levels of CA and TCA decreased in FFA-treated rat hepatocytes, which were normalized again when co-treated with PMP70-specific RNA interference. These data suggest the involvement of PMP70 in transcellular bile salt transport and/or conjugation to taurine.

Notably, expression of Bal, Baat, Ntcp and Bsep, e.g. the other proteins in the conjugation and transcellular bile acid pathway was not changed in rat hepatocytes treated for 24 h with FFA. The differences in cellular and extracellular bile acid concentrations could therefore be directly related to the level of Pmp70 in FFA and/or *Abcd3*-siRNA treated rat hepatocytes.
Newly-synthesized Pmp70 is predominantly targeted to the low-density peroxisomes and appears subsequently in „heavy" peroxisomes (13, 14). The Pmp70 signal is indeed overrepresented in low-density peroxisomes of FFA-treated hepatocytes compared to those from control hepatocytes. Baat is also present in the low-density peroxisome, but does not seem to be more enriched in these fractions after FFA treatment. It will be interesting to determine whether FFA-treatment changes the amount of newly conjugated cholic acid in either low-density and/or high density peroxisomes. If newly sorted PMP70 is immediately active, this could result in preferential accumulation of D_4TCA in low-density peroxisomes. Either way, initial tests should include purification and characterization of the low-density organelles to confirm that these structures are indeed functional peroxisomes.
Following our *in vitro* studies, it is now imperative to obtain support for the involvement of PMP70 in bile salt homeostasis *in vivo*. Pmp70-knockout mice would be the ideal model to analyze this. These animals have been described in abstracts of scientific meetings; however, no detailed characterization of their phenotype is available in peer-reviewed literature so far. Alternatively, siRNA-based approaches could be applied to specifically suppress Pmp70 expression in the liver either by tail vein-injections of siRNA duplexes or short hairpin siRNA expressing adenoviruses. The latter approach has pros and cons: acute suppression of Pmp70 by siRNA may prevent potential compensatory expression of other peroxisomal ABC transporters with overlapping substrate specificity, which is

more likely to occur in Pmp70 knock out mice. However, siRNA-based procedures are never 100% effective and it is unknown what the under limit is of Pmp70 before a physiological effect becomes apparent.
In vitro experiments to further establish the involvement of peroxisomes in bile acid conjugation may include the addition of unconjugated bile acids to purified organelles from a Nycodenz gradient. This experiment would require the use of CoA-activated cholic acid, since plasmamembrane-associated FATP5/Bal/BACS is absent from the organellar fractions. Such experiments could also provide additional information about the contribution and the bile acid conversion rates by low- and high-density peroxisomes.
Bile salts harboring a fluorescent moiety, e.g. fluorescein or Nε-nitrobenzoxadiazolyl (NBD), have been widely used to analyze transport characteristics in hepatocytes and whole liver. In theory, they would be ideal compounds to trace the routing of bile salts through peroxisomes of hepatocytes. However, most of these fluorescent bile salts contain the fluorescent group attached to the side chain, preventing their glycine/taurine conjugation. Moreover, it was recently shown that choly-lysyl-fluorescein (CLF)is actually a very poor substrate for the typical bile salt transporters NTCP and BSEP and predominantly transported by OATP1B3, MRP2 and MRP3 (25). This severely hampers the use fluorescent bile salts to study their intracellular transport. We analyzed cellular uptake and conjugation of cholic acid containing a NBD group at the 3α, 3β, 7α or 7β position. Only for 3α-NBD-CA, we found that it was conjugated to glycine or taurine, though the conversion was very inefficient compared to deuterium-labeled CA. Still, it revealed that the 3α position allows the presence of a fluorescent group and is still a substrate for Bal, Baat and putative intracellular transporters. Testing different fluorescent groups attached to the 3α position of cholic acid may therefore yield fluorescent bile salts that are efficiently handled by genuine bile acid modifying enzymes and transporters. Given the recent findings that one of the most used fluorescent bile acids, CLF, is actually not a substrate for Ntcp and Bsep, further stresses the need for new fluorescently tagged bile acids to trace their transport inside cells (25).

The important question is whether defects in putative peroxisomal bile salt transporters (both the importer and the exporter) would cause a clinical phenotype. Malfunctioning of the peroxisomal bile salt importer could hypothetically cause a change in the bile salt profile towards unconjugated bile acids. Two different scenarios can be envisioned: 1) the unconjugated bile salts are mostly C_{24}-derivatives. This could result from the possibility that independent transporters exist in the peroxisomal membrane for C_{27} (bile salt biosynthesis-intermediates) and C_{24} (intestinal deconjugated) – bile salts. 2) The unconjugated bile salts are mostly C_{27}-derivatives. In this case, transport of the bile salt biosynthesis intermediates into the peroxisomes is hampered and enterohepatic cycling of these "immature" bile salts is very inefficient. The latter condition would be similar to the bile salt profile of patients with Zellweger Syndrome (ZS), where

peroxisome biogenesis is impaired. The bile salt intermediates are partly conjugated though in these patients. Baat is most likely residing in the cytosol in ZS patients, which may account for the residual conjugation activity. In case of a specific blockade of import of C_{27}-bile salt intermediates, we expect that the whole bile salt pool would remain unconjugated, because the cytosolic C_{27} intermediates will be physically separated from peroxisomal Baat.
The impairment of the putative peroxisomal bile salt exporter, on the other hand, may lead to the accumulation of bile salts inside this organelle. In such case, accumulating bile salts could damage the peroxisome and impair its function and biogenesis. In the extreme conditions that all peroxisomes would be involved in bile salt conjugation, this may lead to a Zellweger Syndrome-like phenotype, but would be strictly limited to hepatocytes. In fact, patients with a liver-specific defect in peroxisome biogenesis have been described, where this phenotype was detected in most hepatocytes, while fibroblasts from these patients contained normal peroxisomes (26, 27). Thus, it may very well be these patients have a defect in peroxisomal bile salt export.

The putative activity of cytosolic BAAT is a relevant (and still open) question when discussing the hepatocyte capacity to conjugate bile salts in peroxisomal biogenesis disorders, such as ZS. ZS is characterized by the lack of functional peroxisomes. However, peroxisomal remnants (ghosts) containing PMPs, but lacking most of the matrix enzymes, are detected in the majority of ZS patients (28, 29). Though the subcellular location of BAAT has never been established in ZS patients, we assume that it resides in the cytosol just like catalase.
ZS patients typically accumulate bile salt biosynthesis intermediates like di- and trihydroxycholestanoic acid (D- and THCA). The primary bile acids CA and CDCA are also detected, but at strongly reduced levels. Both the bile salt intermediates and the primary bile salts are only partly conjugated to glycine or taurine. (30, 31). This suggests that BAAT activity is compromised when peroxisomal biogenesis is disturbed, however, it is not completely blocked. Similar observations have been made in studies with *Pex2*-/- knock-out mice, an animal model of Zellweger Syndrome. These mice accumulate C27 bile salt synthesis intermediates in serum, liver and bile, while the C_{24} bile salt concentrations are strongly reduced. Most of these bile salts are unconjugated. Feeding these animal a cholic acid- or ursodeoxycholic acid-containing diet reduced the level of C_{27} bile salt intermediates, but unconjugated bile acids remained dominant in the bile acid pool (32). In contrast, bile acid-fed wild type mice effectively conjugated the bile acids from the diet. Thus, peroxisome deficiency leads to a generalized defect in bile acid conjugation. The residual bile salt-conjugating activity is likely the result of Baat present in the cytosol, indicating that it retains some enzymatic activity at in this subcellular location. Nonetheless, it is clear that the loss of peroxisomal BAAT severely affects bile salt conjugation efficiency and therefore supports our data that in normal conditions it is primarily present in peroxisomes.

The activity of bile salt transporters present in plasma membranes of enterocytes and hepatocytes is modulated by their specific lipid environment, where they associate to cholesterol-enriched microdomains, so-called lipid rafts. It seems likely that bile acid transporters in organelles share this characteristic and are localized to organellar lipid rafts. To determine whether this holds true for the putative peroxisomal bile salt transporter PMP70, we studied whether the peroxisomal membrane contains lipid rafts. Though lipid rafts have been detected in several organellar membranes, this was not particular likely for the peroxisomal membrane, which contains relatively low concentrations of cholesterol.
In chapter 4 (Woudenberg *et al*. 2010 (33)) we describe the existence of peroxisomal lipid rafts and their role in the biogenesis for this organelle. We show that the homologous ABC transporters PMP70 and ALDP are differentially associated to lipids in the peroxisomal membrane as the former resists solubilization with a strong detergent (Triton X-100), whereas the latter only resists the treatment with a mild detergent (Lubrol WX). Also Pex14p was found in Triton X-100 resistance lipid rafts, whereas an interacting partner, Pex13p does not seem to associate with lipid rafts at al. HepG2 cells were depleted from cholesterol, which leads to a mislocalisation of catalase to the cytosol. In addition, ALDP lost its typical peroxisomal location, most likely accumulating in the ER. In contrast, PMP70 and Pex14 retained a largely peroxisome-like location. These processes were largely reversible, as catalase sorting to peroxisomes was restored after repletion of cholesterol in HepG2 cells. However, ALDP sorting was not effectively restored in these cells. These data show that the peroxisomal membrane contains lipid rafts, which are essential for peroxisome biogenesis. Highly homologous (PMP70 and ALDP) and physically interacting (Pex13p and Pex14p) showed different lipid raft association characteristics. The lipid environment of these proteins may strongly affect their activity, either in substrate transport (PMP70 and ALDP) or peroxisome biogenesis (Pex13p and Pex14p).

It has been suggested that the peroxisomal ABC half transporters, including PMP70 and ALDP, may form heterodimers. Formation of such heterodimers could greatly broaden the number of substrates transported by the subgroup of ABC transporters. The fact that PMP70 and ALDP show clear different lipid raft associations seems to argue against the formation of PMP70/ALDP heterodimers in HepG2 cells and hepatocytes. This is in line with the analysis of endogenous PMP70 and ALDP from mouse liver, which revealed that these proteins are predominantly present as homodimers. However, our detergent extraction experiments cannot formally exclude the possibility PMP70 and ALDP co-exist in one microdomain with high internal lipid heterogeneity that still allows the formation of heterodimers. Still, PMP70 and ALDP behave very different in the cholesterol depletion-repletion experiments indicating that ALDP/PMP70 heterodimers are unlikely to be prevalent in HepG2 cells.
Although PMP70 shares the "lipid raft association-feature with the bile acid transporters in plasmamembranes, the current experimental system (cholesterol

depletion-repletion) cannot be used to specifically test whether the presence of PMP70 in lipid rafts regulates its transport activity. Depletion of cholesterol in whole cells will directly affect the activity of the other bile acid transporters also and any effect on bile salt levels in cells or peroxisomes cannot be related to PMP70. This will probably require the *in vitro* reconstitution of PMP70 in membrane vesicles and manipulation of the membrane lipids in transport assays.

To further characterize the peroxisomal lipid rafts, we compared the detergent-extractability and subcellular location of peroxisomal membrane proteins to several well-known markers for these lipid microdomains, including Src-1, flotillin and caveolin-1. Much to our surprise, we found that caveolin-1 appeared to be present in peroxisomal lipid rafts in hepatocytes (chapter 5). Caveolin-1 is one of three caveolins, which are structural components of caveolae that are characteristically found on small endocytotic pits at the plasmamembrane. Previous research on caveolin-1 knock-out mice has shown that it plays a role in liver regeneration and lipid metabolism.
Hepatocytes contain relative low levels of caveolin-1. In the liver, this protein is predominantly detected in endothelial cells. We used cell fractionation procedures, immunofluorescence and immuno-electron microscopy to localize endogenous caveolin-1 in (purified) rat hepatocytes and consistently found that most of the protein was found in peroxisomes. On top of this, also green fluorescent protein (GFP)-tagged caveolin-1 colocalized to peroxisomal markers when expressed in rat hepatocytes. Peroxisomal caveolin-1 retained its characteristic Triton X-100-inextractable feature as observed when present in the plasmamembrane of other cell types. SiRNA-mediated reduction of caveolin-1 in rat hepatocytes as well as livers from caveolin-1 knock mice do not reveal a role of this protein in peroxisome biogenesis. This seems in line with the observation that fenofibric acid strongly repressed the expression of caveolin-1 while this PPARα agonist induced peroxisome proliferation. This could even imply that shutting down the expression of caveolin-1 is a prerequisite for (the initiation of) peroxisomal proliferation.
Alternatively, peroxisomal caveolin-1 may be involved in lipid and/or bile salt metabolism. Caveolin-1 knock out mice have not yet been studied with respect to bile salt homeostasis. It is known, however, that bile salt signaling is important for liver regeneration, a process that is disturbed in caveolin-1 knock out mice. It seems therefore timely to determine a putative role of caveolin-1 in bile salt homeostasis. The work reported in this thesis provides experimental tools to study this: caveolin-1 expression can be suppressed in primary rat hepatocytes subsequently exposed to D_4CA to analyze the conjugation and transcellular transport efficiency. These studies can be complemented by analyzing the bile acid profile in blood, liver and bile in caveolin-1 -/- mice either on fed a control diet or a cholic acid-containing diet.

In conclusion, this thesis shows that the enterohepatic cycle of bile acids does not only require bile acid transport across the plasmamembrane of hepatocytes and

enterocytes, but also across peroxisomal membranes inside hepatocytes. The 70-kDa peroxisomal membrane protein (PMP70) is likely involved in the import of bile acids into peroxisomes to become conjugated to taurine or glycine. Like plasmamembrane bile acid transporters, PMP70 is associated to lipid rafts, which are likely to control its subcellular sorting and/or transport activity. Peroxisomal lipid rafts also contained caveolin-1, a protein involved in lipid and cholesterol transport, but in most other cells resides in the plasmamembrane. These results warrant follow up studies to identify the peroxisomal bile acid transporters as well as an in-depth analysis of the role of caveolin-1 in bile acid homeostasis.

References

1. Pellicoro A, van den Heuvel FA, Geuken M, Moshage H, Jansen PL, Faber KN. Human and rat bile acid-CoA:amino acid N-acyltransferase are liver-specific peroxisomal enzymes: implications for intracellular bile salt transport. Hepatology. 2007 Feb;45(2):340-8.
9. Antonenkov VD, Sormunen RT, Hiltunen JK. The behavior of peroxisomes in vitro: mammalian peroxisomes are osmotically sensitive particles. Am J Physiol Cell Physiol 2004;287:C1623-C1635.
10. Leighton F, Coloma L, Koenig C. Structure, Composition, Physical-Properties, and Turnover of Proliferated Peroxisomes - Study of Trophic Effects of Su-13437 on Rat-Liver. Journal of Cell Biology 1975;67(2):281-309.
11. Verheyden K, Fransen M, Van Veldhoven PP, Mannaerts GP. Presence of small GTP-binding proteins in the peroxisomal membrane. Biochim Biophys Acta 1992;1109:48-54.
12. Kukongviriyapan V, Stacey NH. Kinetics of taurocholate efflux from freshly isolated suspensions and primary cultures of rat hepatocytes. Hepatology. 1990 May;11(5):750-6.
2. Li T, Chiang JY. Regulation of Bile Acid and Cholesterol Metabolism by PPARs. PPAR Res. 2009;2009:501739
7. Carlton VE, Harris BZ, Puffenberger EG, Batta AK, Knisely AS, Robinson DL, Strauss KA, Shneider BL, Lim WA, Salen G, Morton DH, Bull LN. Complex inheritance of familial hypercholanemia with associated mutations in TJP2 and BAAT. Nat Genet. 2003 May;34(1):91-6.
8. Barbarito E, Batta AK, Salen G, Morton HD., Carlton V, Bull LN, Shneider BL. High serum and urinary unconjugated bile acid concentrations are associated with homozygous mutation in bile acid coenzyme A: Amino acid N-acyltransferase (BAAT). Gastroenterology 2003;124(4); supplement 1:A60
3. Hunt MC, Yang YZ, Eggertsen G, Carneheim CM, Gåfvels M, Einarsson C, Alexson SE. The peroxisome proliferator-activated receptor alpha (PPARalpha) regulates bile acid biosynthesis. J Biol Chem. 2000 Sep 15;275(37):28947-53
4. Kok T, Bloks VW, Wolters H, Havinga R, Jansen PL, Staels B, Kuipers F. Peroxisome proliferator-activated receptor alpha (PPARalpha)-mediated regulation of multidrug resistance 2 (Mdr2) expression and function in mice. Biochem J. 2003 Feb 1;369(Pt 3):539-47.
5. Inoue Y, Yu AM, Inoue J, Gonzalez FJ. Hepatocyte nuclear factor 4alpha is a central regulator of bile acid conjugation. J Biol Chem. 2004 Jan 23;279(4):2480-9.
6. Solaas K, Kase BF, Pham V, Bamberg K, Hunt MC, Alexson SE. Differential regulation of cytosolic and peroxisomal bile acid amidation by PPAR alpha activation favors the formation of unconjugated bile acids. J Lipid Res. 2004 Jun;45(6):1051-60.
22. Yoshihara T, Hamamoto T, Munakata R, Tajiri R, Ohsumi M, Yokota S. Localization of cytosolic NADPdependent isocitrate dehydrogenase in the peroxisomes of rat liver cells: Biochemical and immunocytochemical studies. Journal of Histochemistry & Cytochemistry 2001;49(9):1123-1131.
23. Rokka A, Antonenkov VD, Soininen R, Immonen HL, Pirilä PL, Bergmann U, Sormunen RT, Weckström M, Benz R, Hiltunen JK. Pxmp2 is a channel-forming protein in Mammalian peroxisomal membrane. PLoS One. 2009;4(4):e5090.
24. Meinecke M, Cizmowski C, Schliebs W, Krüger V, Beck S, Wagner R, Erdmann R. The peroxisomal importomer constitutes a large and highly dynamic pore. Nat Cell Biol. 2010 Mar;12(3):273-7.
13. Wilcke M, Hultenby K, Alexson SE. Novel peroxisomal populations in subcellular fractions from rat liver. Implications for peroxisome structure and biogenesis. J Biol Chem. 1995 Mar 24;270(12):6949-58.
14. Lüers G, Hashimoto T, Fahimi HD, Völkl A. Biogenesis of peroxisomes: isolation and characterization of two distinct peroxisomal populations from normal and regenerating rat liver.J Cell Biol. 1993 Jun;121(6):1271-80.
15. Wilcke M, Alexson SE. Differential induction of peroxisomal populations in subcellular fractions of rat liver. Biochim Biophys Acta. 2001 Jan 12;1544(1-2):358-69.
16. Yamamoto K, Fahimi HD. Biogenesis of peroxisomes in regenerating rat liver. I. Sequential changes of catalase and urate oxidase detected by ultrastructural cytochemistry. Eur J Cell Biol. 1987 Jun;43(3):293-300.
17. Ghosh MK, Hajra AK. A rapid method for the isolation of peroxisomes from rat liver. Anal Biochem. 1986 Nov 15;159(1):169-74.
18. Völkl A, Mohr H, Fahimi HD. Peroxisome subpopulations of the rat liver. Isolation by immune free flow electrophoresis. J Histochem Cytochem. 1999 Sep;47(9):1111-8.

19. Heinemann P, Just WW. Peroxisomal protein import. In vivo evidence for a novel translocation competent compartment. FEBS Lett. 1992 Mar 30;300(2):179-82.
20. Veenhuis M, Sulter G, van der Klei I, Harder W. Evidence for functional heterogeneity among microbodies in yeasts. Arch Microbiol. 1989;151(2):105-10.
21. Waterham HR, Keizer-Gunnink I, Goodman JM, Harder W, Veenhuis M. Development of multipurpose peroxisomes in Candida boidinii grown in oleic acid-methanol limited continuous cultures. J Bacteriol. 1992 Jun;174(12):4057-63.
25. de Waart DR, Häusler S, Vlaming ML, Kunne C, Hänggi E, Gruss HJ, Oude Elferink RP, Stieger B. Hepatic transport mechanisms of cholyl-L-lysyl-fluorescein. J Pharmacol Exp Ther. 2010 Jul;334(1):78-86.
26. Espeel M, Mandel H, Poggi F, Smeitink JA, Wanders RJ, Kerckaert I, Schutgens RB, Saudubray JM, Poll-The BT, Roels F. Peroxisome mosaicism in the livers of peroxisomal deficiency patients. Hepatology. 1995 Aug;22(2):497-504.
27. Mandel H, Espeel M, Roels F, Sofer N, Luder A, Iancu TC, Aizin A, Berant M, Wanders RJ, Schutgens RB. A new type of peroxisomal disorder with variable expression in liver and fibroblasts. J Pediatr. 1994 Oct;125(4):549-55.
28. Santos MJ, Henderson SC, Moser AB, Moser HW, Lazarow PB. Peroxisomal ghosts are intracellular structures distinct from lysosomal compartments in Zellweger syndrome: a confocal laser scanning microscopy study. Biol Cell. 2000 Apr;92(2):85-94.
29. Shimozawa N, Suzuki Y, Zhang Z, Imamura A, Kondo N, Kinoshita N, Fujiki Y, Tsukamoto T, Osumi T, Imanaka T, Orii T, Beemer F, Mooijer P, Dekker C, Wanders RJ. Genetic basis of peroxisome-assembly mutants of humans, Chinese hamster ovary cells, and yeast: identification of a new complementation group of peroxisome-biogenesis disorders apparently lacking peroxisomal-membrane ghosts. Am J Hum Genet. 1998 Dec;63(6):1898-903.
30. Clayton PT, Patel E, Lawson AM, Carruthers RA, Collins J. Bile-Acid Profiles in Peroxisomal 3-Oxoacyl-Coenzyme-A Thiolase Deficiency. Journal of Clinical Investigation 1990;85(4):1267-1273.
31. Bootsma AH, Overmars H, van Rooij A, van Lint AEM, Wanders RJA, van Gennip AH, et al. Rapid analysis of conjugated bile acids in plasma using electrospray tandem mass spectrometry: Application for selective screening of peroxisomal disorders. Journal of Inherited Metabolic Disease 1999;22(3):307- 310.
32. Keane MH, Overmars H, Wikander TM, Ferdinandusse S, Duran M, Wanders RJ, et al. Bile acid treatment alters hepatic disease and bile acid transport in peroxisome-deficient PEX2 Zellweger mice. Hepatology 2007; 45: 982-997
33. Woudenberg J, Rembacz KP, Hoekstra M, Pellicoro A, van den Heuvel FA, Heegsma J, van Ijzendoorn SC, Holzinger A, Imanaka T, Moshage H, Faber KN. Lipid rafts are essential for peroxisome biogenesis in HepG2 cells. Hepatology.

CHAPTER 7

Summaries

Summary

The liver is a central organ in regulating body homeostasis. It controls body temperature, protein, glucose and fat metabolism as well as the removal of toxic (waste) products. It plays an integrative function in the whole organism by cooperation with the circular and digestive system. This feature of the liver allows for the effective exchange of nutrients between every cell in the body coupled to the neutralization and elimination of metabolic waste products.
A main function of the liver is the production of bile, which is a mixture of water, phospholipids, cholesterol and bile salts. Bile salts are synthesized from cholesterol in the parenchymal cells of the liver, the hepatocytes. Together with phospholipids, bile acids form mixed micelles that are the fat-solubilizing particles that keep dietary fats in solution for absorption in the intestine. At the same time they are crucial for excretion of cholesterol and toxic waste products via the feces.
Peroxisomes are single membrane-bound organelles present in cells of all eukaryotes. In mammals, they are particularly abundant in the liver. They are responsible for a great variety of metabolic processes, including breakdown of very-long chain acids, D-amino acids, and polyamines and the biosynthesis of plasmalogens and bile salts. Peroxisomes are essential organelles containing a wide range of enzymes located inside this organelle to perform the diverse metabolic activities. In addition, specific substrate transporters are located in the peroxisomal membrane to fuel the metabolic processes and remove their products (ATP, fatty acids and bile salts).
Bile salts biosynthesis involves at least 13 different enzymes located to various organelles in liver hepatocytes. The bile salt biosynthesis pathway consists of two main routes and starts either in the ER (the "classical pathway" involving CYP7A1) or in the mitochondria (the so-called "acidic pathway" involving CYP27A1). Both routes yield CoA-activated C-27 bile acid biosynthesis intermediates and converge in peroxisomes where the primary C-24 bile salts cholic acid (CA) and chenodeoxycholic acid (CDCA) are formed. The final step of bile salt synthesis is the conjugation of CA and CDCA to either taurine or glycine. The sole enzyme responsible for bile acid conjugation in humans is bile acid-amino acid N-acytransferase (BAAT), which resides (most probably exclusively) in liver peroxisomes. After export from peroxisomes, bile salts are then transported by the Bile Salt Export Pump (BSEP) from the hepatocytes to the bile. This way, bile salts enter the enterohepatic circulation, where over 95% will be reabsorbed in the intestine, specifically at the terminal ileum, and return back to the liver via the portal vein for recycling. Bile salts returning from the intestine are imported into hepatocytes via the sodium-taurocholate cotransporting polypeptide (NTCP). The amount of bile salts that is lost via the feces is compensated for by *de novo* bile salt synthesis in the liver.
Bile salts in the intestine may undergo modifications by intestinal bacterial flora. These modifications include deconjugation of bile salts from taurine or glycine. These de-conjugated bile salts need to be re-conjugated by BAAT for effective

cycling between liver and ileum. Previous studies described BAAT residence in both the cytoplasm and peroxisomes. It seemed logical, as the dual location comfortably explains the function of this enzyme in *de novo* bile salt biosynthesis as well as in bile salt reconjugation. Peroxisomal BAAT was proposed to be involved solely in *de novo* synthesis of bile salts, while its cytoplasmic pool has been proposed to play a role in the reconjugation of deconjugated bile acids returning from the intestine. However, the dual location of BAAT was primarily based on cell fractionation experiments in which BAAT was detected in cytosolic and peroxisome-enriched fractions. However, peroxisomes are fragile organelles that may easily rupture during such experimental procedures and over 80% of the peroxisomal matrix protein content may leak out of these organelles and incorrectly designated as (partly) cytosolic. Recent findings based on digitonin permeabilization and (immuno) fluorescence identified BAAT as a typical peroxisomal protein in both rat and human hepatocytes. The location of BAAT inside peroxisomes has consequences for bile salt transport inside hepatocytes and requires peroxisomal bile salt transporters that are not identified to date.

In this thesis, we aimed to answer the question whether C-24 bile salts transit through hepatocyte peroxisomes for reconjugation. In **chapter 2**, we used primary rat hepatocytes and exposed them to deuterium-labeled cholic acid (D_4CA) that represent deconjugated bile acids returning to the liver from the intestine in this experimental system. Using this novel assay, we demonstrated a time-dependent conversion of D_4CA to the taurine and glycine-conjugates (D_4TCA and D_4GCA). Within 24 h, 100 uM D4CA added to the culture medium of 1 million hepatocytes was completely converted to D4TCA/D4GCA. A transient cellular accumulation of D4TCA/D4GCA was detected peaking at approximately 600-700 uM 3 h after adding D4CA to the medium. Digitonin permeabilisation of these hepatocytes revealed that the majority of D_4TCA remains associated to the cellular fractions when treated with 30 ug/mL digitonin, which fully releases all cytosolic proteins. Complete D4TCA release was only observed when hepatocytes were treated with high (500 ug/ml) concentrations of digitonin, which also release peroxisomal catalase. This indicated that D_4TCA is retained in a cell compartment of relatively low cholesterol membrane content, a typical feature of the peroxisomal membrane. To further prove that newly formed conjugates are present in peroxisomes of isolated rat hepatocytes, we performed cell fractionation experiments using an optimized procedure aimed at minimizing the osmotic damage to this organelle. We detected D_4TCA in highly purified peroxisomal fractions of these cells. We conclude that active transport of deuterated cholic acid into peroxisomes had occurring after which it was taurine conjugated. Thus, the enterohepatic cycling of unconjugated bile salts includes their shuttling through hepatocyte peroxisomes.

Our next goal was to try to determine which peroxisomal membrane protein (PMP) could be involved in transport of bile salts into this organelle. Extensive data is available on transporters responsible for bile salt transport across plasmamembranes in hepatocytes and enterocytes. Peroxisomal (and other organellar) bile salt transporters remain unknown. Previously, it has been found

that for the efficient translocation of C-27 bile salts inside peroxisomes ATP is required. This suggested an active transport of bile salt biosynthetic intermediates. However, no candidate transporter has been identified so far. It has also been shown that conjugated bile salts are exported out of peroxisomes in a passive transport, not requiring an energy supply. In **chapter 3**, we studied whether the Peroxisomal Membrane Protein of 70-kDa (Pmp70) is involved in the bile salt re-conjugation process. Although Pmp70 is the most dominant peroxisomal membrane protein in rat liver, very limited data is available concerning its function and its substrates. The ATP-binding site of Pmp70 faces the cytosol, which suggests that this protein transports substrates into peroxisomes. We exposed primary rat hepatocytes to fenofibric acid (FFA), a potent agonist of Peroxisome Proliferator-Activated Receptor Alpha (PPARα). PPARα stimulation in rodents increases peroxisome proliferation. Pmp70 is one of PPARα target genes and its expression is elevated in the presence of FFA. Additionally, we inhibited the expression of Pmp70 with small interfering RNA (siRNA). We manipulated the expression of Pmp70 in primary rat hepatocytes that were subsequently subjected to the "CA-conjugation and intracellular transport assay" described in chapter 2, to study the glycine/taurine conjugation and transcellular transport of D_4CA. We show that the induction of Pmp70 expression increases the D_4TCA accumulation in the medium, while the intracellular levels of D_4TCA and D_4CA were reduced. In the complementary approach, we found that siRNA-mediated inhibition of PMP70 reversed the FFA-induced Pmp70 overexpression and increased the intracellular levels of D4CA and D4TCA while D_4TCA levels in the medium decreased. Importantly, other proteins that are involved in bile acid re-conjugation pathway (NTCP, FATP5, BAAT and BSEP) were not affected by FFA and/or siRNA treatment. These data suggest a role for Pmp70 in the transport of unconjugated bile salts into peroxisomes to become conjugated to taurine and efficiently exported from hepatocytes.

The activity of bile salt transporters present in plasma membranes of enterocytes and hepatocytes is modulated by their specific lipid environment, where they may associate to cholesterol-enriched microdomains, so-called lipid rafts.

It seems likely that bile acid transporters in organelles share this characteristic and are localized to organellar lipid rafts. To determine whether this holds true for the putative peroxisomal bile salt transporter PMP70, we studied whether the peroxisomal membrane contains lipid rafts. Though lipid rafts have been detected in several organellar membranes, this was not particular likely for the peroxisomal membrane, which contains relatively low concentrations of cholesterol. In **chapter 4**, however, we do describe the existence of peroxisomal lipid rafts and their role in the biogenesis for this organelle. We show that the homologous ABC transporters PMP70 and Adrenoleukodystrophy protein (ALDP) are differentially associated to lipid rafts in the peroxisomal membrane, as the former resists solubilization with a strong detergent (Triton X-100), whereas the latter only resists the treatment with a mild detergent (Lubrol WX). Also Pex14p was found in Triton X-100-resistance lipid rafts, whereas an interacting partner, Pex13p is not associated with lipid rafts

at all. HepG2 cells were depleted from cholesterol thereby depleting it from lipid rafts, which leads to a mislocalisation of catalase to the cytosol. In addition, ALDP lost its typical peroxisomal location, most likely accumulating in the ER. In contrast, PMP70 and Pex14 remained predominantly present in peroxisomes. These processes were partly reversible, as catalase sorting to peroxisomes was restored after repletion of cholesterol in HepG2 cells. In contrast, ALDP sorting was not effectively restored in these cells. These data show that the peroxisomal membrane contains lipid rafts, which are essential for peroxisome biogenesis. Highly homologous (PMP70 and ALDP) and physically interacting (Pex13p and Pex14p) showed different lipid raft association characteristics. The lipid environment of these proteins may strongly affect their activity.

To further characterize the peroxisomal lipid rafts, in **chapter 5** we compared the detergent-extractability and subcellular location of peroxisomal membrane proteins to several well-known markers of lipid microdomains, including Src-1, flotillin and caveolin-1. Much to our surprise, we found that caveolin-1 appeared to be present in peroxisomal lipid rafts in hepatocytes. Caveolin-1 is one of three caveolins, which are structural components of caveolae that are characteristically found on small endocytic pits at the plasmamembrane. Caveolin-1 expression in hepatocytes is relatively low, in particular when compared to endothelial cells. Cell fractionation and confocal laser scanning microscopy on purified hepatocytes revealed that most of the caveolin-1 in hepatocytes was associated with peroxisomes. Also, artificially expressed GFP-tagged caveolin-1 accumulated in catalase-positive organelles in hepatocytes. FFA treatment strongly reduced caveolin-1 expression in hepatocytes while it stimulated peroxisome proliferation. No aberrant peroxisome morphology was detected in liver tissue from caveolin-1 knockout mice, indicating that it is not an important factor for peroxisome biogenesis. Previous research on these mice revealed that they show impaired liver regeneration and lipid metabolism.

In conclusion, this thesis shows that the enterohepatic cycle of bile acids does not only require bile acid transport across the plasmamembranes of hepatocytes and enterocytes, but also across peroxisomal membranes inside hepatocytes. The 70-kDa peroxisomal membrane protein (PMP70) is likely involved in the import of bile acids into peroxisomes to become conjugated to taurine or glycine. Like plasmamembrane bile acid transporters, PMP70 is associated to lipid rafts, which likely controls its subcellular sorting and/or transport activity. Peroxisomal lipid rafts also contained caveolin-1, a protein involved in lipid and cholesterol transport. These results warrant follow up studies to identify the peroxisomal bile acid transporters as well as an in-depth analysis of the role of caveolin-1 in bile acid homeostasis.

Samenvatting

De lever is een centraal orgaan in het lichaam voor de regulatie van lichaamstemperatuur, eiwit, glucose en vetmetabolisme en het elimineren van toxische afval producten. De lever speelt in het lichaam een integrerende rol in de samenwerking van het darmstelsel met de systemische circulatie. Hierdoor is de lever uitermate geschikt voor het effectief verwerken van nutriënten uit de darmen en het in stand houden van systemische bloedspiegelwaardes. Zo balanceert de lever toevoer van nutrienten aan alle lichaamscellen en filtratie en eliminatie van metabole eindproducten uit het lichaam.
Een belangrijke functie van de lever is het aanmaken van gal. Gal is een mengsel van water, fosfolipiden, cholesterol, galzouten en afvalstoffen. Galzouten worden gemaakt van cholesterol in hepatocyten, het meest voorkomende celtype in de lever die het zgn. leverparenchym vormen. Samen met fosfolipiden vormen galzouten gemixte micellen die in de darm dieëtvetten emulsificeren voor een efficiënte absorptie. Tegelijkertijd is gal cruciaal voor het uitscheiden van cholesterol en afvalstoffen uit het lichaam via de feces.
Peroxisomen zijn celorganellen met een enkelvoudige membraan en komen in alle eukaryoten voor. In zoogdieren zijn peroxisomen vooral zeer talrijk verrijkt aanwezig in de lever en vooral in hepatocyten aanwezig. Ze zijn betrokken bij diverse metabolische processen, zoals het afbreken van (zeer) lange vetzuurketens, D-aminozuren en polyamines, maar ook biosynthese van plasmalogens en galzouten. Peroxisomen zijn essentiële organellen waarin een breed scala aan enzymen aanwezig is voor de diverse metabole functies. Hiervoor zitten in de peroxisomale membraan specifieke peroxisomale transporters die de peroxisomale enzymen voorzien van substraten en die de producten verwijderen (ATP, vetzuren en galzouten).
Bij de galzoutsynthese zijn tenminste 13 verschillende enzymen betrokken. Deze zijn verspreid over diverse organellen, waaronder het endoplasmatisch reticulum (ER), mitochondriën en peroxisomen. De galzoutbiosynthese kan via 2 routes verlopen, de klassieke en zure route. In de klassieke route is de eerste stap het omzetten van cholesterol door Cytochroom P450 (CYP) 7A1 in het ER. Bij de zure route verloopt de omzetting van cholesterol via CYP27A1 in de mitochondriën. In beide gevallen worden CoA-geactiveerde C-27 galzout intermediairen gevormd die samenkomen in het peroxisoom. Hier worden de primaire C-24 galzuren, cholaat (CA) en chenodeoxycholaat (CDCA) gesynthetiseerd. De laatste stap in het proces van galzoutsynthese is het conjugeren van CA en CDCA met Glycine of Taurine. Bile acid-amino N-acyltransferase (BAAT) is het enige enzym dat galzuren kan conjugeren. Het enzym BAAT komt -waarschijnlijk exclusief- in leverperoxisomen voor. Na transport uit de peroxisoom worden galzouten via de Bile Salt Export Pump (BSEP) uit hepatocyten de gal in getransporteerd voor het doorlopen van de enterohepatische kringloop. Meer dan 95% van de galzouten in gal zal in de darmen worden geabsorbeerd, met name in het terminaal ilieum, waarna ze via de poortader terugkomen in de lever. Circulerende galzouten

worden via de Sodium-dependent Taurocholate Co-transporting Peptide (NTCP) de hepatocyt in geïmporteerd. De galzouten die verloren gaan via de feces worden in de lever met *'de novo'* synthese gecompenseerd.
In de darmen kunnen galzouten gemodificeerd worden door de aanwezige darmflora. Het verwijderen van de Glycine of Taurine groep ("deconjugatie") is een veel voorkomende modificatie van galzouten in de darm. Gedeconjugeerde galzouten worden opnieuw geconjugeerd in de hepatocyt door BAAT voor effectief transport tussen lever en darm. In vorig onderzoek is beschreven dat BAAT zowel in het cytosol als in het peroxisoom aanwezig is. Deze verschillende intracellulaire locaties van BAAT zouden specifiek verantwoordelijk kunnen zijn voor de conjugatie van *'de novo'* gesynthetiseerde en gereconjugeerde galzouten. Peroxisomaal BAAT zou dan alleen betrokken zijn bij *'de novo'* galzoutbiosynthese, terwijl cytosolisch BAAT een rol zou spelen bij reconjugatie van gedeconjugeerde galzouten uit de darmen. De reden waarom men aanneemt dat BAAT zowel in peroxisomen als in het cytosol voorkomt, is gebaseerd op celfractioneringsexperimenten waain BAAT zowel in het cytosol als in de peroxisomale fractie werd aangetoond. Het is echter bekent dat de peroxisomal membraan gemakkelijk kapot gaat tijdens dergelijke celfractionerings experimenten, waarbij wel meer dan 80% van de peroxisomale enzymen uit deze organellen lekken en onterecht als "cytosolisch" worden gekwalificeerd .. Recent is met meer geraffineerde methodes, zoals digitonine permeabilisatie en (immuno) fluorescentie microscopie, BAAT voornamelijk, zo niet exclusief, peroxisomaal aanwezig in zowel ratten- als humane hepatocyten. De peroxisomale lokalisatie van BAAT heeft consequenties voor het transport van galzouten in hepatocyten. Voor reconjugatie moeten galzouten namelijk eerst de peroxisoom in geimporteerd worden. Een peroxisomale galzouttransporter die dit doet is nog niet geïdentificeerd.
In dit proefschrift hebben we geprobeerd om de vraag te beantwoorden of C24 galzouten voor reconjugatie door peroxisomen van hepatocyten gaan. In hoofdstuk 2 zijn primaire ratten hepatocyten blootgesteld aan deuterium-gelabeld cholaat (D_4CA). Iin dit experiment staat D_4CA model voor de gedeconjugeerde galzouten die vanuit de darm terugkeren naar de lever. Met deze nieuwe methode hebben we een tijdsafhankelijke omzetting van D_4CA in taurine-en glycine conjugaten (D_4TCA en D_4GCA) aangetoond. Binnen 24 uur was van de 100 µM D_4CA die aan kweekmedium met 1 miljoen hepatocyten was toegediend, volledig omgezet in D_4TCA/D_4GCA. Een tijdelijke cellulaire ophoping van D_4TCA/D_4GCA werd waargenomen, met een maximum van ca. 600-700 µM na 3 uur incubatie met D_4CA. Permeabilisatie van hepatocyten met digitonine (30 µg/mL) liet zien dat het grootste deel van D_4TCA geassocieerd bleef met cellulaire fracties, terwijl alle cytosolische eiwitten wel vrijkwamen. Het volledig vrijkomen van D_4TCA uit hepatocyten werd bereikt wanneer er een hoge concentratie digitonine (500 µg/mL) werd gebruikt. Bij deze concentratie kwam ook het peroxisomale matrix eiwit Catalase vrij. Deze bevindingen met digitonine permeabilisatie duidde er op dat D_4TCA opgesloten zit in een cel compartiment met lage concentraties

cholesterol in de membraan, hetgeen karakteristiek is voor peroxisomen. Om verder te bewijzen dat nieuw-gevormde galzoutconjugaten in peroxisomen van ratten hepatocyten zitten, hebben we een nieuwe celfractioneringsmethode ontwikkeld. Deze methode is zodanig geoptimaliseerd dat osmotische schade aan peroxisomen wordt geminimaliseerd. In deze fractioneringsexperimenten hebben we D_4TCA in een zeer zuivere peroxisomale fractie kunnen detecteren. Hiermee concluderen we dat er transport van deuterium-gelabeld cholaat de peroxisoom in heeft plaats gevonden, waarna het met Taurine is geconjugeerd. Dit is het eerste experimentele bewijs dat ongeconjugeerde (C-24) galzouten die zich in de enterohepatische circulatie bevinden voor reconjugatie door peroxisomen van hepatocyten gaan.
Ons volgend doel was het identificeren van een peroxisomaal membraaneiwit (PMP) dat mogelijk betrokken is bij het importeren van galzouten. Er is een uitgebreide hoeveelheid data beschikbaar over transporters in hepatocyten en enterocyten die galzouten over plasmamembranen transporteren. Voor peroxisomen, maar ook andere organellen, zijn dergelijke galzouttransporters nog niet geïdentificeerd.
In het verleden is aangetoond dat voor efficiente translocatie van C-27 galzouten naar de peroxisoom ATP nodig is. Dit wijst op een aktief transport van galzout intermediairen in de *'de novo'* synthese route. Men heeft ook aangetoond dat geconjugeerde galzouten d.m.v. passief transport, zonder energie verbruik, de peroxisoom uitgaan.
In hoofdstuk 3 hebben we de mogelijke betrokkenheid van het Peroxisomal Membrane Protein – 70 kDa (PMP70) bij reconjugatie van galzouten bestudeerd. Hoewel PMP70 het meest dominante peroxisomale eiwit is in rattenlever, is er relatief weinig over de functie en substraatspecificiteit van dit eiwit bekend. De ATP – bindingsplaats van PMP70 is gericht naar het cytosol. Dit suggereert dat dit eiwit betrokken is bij de import van substraten de peroxisoom in. We hebben primaire ratten hepatocyten blootgesteld aan fenofibraatzuur (FFA), een effectieve agonist van de transcriptiefactor Peroxisome Proliferator Activated Receptor alpha (PPARα). PPARα activatie stimuleert peroxisoom proliferatie in knaagdieren. Ook Pmp70 expressie staat onder controle van PPARα en wordt geïnduceerd in aanwezigheid van FFA. Daarnaast hebben we de expressie van Pmp70 geremd m.b.v. "small interfering RNA's" (siRNA). We hebben de expressie van Pmp70 in ratten hepatocyten gemanipuleerd om vervolgens met de in hoofdstuk 2 beschreven, "CA-conjugatie en intracellulaire transport proeven", de glycine/taurine conjugatie en transport van D_4CA te bestuderen. We laten zien dat inductie van Pmp70 expressie een verhoging van D_4TCA in het medium geeft, terwijl de intracellulaire nivo's van D_4TCA en D_4CA verlaagd zijn. Het complementaire experiment, waarbij Pmp70 expressie geremd wordt d.m.v. siRNA, voorkwam de FFA-geïnduceerde overexpressie van Pmp70 en verhoogde de intracellulaire nivo's van D_4CA en D_4TCA, terwijl D_4TCA in het medium verlaagd was. De behandeling met FFA en siRNA had geen effect op andere eiwitten die een effect zouden kunnen hebben op galzout re-conjugatie (NTCP,

FATP5, BAAT en BSEP). Deze data suggereren een rol voor Pmp70 in het transport van ongeconjugeerde galzouten de peroxisoom in, om vervolgens met Taurine geconjugeerd te worden voor efficiënte excretie uit peroxisomen en vervolgens uit hepatocyten.
De activiteit van galzout transporters in de plasmamembraan van enterocyten en hepatocyten wordt gemoduleerd door de specifieke lipide omgeving in de membraan. Verschillende galzout transporters zitten in zgn. "lipid rafts". Dit zijn microdomeinen in cellulaire membranen die een relatief hoge concentratie cholesterol bevatten.
Het is waarschijnlijk dat galzouttransporters in membranen van organellen deze karakteristiek delen met galzout transporters in plasmamembranen en dus ook gelokaliseerd zijn in lipid rafts. Om te bepalen of dit van toepassing is op de vermoedelijke peroxisomale galzout transporter PMP70 hebben we eerst gekeken of lipide rafts überhaupt aanwezig zijn in de peroxisomale membraan. Hoewel lipide rafts gevonden zijn membranen van verschillende organellen , was dit niet erg waarschijnlijk voor de peroxisomale membraan , aangezien die een relatief lage concentratie cholesterol bevat. Echter, in hoofdstuk 4 beschrijven we het bestaan van peroxisomale lipide rafts en hun rol in de biogenese van dit organel. Op basis van biochemische extractie experimenten definiëren we op zijn minst 2 verschillende lipide rafts in de peroxisomale membraan van HepG2 cellen, een modelcellijn voor humane hepatocyten. PMP70 is aanwezig in een lipide raft die bestand is tegen extractie met een sterk detergent (is een zeepachtige stof), Triton X-100. Ook Pex14p, een eiwit dat betrokken is bij eiwitimport in peroxisomen, zit in deze Triton X-100 lipide rafts. Opmerkelijk is dat een eiwit wat erg veel op PMP70 lijkt en ook in de peroxisomale membraan zit, het Adrenoleukodystrophy protein (ALDP) niet in Triton X-100 lipide rafts zit maar juist in lubrol WX (een zwakker detergent) lipide rafts. Pex13p, een ander eiwit betrokken bij eiwitimport in peroxisomen, was niet aanwezig in lipide rafts, hetgeen ook verrassend is omdat bekend is dat dit een eiwitcomplex vormt met Pex14p. Als de HepG2 cellen werden gedepleteerd van cholesterol om de lipide rafts te onttrekken van de membraan, dan leidde dit tot de mislokalisatie van Catalase naar het cytosol. OokALDP verloor zijn typische peroxisomale lokalisatie en accumuleerde waarschijnlijk in het ER. Daarentegen bleven PMP70 en Pex14p voornamelijk geassocieerd met peroxisomen. Als vervolgens deze HepG2 cellen opnieuw cholesterol toegediend kregen, werd catalase weer efficiënt in peroxisomen opgenomen. Er werd echter niet een noemenswaardig herstel van ALDP transport naar de peroxisomen waargenomen. Deze resultaten tonen aan dat er lipide rafts in de peroxisomale membraan aanwezig zijn, die noodzakelijk zijn voor de vorming van dit organel. Opmerkelijk was dat de sterk homologe PMP70 en ALDP en de eiwitcomplex-vormende Pex13p en Pex14p een verschillende lipide raft associatie lieten zien. De lipide omgeving van deze eiwitten zou sterk van invloed kunnen zijn op hun activiteit.
Om peroxisomale lipide rafts verder te karakteriseren, hebben we in hoofdstuk 5 detergents extracties en subcellulaire lokaties van peroxisomale membraaneiwitten

vergeleken met een aantal wel bekende lipide microdomein merkers, nl. Src-1, flotillin en Caveolin-1. Tot onze grote verrassing zagen we dat caveolin-1 in hepatocyten aanwezig is in peroxisomale lipid rafts. Caveolin-1 is één van de drie Caveolines, die een structurele component zijn van Caveolea en normaal gesproken op de endocytotische instulpingen van de plasmamembraan zit. Caveolin-1 expressie is relatief laag in hepatocyten, vooral als de expressie wordt vergeleken met endotheel cellen in de lever. Celfractionering en confocale laser scanning microscopie van gezuiverde hepatocyten onthulde dat het merendeel van het caveolin-1 in hepatocyten geassocieerd was met peroxisomen. Ook artificiële expressie van GFP-gelabeld caveolin-1 in hepatocyten hoopte zich op in organellen die catalase bevatten, de karakteristieke merker voor peroxisomen. FFA stimulatie verlaagt Caveolin-1 expressie in hepatocyten, terwijl peroxisoomproliferatie juist werd geïnduceerd. In Caveolin-1 knock out muizen werden geen afwijkingen gevonden in peroxisoom morfologie. Dit suggereert dat het geen belangrijke factor is voor peroxisoombiogenese. Uit vorig onderzoek met deze muizen is gebleken dat er sprake was van een verstoorde leverregeneratie en vetmetabolisme.
In conclusie, dit proefschrift laat zien dat de enterohepatische circulatie van galzouten niet alleen afhankelijk is van galzouttransporters in de plasmamembraan van hepatocyten en enterocyten, maar ook van transport door de peroxisomale membraan in hepatocyten. Het 70-kDa peroxisomale membraan eiwit (PMP70) is waarschijnlijk betrokken bij transport van galzouten in peroxisomen voor conjugatie met Taurine of Glycine. Vergelijkbaar met galzouttransporters in de plasmamembraan is PMP70 ook geassocieerd met lipide rafts, die waarschijnlijk de subcellulaire lokalisatie en/of transport activiteit controleren. Peroxisomen in hepatocyten bevatten Caveolin-1, een eiwit dat betrokken is bij lipiden en cholesterol transport, i.t.t. de meeste andere cellen waar het in de plasmambembraan gevonden wordt Deze resultaten geven een goede aanleiding voor vervolgonderzoek voor het identificeren van de peroxisomale galzouttransporters, maar ook een gedetailleerde analyse van de rol die Caveolin-1 speelt in galzouthomeostase.